TWIN-CORE OFFSET FIBRE AND ITS APPLICATIONS

By

Jiancong (Raymond) ZHANG

A thesis submitted
in partial fulfilment of the requirement
for the Degree of
Master of Engineering Science

Department of Communication
School of Electrical Engineering
The University of New South Wales

Submitted: June 1993

CERTIFICATE OF ORIGINALITY

I hereby declare that this submission is my own work and that, to the best of my knowledge and belief, it contains no material previously published or written by another person nor material which to a substantial extent has been accepted for the award of any other degree or diploma of a university or other institute of higher learning, except where due acknowledgement is made in the text.

(Signed).

Acknowledgments

I would like to express my heartfelt gratitude to my supervisor, Prof. P. L. Chu, for his guidance and encouragement not only during the course of this research, but also in my most difficult time of studying, when I commenced course work as a Graduate Diploma candidate in the University. I also wish to thank him for patiently proof reading my thesis using his precious private time.

My special thanks to Dr. G. D. Peng for teaching me the experimental skill and for his helps in many area. I also thank him for proof reading my thesis.

I wish to thank Mr. T. Whitbread for his kind and patient help in many area, including the use of the experimental apparatus, discussions and suggestions in the application of computer softwares and hardware, etc. His advise and support is really appreciated. I also thank Mr. P. Allen for his helps.

I am indebted to all my colleague in the Optical Communication Group (OCG). Thanks to Tjugi for his help in many area and let me read his M.Eng.Sc. thesis. Thanks to Chris for sharing his experience in making and experimenting twin-core D fibres with me and let me read his M.Eng.Sc. thesis. Thanks to Fan for patiently helping me making and measuring preforms. Thanks to Granpayeh for his helpful discussions and support in writing the Pascal program. Thank to all the members in OCG for their helps in many area which cannot be mentioned in full, especially to Maxing and Yanling.

Finally, thanks to my relatives and family for their years of concern and encouragement. My sincere thanks go to my uncle Manwong Cheung and his

family for their spiritual encouragement and financial support in these years. Most importantly, I wish to show my gratefulness to my greatest mother, who brought me up alone since my father passed away when I was a child, for her love, understanding and encouragement.

Table of Contents

Abstract

In this thesis, basic concepts of conventional single mode fibres are reviewed and the twin-core offset fibres are proposed and analysed. The procedure of design and fabrication of twin-core offset fibres is also given. A proposal to construct a twin-core offset fibre directional coupler is given along with some of its applications. Experiments carried out for twin-core offset fibres and directional couplers are presented and the results of the experiments are discussed.

List of Figures

List of Tables

List of Symbols

TOF	Twin-core offset fibre
TOFDC	Twin-core offset fibre directional coupler
P	Power
λ	Free space wavelength
n_1	Refractive index of the core
n_2	Refractive index of the inner cladding
n_2'	Refractive index of the outer cladding
n_{2eff}	Effective index of the claddiong
Δn	Index difference
Δn_{eff}	Effective index difference
n_3	Refractive index of the surrounding medium
Δ	Relative index difference
Δ_{eff}	Effective relative index difference
V	Normalised frequency
U	Core modal parameter
W	Cladding modal parameter
β	Propagation constant of the fundamental mode
$\beta_{+/-}$	Propagation constant of even and odd fundamental modes
ρ	core radius of the fibre core

κ	Free space wave nomber
$J_0(\,), J_1(\,)$	Bessel function of order zero and one
$K_0(\,), K_1(\,)$	Modified Hankel function of order zero and one
r	radius from fibre axis
E	Electric field
$E_{a/b}$	Electric field of care a and core b
$P_{a/b}$	Power gurded by core a and core b
r_0	Spot size
$\Psi(r)$	Radial amplitude distribution
$\Psi_{+/-}$	Field amplitude contribution of even and odd modes
d	Core separation of a twin-core fibre
d'	Core edge separation of a twin-core fibre d'=d-2ρ
C	Coupling coefficient
z	Fibre length
L_c	Coupling length
D_s	Fibre diameter of a primary preform
ρ_s	Radius of primary preform
D_D	Diameter of a D shaped single-core preform
d_{D1}	Core to D surface distance of a D single-core preform
d_{nt}	Core sepatation of a normal twin-core preform
D_{nt}	Diameter of a normal twin-core preform

d_{to}	Core separation of twin-core offset preform
D_{to}	Diameter of twin-core offset preform
S_{to}	Minimum distance of core to preform surface of a twin-core offset preform
MCVD	Modified chemical vapour deposition
n_{2effi}, n_{2effx}	Minimum and maximum effective cladding index
Δ_{effi}, Δ_{effx}	Minimum and maximum effective relative index difference
λ_{min}, λ_{max}	Minimum and maximum operation wavelength
R_s	Splitting ration of a directional coupler
P_4	Coupled output power of a directional coupler
P_2	Throughput power of a directional coupler
P_1	Input power of a directional coupler
A_s	Splitting ration in decibel
A_d	Directivity of a directional coupler in decibel
A_i	Insertion loss of a directional coupler in decibel

Chapter 1

Introduction

1.1 Overview of the topic

Twin-core Offset Fibre (TOF) is a new type of optical fibre which is proposed, designed, fabricated and analysed firstly in our laboratory. By utilising the special properties of a TOF, a new type of tunable directional couplers, the Twin-core Offset Fibre Directional Couplers (TOFDC), can be made.

The purpose of this the thesis is to report the studies in analysis, design, fabrication and experimentation with TOF and TOFDC.

Single-mode fibres have much greater bandwidth and lower fibre attenuation than multimode fibres. In addition, the propagation characteristics of the single-mode fibres are independent of the launch condition whereas this is not the case for multimode fibers [1] [2]. Due to the many advantages of the single-mode fibres over the multimode fibres, most of the optical fibre communication systems use the single-mode fibre as the transmission media, and hence the single mode fibres and single-mode directional couplers play a much more important role in modern communication systems.

There are two main types of optical directional couplers: the bulk optics and the fibre-optics. Bulk optical directional couplers requires the transformation of a guided beam from the fibre into a free beam which passes through couplers and then relaunch the beam into another fibre again. This introduces extra losses. Fibre-optic directional coupler operates on guided wave beams of the fibre. Fibre-optic directional couplers are preferable in optical fibre communication systems due to their lower insertion loss, better stability, and more suitable size than their bulk counterparts [3].

The fibre and directional coupler considered in thesis are single-mode fibre and fibre-optic single-mode directional (four-port) coupler.

1.2 Contents of this thesis

In chapter 2 of the thesis, the basic concepts of a normal single-mode fibre are reviewed, some formulas for calculating the basic parameters of normal fibres with step index profile are introduced. Because a core(s) offset fibre is merely a modified normal fibre, and also because the properties of a core(s) offset fibre can be analysed by its equivalent step index profile, a revision of the basic concepts of normal single-core and twin-core mono-mode fibres is very helpful for later analysis of the core(s) offset fibre.

Chapter 3 proposed a new type of optical fibre, the twin-core offset fibre (TOF). We then perform an analysis in the single-core and twin-core offset fibre (cores close to the fibre surface). The operational principle of core(s) offset fibres is

explained. The formulas for normal fibres are modified so that they can be used in the analysis of core(s) offset fibres.

Chapter 4 developed a design technique for fabricating twin-core offset fibres. There are five steps in the TOF fabrication process and formulas are provided for each step. A set of designed parameters are calculated for our required TOF in this chapter.

Chapter 5 describes our procedure in making the required twin-core offset fibre. The parameters of our fabricated TOF are measured.

Chapter 6 introduces a new idea of making tunable optical directional coupler, based on twin-core offset fibres. We call the Twin-core Offset Fibre Directional Coupler (TOFDC). The operational principle of the TOFDCs is described and some formulas for characterising the TOFDCs are presented. Several applications of the TOFDCs are proposed.

Chapter 7 reports our experiment and results on the twin-core offset fibres. Discussions on the experimental results are also included.

Chapter 8 summarises our works in preparing this thesis and provides comments on the results obtained and gives suggestions for further improvements.

Appendix A is a Pascal program to calculate electric field distribution in a normal single-core fibre. Appendix B and Appendix C are Pascal programs for calculating and plotting the relations among different parameters of twin-core fibres (they need minor modification for calculating some other relationship of twin-core fibre parameters except those shown in the program).

Appendix D is a Pascal program for calculating and plotting relation between coupling coefficient and operation wavelength from experiment data.

1.3 Original contributions of the thesis

There are four original contributions in this thesis.

Firstly, a new type of fibres, the twin-core offset fibres (TOF), are proposed and it has been analysed both theoritally and experimentally. Although the twin-core D fibres, which has similar properties as twin-core offset fibres, had been fabricated in our laboratory, it is hard to obtain a twin-core D fibre with the exact required parameters using the preform drawing method because its cross-sectional shape, thickness and hence core radius, core separation, etc, vary during the fibre drawing process. ON the other hand, twin-core D fibre fabricated by fibre polishing method can not be very long. A long TOF with uniform and controled parameters is easy to obtain. In addition, little analysis has been done on twin-core D fibre previously. In this thesis, we study TOF both theoretically and experimentally, the result can be applied to twin-core D fibres.

Secondly, a systematical method of designing and fabricating twin-core offset fibres is developed. The method is based on the existing general twin-core fibre fabrication method, but its advantage is that it provides a step by step cntrol of not only the TOF fabrication process, but also the general twin-core fibres.

Thirdly, a new type of tunable directional couplers, the twin-core offset fibre directional coupler (TOFDC) is proposed and analysed. The advantage of

TOFDC is that they can provide more convenient and smooth variation on the power splitting ratio and less disturbance to the coupler/fibre connection.

Finally, an automated computer program to obtain coupling coefficient of any twin-core fibres in the required wavelength range has been written. With the results of a classic P vs λ (power versus wavelength) measurement, the program gives an exact coupling coeffcient as a function of wavelength (instructions will be given once you start to run the program).

References of chapter 1:

1 Kapron F.P: Critical review of fiber-optic communication technology: optical fibers. Proc.SPIE 425, 1-16, 1984.

2 Gambling W.A., Matsumura H.:"A comparison of single-mode and multimode fibers for long-distance telecommunications", in Fiber and Integrated Optics, ed. by D.B.Ostrowski (Plenum, New York), pp.333-343,1979.

3 Neumann E. -G.: Single-mode fibers Fundamentals, Springer-Verlag, Berlin, 1988, Chapter 7.

Chapter 2

Basic Concepts of Conventional Single-mode Fibres

2.1 Introduction to Chapter 2

In this chapter, the basic concepts of the conventional single-mode fibres are reviewed. In perticular, we discuss the main parameters and variables that characterise a single-mode fibre such as the relative index difference Δ, the normalised frequency V, the core modal parameter U, the cladding modal parameter W, and the coupling coefficient C, etc, are described. The most important formulas for calculating the parameters of normal single-mode fibres with step-index profile are presented. Since the normalised frequency for single-mode operation of fibres with arbitrary profiles depends primarily on the profile 'volume' and is relatively insensitive to profile shape, we believe that there is an equivalent step-index profile for core(s) offset fibres and non-step-index fibres, from which we can analyse the properties of these fibres more easily (except the pulse dispersion property which is not a concern in this thesis).

2.2 Single-core Fibres

2.2.1 Principles

Optical communications using light beam in free space have three main problems. Firstly, the light beam propagates in a straight path such that any obstacle in its path blocks it; Secondly, the beam can be scattered by rain, fog, or snow when it is transmitted through the atmosphere; Thirdly, the beam will diverge when it propagates in a homogeneous medium, leading to a decrease in optical power transmitted per unit area (due to the increase in beam diameter). For these reasons, there are only a few optical communication systems operating in free space propagation, for instance, between two tall buildings or between two satellites in space.

To overcome these problems, optical fibres are introduced to guide the light beams. The principle of the wave guiding in a fibre is that the higher refractive index in the region around the fibre axis reduces the phase velocity of the centre part of a light beam causing the wavefronts in this part retarded relative to the outer part, and hence produce a focusing (or converging) effect on the light beam. By using optical fibres, light signal can avoid diffraction spreading and transmitting along a curved path without being influenced by the changing properties of the atmosphere. A picture of a "unclad" fibre is shown in Figure 2.2.1.1.

The "unclad" fibres can excite many "modes" due to their large core and large index difference between core and the surrounding air. The unwanted multimode dispersion (and hence pulse spreading) is then incurred because of the phase

velocity difference between different modes. The "unclad" fibres never became a practical communication channel.

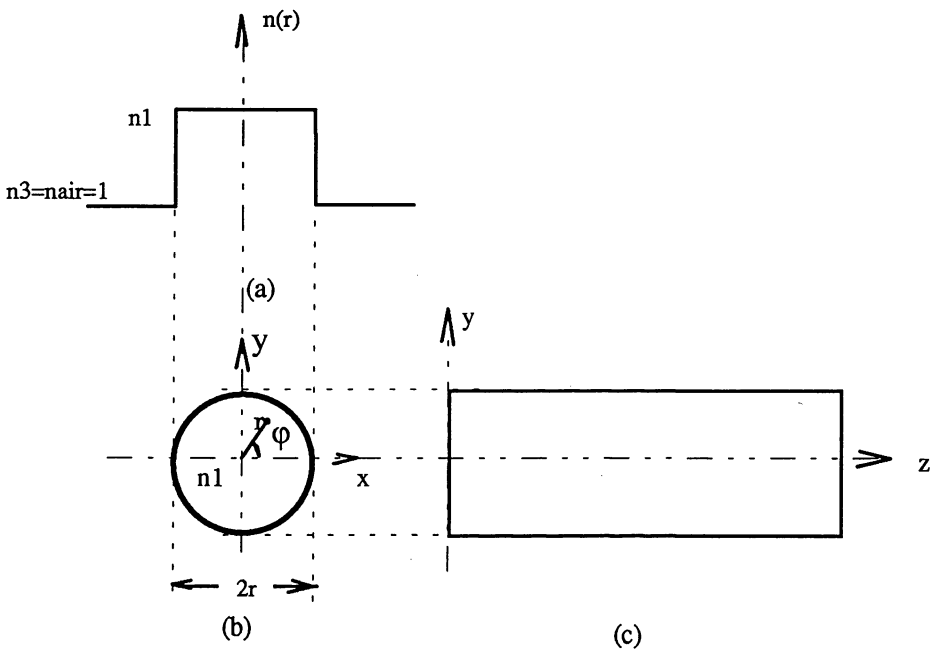

Figure 2.2.1.1 "Unclad" fibre
(a) Refractive index profile
(b), (c) Cross-sectional view

In the mid- 1960s, the "core-cladding" (or "weakly guiding") structure was introduced [1, 2]. In these structure, the light-guiding central portion (called "core") is surrounded by a dielectric layer (called "cladding") having a refractive index slightly (0.1-1%) lower than that of the core. Figure 2.2.1.2 shows a typical weakly-guiding fibre with step-index profile.

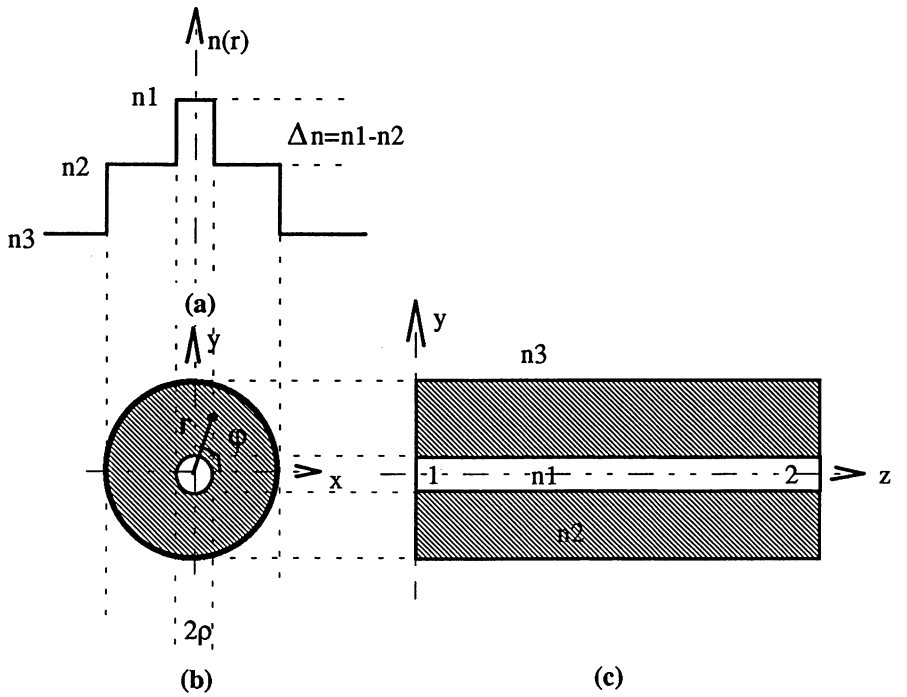

Figure 2.2.1.2 "Core-cladding" fibre

(a) Refrective index profile

(b), (c) Cross-sectional view of x-y plane

2.2.2 Parameters and Characteristics

Because most of the properties of a fibre with arbitrary index profile can be characterised and analysed by its ESI (Equivalent Step Index) parameters [3], and because the fibres discussed in this thesis are near step-index profiled and single-moded, only the parameters that characterise single-mode fibres with step index profile are reviewed in this chapter.

The main parameters that characterise typical single-core single-mode fibres of step-index profiled include [4 5]: the index difference

$$\Delta n = n_1 - n_2 \qquad (2.2.2.1)$$

or relative index difference

$$\Delta = \frac{n_1^2 - n_2^2}{2n_1^2} \approx \frac{n_1 - n_2}{n_1} \text{ (for weakly guiding , ie } \Delta n < 0.01) \qquad (2.2.2.2)$$

where n_1, n_2 and n_3 are refractive index of the core, cladding and surrounding medium respectively; n_3 does not influence the light propagation in the conventional fibre. The normalised frequency (or fibre parameter [6 7])

$$V = \kappa\rho\sqrt{n_1^2 - n_2^2} = \frac{2\pi}{\lambda}\rho\sqrt{n_1^2 - n_2^2} = \frac{2\pi}{\lambda}\rho \cdot n_1\sqrt{2\Delta} \qquad (2.2.2.3)$$

where ρ is the core radius of the fibre, κ ($=\frac{2\pi}{\lambda}$, λ is the free-space wavelength used) is the free-space wave number. V is a very useful parameter for measuring the confinement ability of a fibre to wave modes (V=2.405 is the cutoff condition for first higher order LP_{11} modes in a circular step-profile fibre. The cutoff condition for the j^{th} higher modes is $U_j = V$ *or* $W_j = 0$ [8 9] where U and W will be explaned later). In the single-mode fibre, all the higher order modes are not guided and only the two orthogonally polarised fundamental HE_{11} (or LP_{01}) modes can propagate in the fibre. The core modal (fundamental HE_{11} mode) parameter

$$U = \rho\sqrt{\kappa^2 n_1^2 - \beta^2}$$

$$\approx 2.405\frac{V}{V+1}\left[1-\frac{2.405^2}{6(V+1)^3}-\frac{2.405^4}{20(V+1)^5}\right] \qquad (2.2.2.4)$$

$$(for \cdot 1.5 \le V \le 2.5)$$

the cladding modal parameter (bound mode)

$$W = \rho\sqrt{\beta^2 - k^2 n_2^2}$$

$$\approx 1.1428V - 0.996\,(for \cdot 1.5 \le V \le 2.5) \qquad (2.2.2.5)$$

where β is the propagation constant of the fundamental mode with $n_2\kappa < \beta < n_1\kappa$; The error in W made by using the approximation is smaller than 0.1% [10, 11]. W is also called the cladding decay parameter because W/ρ determines the decay rate of the field level in the cladding (the reciprocal of the W/ρ, ie, the quantity ρ/W, is a measure for the field extent in the cladding); A relation among β, U, W and V are:

$$\beta = \kappa \cdot n_1\sqrt{1-2\Delta\left(\frac{U^2}{V^2}\right)} \qquad (2.2.2.6)$$

$$V^2 = U^2 + W^2 \qquad (2.2.2.7)$$

and

$$U\frac{J_1(U)}{J_0(U)} = W\frac{K_1(W)}{K_0(W)} \qquad (2.2.2.8)$$

β can be approximated by $\beta \cong \kappa n_1 \cong k n_2$ in extremely weakly guiding fibre and hence the modes in extremely weakly guiding fibres can be treated as TEM (Transversal ElectroMegnetical wave). Eq.(2.2.2.7) and (2.2.2.8) is called the "sum rule" [12] and the "characteristic equation for the fundamental mode of a step-index fiber" [13] [14], Eq.(2.2.2.4) and (2.2.2.5) are actually the solutions of equations (2.2.2.7) and (2.2.2.8). The spot size of a single-mode fibre (or spot size of the fundamental mode) [15]

$$r_0 = \frac{\rho}{\sqrt{2}}\left[0.65 + \frac{1.619}{V^{3/2}} + \frac{2.879}{V^6}\right] \qquad (2.2.2.9)$$

Formula (2.2.2.9) is the most generally used formula for spot size calculation (it is called spot size related to launching w_G in [16]). Generally speaking, the spot size obtained from different definitions are quite similar [17].

In a glass fibre with a small refractive-index difference, one of the two fundamental HE_{11} modes have a transversal components of its electric field vector, eg, E_x, much larger compared to the other transversal component E_y and the longitudinal component E_z. Neglecting losses, the equation describing the instantaneous spatial distribution of the dominant component of the electric field in a fundamental mode propagating in the positive z-direction at time t is:

$$E_x(r,z,t) = \psi(r)\cos(\omega t - \beta z) \qquad (2.2.2.10)$$

where ω is the angular frequency and others is as indicated before; For arbitrary refractive-index profile in the core, the radial amplitude distribution $\psi(r)$ in the homogeneous cladding is

$$\psi(r) = \frac{K_0(Wr/\rho)}{K_0(W)} \qquad (2.2.2.11)$$

K_0 is the modified Hankel function of zero order. In the core, $\psi(r)$ depends on the particular refractive-index profile. From the refractive-index profile n(r), for a given operating wavelength λ, the $\psi(r)$ and propagation constant β of the fundamental fibre mode in the core can be obtained by solving the scalar wave equation [18]

$$\frac{\partial^2\psi(r)}{\partial r^2} + \frac{\partial\psi(r)}{r\partial r} + [n^2(r)\cdot k^2 - \beta^2]\cdot\psi(r) = 0 \qquad (2.2.2.12)$$

The analytical solution for equation (2.2.2.12) are available only for fibres with step-index [19] and parabolic-index profiles [20] [21]. The $\psi(r)$ in the core of the step-index fibre is

$$\psi(r) = \frac{J_0(Ur/\rho)}{J_0(U)} \qquad (2.2.2.13)$$

J_0 is the Bessel function of zero order. It can be summarised as

$$\psi(r) = \begin{cases} \dfrac{J_0(U\,r/\rho)}{J_0(U)} & r \le \rho \\ \dfrac{K_0(W\,r/\rho)}{K_0(W)} & r > \rho \end{cases} \qquad (2.2.2.14)$$

The $\psi(r)$ in both the core and cladding for the fundamental mode can be approximated by the Gaussian Approximation [22] as

$$\psi(r) = \psi_0 \cdot \exp\left[-\left(\frac{r}{r_0}\right)^2\right] \qquad (2.2.2.15)$$

where r_0 is the spot size of the fundamental mode which can be obtained from the formula (2.2.2.9) and ψ_0 is a constant amplitude determined by the power transmitted by the Gaussian field being equal to the power transmitted by the true mode.

For single-mode fibres with homogeneous cladding, the field in the cladding is more like an exponential function than a Gaussian function. Problems may arise in using the Gaussian Approximation when the decay rate W of the evanescent field in the cladding is of importance, eg, when analysing cross-talk between guides, or when designing directional couplers. In these cases, it is better to characterise the transverse field extent of the fundamental fibre mode by the field extent ρ/W in the cladding instead of by the spot size.

For weakly guiding fibres with a small relative refractive-index difference, the other two components of the electric field E_y and E_z are very small as compared to the dominant component, although they are not identical to zero.

The electric field distribution of a normal single-core single-mode fibre is shown in Figure 2.2.3 (calculated from the program shown in Appendix A).

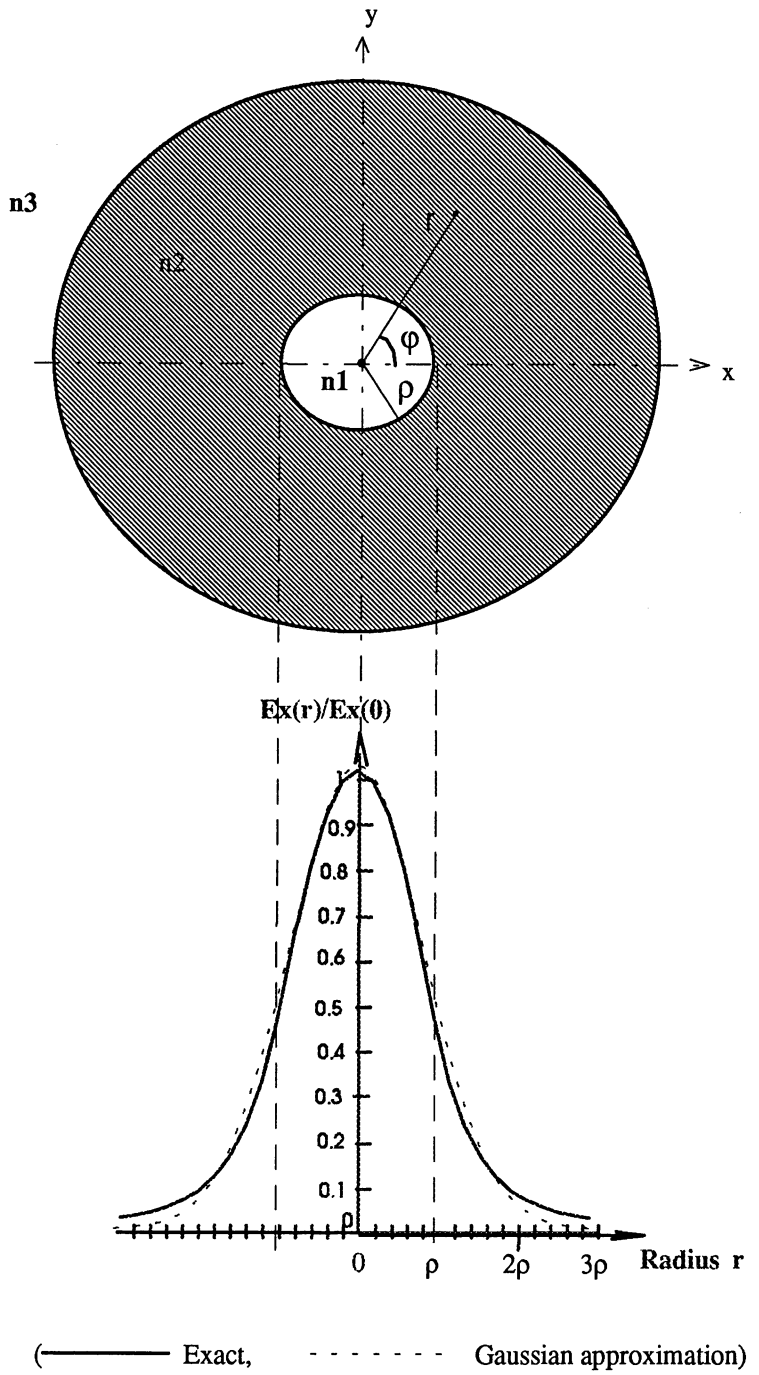

Figure 2.2.2.1. Electric field distribution of conventional single-core fibre

2.3 Twin-core Fibres

2.3.1 Principles

When the two cores of a twin-core single-mode fibre are very close and parallel to each other, the fundamental evanescent field of one core extends to the other core and excites a fundamental field in the second core. The excited field in turn interacts with the field of the first core. Consequently, there is a coupling (or exchange) of power between the two cores as the fields propagate. The power coupling between the two cores of a twin-core fibre is usually undesirable in data communication system since the transmission data may be corrupted or distorted. Nevertheless, it is very useful for applications in sensor systems. Twin-core single-mode fibres can be used for making optical devices such as attenuators, power splitters and combiners, directional couplers, switches, taps, wavelength filters, wavelength multiplexers and demultiplexers [23] [24], resonators, etc. Figure 2.3.1.1 shows a normal twin-core fibre (cores in the centre of the fibre) with common cladding and identical cores.

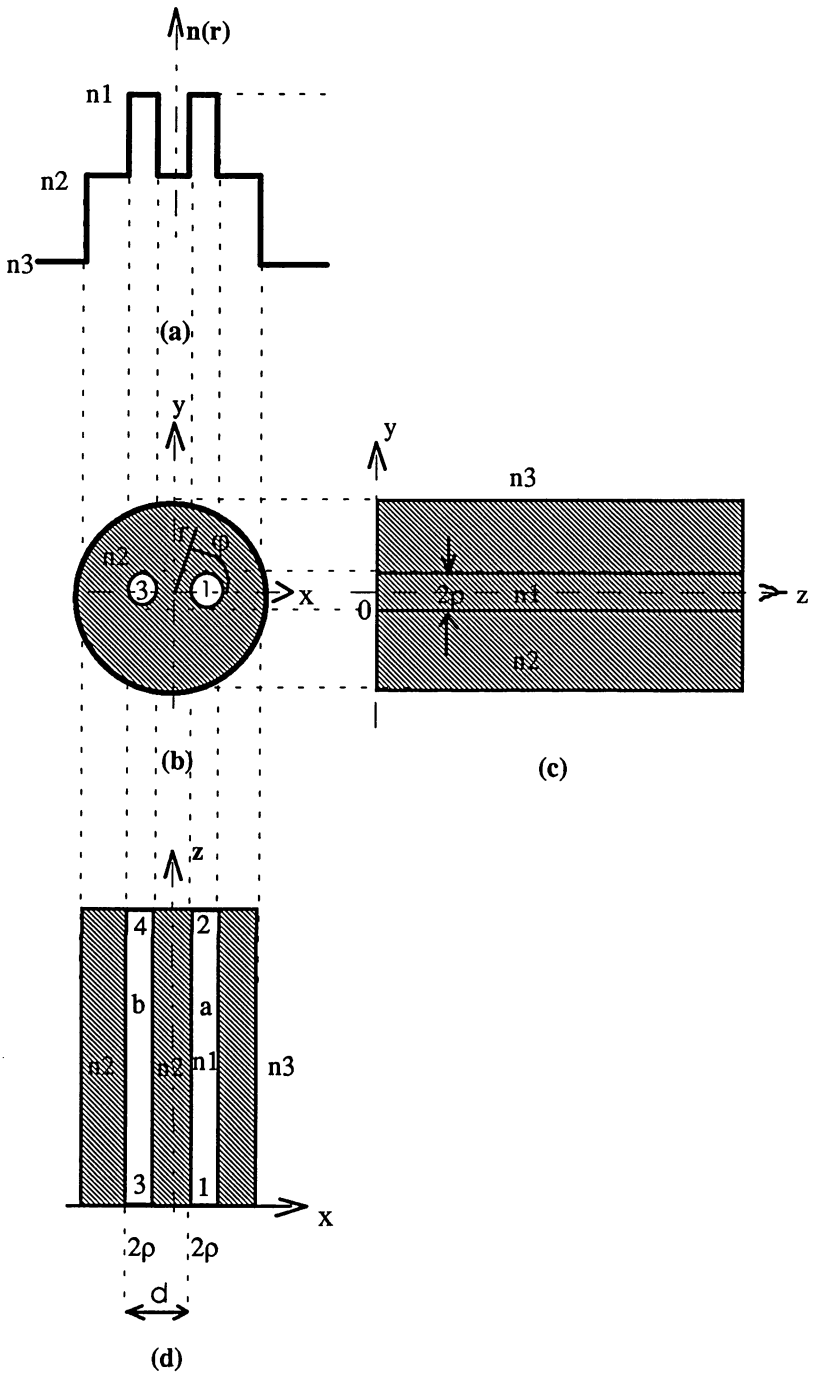

Figure 2.3.1.1 Conventional twin-core fibre

(a) Refractive index profile

(b), (c), (d), Cross-sectional view

2.3.2 Parameters and Characteristics

The fibre in figure 2.3.1.1 is symmetric about the y and x plane, where each core of the fibre (core a and b) has a step-index profile. In this thesis, only the twin-core fibre with step-index profile, symmetric about y-z plane, and homogeneous both in the core and cladding are considered. If a fibre is not exactly step-index profiled, we can find its equivalent step-index profile. Because each twin-core fibre used in our experiment is made by fusing two D-shaped single-core preform (which are cut from same single-core preform) together and then drawing, the two cores of our twin-core fibres is supposed to be nearly identical, we also suppose the cores and cladding are homogeneous.

Assumming that only x-polarised modes are involved, the fundamental electric field of the above structure (figure 2.3.1.1) is given everywhere by

$$E_x = b_+\psi_+ cos(\omega t - \beta_+ z) + b\_\psi\_ cos(\omega t - \beta\_ z) \qquad (2.3.2.1)$$

where b_+ and $b\_$ are modal amplitudes, ψ_+ and $\psi_$are the two fundamental solutions of the scalar wave equation satisfying

$$\psi_+ = \psi_a + \psi_b$$
$$\psi\_ = \psi_a - \psi_b \qquad (2.3.2.2)$$

where ψ_a and ψ_b are the fundamental solutions for core a and core b in isolation as indicated in Sec.2.2. β_+ and $\beta_$in Eq. (2.3.2.1) are the propagation constants associated with ψ_+ and $\psi\_$, they satisfying

$$\beta_+ = \beta + C$$
$$\beta_- = \beta - C \qquad (2.3.2.3)$$

where β is the propagation constant common to ψ_a and ψ_b (propagation constant of the fundamental mode of core a and core b in isolation as indicated in Sec.2.2), C is the coupling coefficient that will be explained later. For fibre with length z, the electric fields in core a and core b can be approximated by

$$E_a = 2b_+ \psi_a e^{i\beta z} \cos(Cz)$$
$$E_b = 2ib_+ \psi_b e^{i\beta z} \sin(Cz) \qquad (2.3.2.4)$$

The power flow $P_a(z)$ and $P_b(z)$ in each core is obtained by integrating the intensity $(n_1/2)(\varepsilon_0/\mu_0)^{1/2}|E_a|^2$ or $(n_1/2)(\varepsilon_0/\mu_0)^{1/2}|E_b|^2$ over the infinite cross-section. Assuming $P_a(0) = 1$ and $P_b(0) = 0$, we deduce that

$$P_a(z) = \cos^2(C \cdot z) \qquad (2.3.2.5.a)$$

$$P_b(z) = \sin^2(C \cdot z) \qquad (2.3.2.5.b)$$

From equation (2.3.2.5) we can see that the power coupling of two identical cores of a lossless twin-core fibre cause a complete periodic interchange of power. The total power is preserved

$$P_a(z) + P_b(z) = 1 \qquad (2.3.2.6)$$

Figure 2.3.2.1 illustrate the power splitting across the two cores of a twin-core fibre for the case of two identical cores; As we can see from Eq. (2.3.2.5), (2.3.2.6) and figure 2.3.2.1, after a length z, for which

$$C \cdot z = \frac{\pi}{2} \tag{2.3.2.7}$$

all the power is in the core b; when $C \cdot z = \pi$, all power is back to core a again; The period L_c of power exchange is then related to the coupling coefficient C by

$$L_c = \frac{\pi}{2C} = \frac{\pi}{\beta_+ - \beta_-} \tag{2.3.2.8}$$

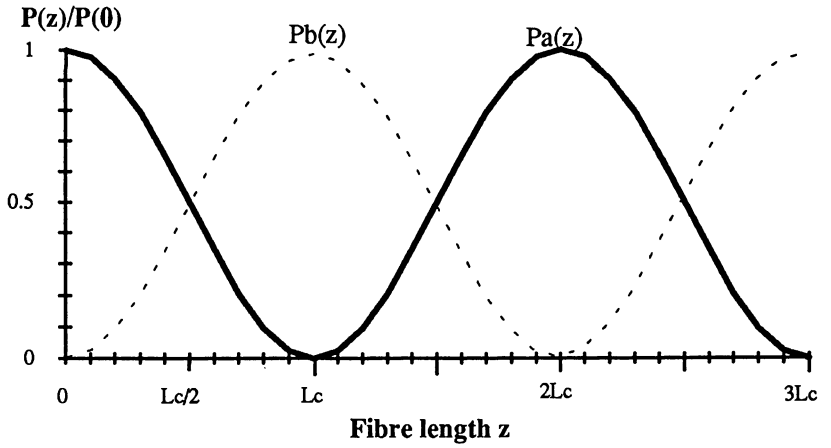

Figure 2.3.2.1 Power coupling between two identical cores along twin-core single-mode fibre

L_c is defined as the coupling length which is the distance along the fibre in which there is total transfer of power from one core to the other. L_c is one of the measures of the power coupling strength.

The strength of the coupling is determined by the degree of overlapping of the fields of the two cores, which is a function of the separation of the fibre cores d and the extent to which the field spreads into the cladding ρ/W (note that the power splitting rate is a function of the coupling strength and length of the coupling region). Figure 2.3.2.2 shows the fundamental field overlapping of the two cores of a twin-core fibre.

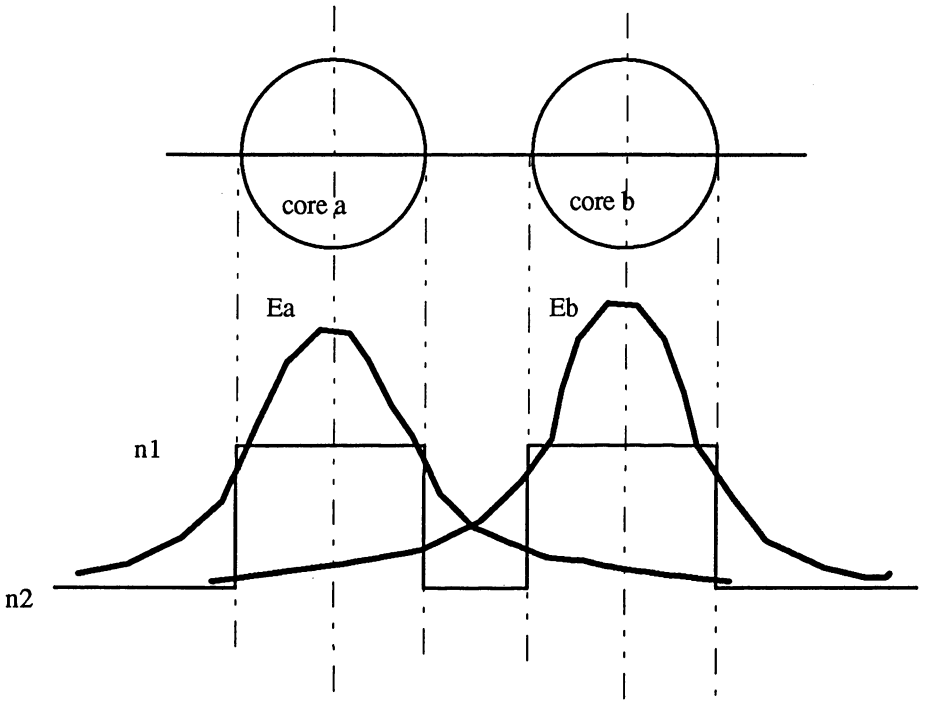

Figure 2.3.2.2 Electric fields overlap between two cores

The field coupling strength from one core to the other is more generally expressed by the coupling coefficient. For a twin-core fibre with identical cores that are both single-moded and have step refractive index profile, the coupling coefficient from one core to the other, and vice versa, can be calculated from a formula [25] [26] [27] [28] [29]:

$$C = C_{ab} = C_{ba}$$

$$= \kappa\left\{\int_{A_-} (n - n_a)\psi_a \psi_{+,-} dA\right\} \Big/ \int_{A_-} \psi_a \psi_{+,-} dA$$

$$\cong \frac{2\pi}{\lambda}\left\{\int_{A_-} (n - n_a)\psi_a \psi_b dA\right\} \Big/ \int_{A_-} \psi_a^2 dA$$

$$= \frac{(2\Delta)^{1/2}}{\rho} \frac{U^2}{V^3} \frac{K_0(W d/\rho)}{K_1^2(W)}$$

$$\cong \left\{\frac{\pi \cdot \Delta}{Wd\rho}\right\}^{1/2} \frac{U^2}{V^3} \frac{\exp(-W d/\rho)}{K_1^2(W)} \qquad (2.3.2.9)$$

where Δ, ρ, d, U, V, W are explained in section 2.2, K_0 and K_1 are modified Hankel functions of zero and first order respectively. The last approximate form of Eq. (2.3.2.9) is accurate enough when cores are well separated electromagnetically, ie. $Wd/\rho >> 1$. When V is very small, we have $U \cong V$ and $K_1(W) \cong 1/W$, C then becomes

$$C \cong \frac{(2\Delta)^{1/2}}{\rho} \frac{W^2}{V} K_0(W d/\rho) \qquad (2.3.2.10)$$

C is a real value [30] and is proportional to the third power of the wavelength [31] when the two cores (and also the cladding of cores) are identical and in single-mode operation:

$$C = k\lambda^3 \qquad (2.3.2.11)$$

We know that a mode is "cutoff" when $\beta_{+,-} = \kappa n_2$. Substituting this into equation (2.3.2.3), using equation (2.3.2.10) and the exact form of equation(2.2.2.6), (2.2.2.7), we find that the ψ_+ mode propagates for all values of V while the ψ_- mode is cutoff when $V = V_{co}$, where [32]

$$V_{co} \cong \left\{ \frac{8}{0.967+4\ln(d/\rho)} \right\}^{1/2} \qquad (2.3.2.12)$$

Section 2.2 shows that the upper bound of the V value for fundamental mode operation in a single-core fibre is 2.405, combining the lower bound for a twin-core fibre in Eq.(2.3.2.12), we obtained the V range for fundamental mode operation in a twin-core fibre

$$\left\{ \frac{8}{0.967+4\ln(d/\rho)} \right\}^{1/2} < V < 2.405 \qquad (2.3.2.13)$$

Figure 2.2.2.3 shows the relation between the coupling coefficient C and the wavelength λ, when core index is 1.464, cladding index is 1.460, core separation is 9μm and core raidus is 3μm (Appendix B is the Pascal program to plot the curve). It indicates that C increases as λ increases. Fig.2.3.2.4 shows the relation between normalised coupled power $P_4/(P_2+P_4)$ and wavelength λ. It indicates that the swap of power between two cores become more frequent as wavelength increases. Fig.2.3.2.5 shows the relation between the coupling coefficient C and the relative index difference Δ of different normalised separation d/ρ (Appendix C is the Pascal program to plot this curve). It indicates that the greater the Δ, the smaller the C. It also indicates that C decreases as d/ρ increases. Fig.2.3.2.6 is

the relation between C and normalised frequency V. It indecates that C decreases as V increases.

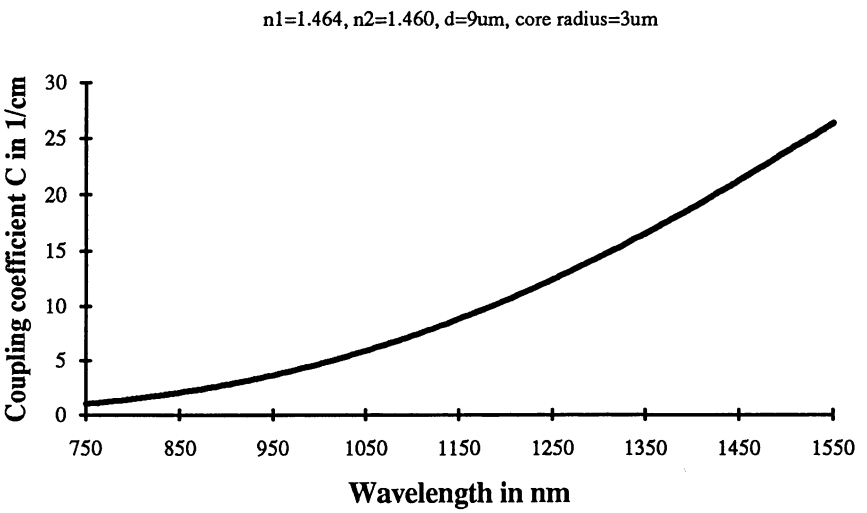

Figure 2.3.2.3 Coupling coefficient vs wavelength

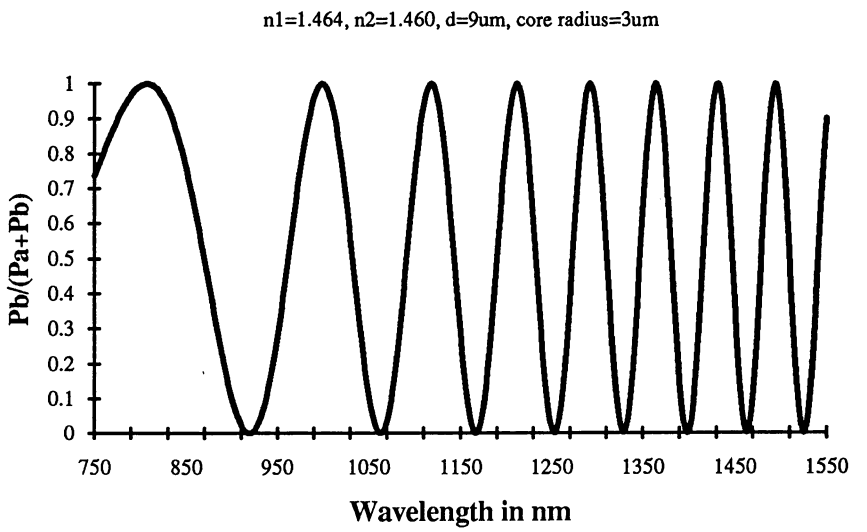

Figure 2.3.2.4 Power splitting ratio vs wavelength

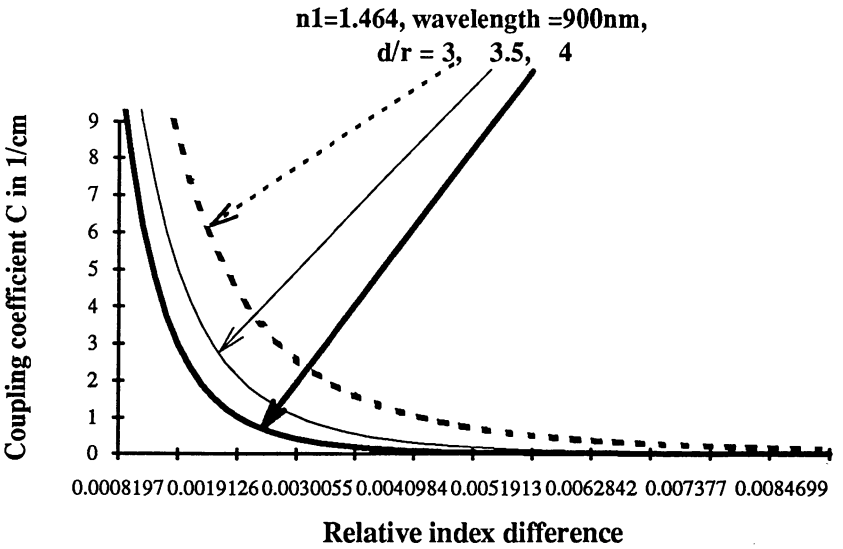

Figure 2.3.2.5 Coupling coefficient vs relative index difference

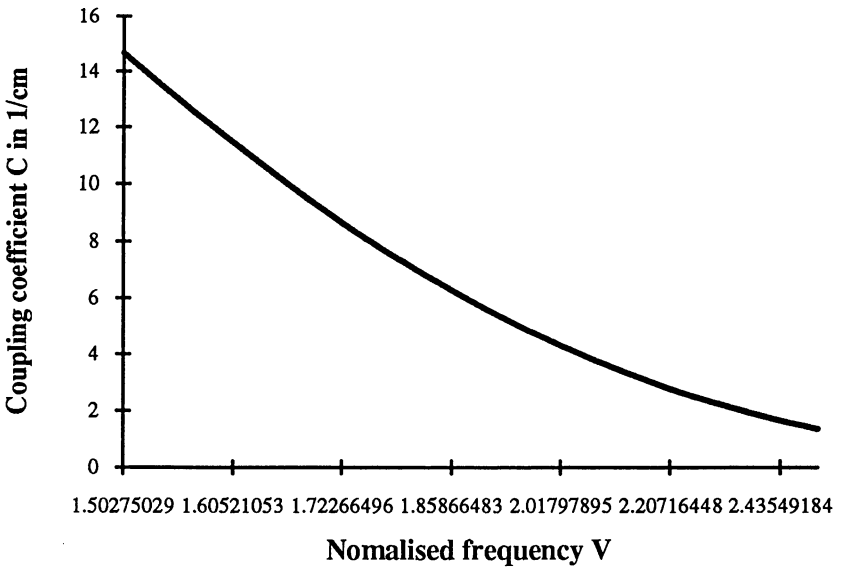

Figure 2.3.2.6 Coupling coefficient C vs normalised frequency V

Reference of Chapter 2

1 Gloge D., Weakly guiding fibers, Appl, Opt. 10, No. 10, 2252-2288, 1971.

2 Snyder A. W.: Asymptotic expressions for eigenfunctions and Eigenvalues of directric or optical waveguides, IEEE. Trans. Microwave Theory Tech. 17, 1130-8, 1969.

3 Jeunhomme L.B., Single-mode fiber optics principles and applications, Marcel Ddekker, inc., 1983, Chapter 1.

4 Snyder A. W., Love J. D.: Optical Waveguide Theory, Chapman and Hall, London, 1983, Chapter 11, Chapter 13-Chapter 15.

5 Neumann E. -G.: Single-mode fibers Fundamentals, Springer-Verlag, Berlin, 1988, Chapter 4 and Chapter 5

6 Snitzer E.: Cytindrical dielectric waveguide modes. J. Opt. Soc. Am. 51, 491-498, 1961.

7 Snyder A.W.: Asymptotic expressions for eigenfunctions and eigenvalues of a dielectric or optical waveguide. IEEE Trans. MTT-17, 1130-1138, 1969.

8 Okoshi T.: Optical Fibers, Academic Press, 1982, Chapter 4 and Chapter 5.

9 Snyder A. W., Love J. D.: Optical Waveguide Theory, Chapman and Hall, London, 1983, Chapter 11.

10 Rudolph H.-D., Neummann E.-G.: Approximations for the eigenvalues of the fundamental mode of a step-index glass fiber waveguide. Electron. Lett. 29, 328-329, 1976.

[11] Neumann E. -G.: Single-mode fibers Fundamentals, Springer-Verlag, Berlin, 1988, Chapter 5.

[12] Garrett I., Todd C.J.: Review: Components and systems for long-wavelength monomode fiber transmission. Opt. Quantum Electron. 14, 95-143, 1982.

[13] Snyder A.W.: Asymptotic expressions for eigenfunctions and eigenvalues of a dielectric or optical waveguide. IEEE Trans. MTT-17, 1130-1138, 1969.

[14] Gloge D.: Weakly guiding fibers. Appl. Opt. 10, 2252-2258, 1971

[15] Marcuse D.: Loss analysis ofsingle-mode fiber splices. Bell Syst. Tech. J. 56, 703-718, 1977

[16] Neumann E. -G.: Single-mode fibers Fundamentals, Springer-Verlag, Berlin, 1988, Chapter 10.

[17] Neumann E. -G.: Single-mode fibers Fundamentals, Springer-Verlag, Berlin, 1988, Chapter 10.

[18] Snyder A.W., Love J.D.: Optical Waveguide theory, Chapman and Hall, London, 1983, Chapter 11.

[19] Snyder A.W.: Asymptotic expressions for eigenfunctions and eigenvalues of a dielectric or optical waveguide. IEEE Trans. MTT-17, 1130-1138, 1969.

[20] Streifer W., Kurtz C.N.: Scalar analysis of radially inhomogeneous guiding media. J. Opt. Soc. Am. 57, 779-786, 1967

[21] Meunier J.P., Pigeon J., Massot J.N.: Perturbation theory for the evaluation of the mormalized cutoff frequencies in radially inhomogeneous fibers. Electron Lttt. 16, 27-29, 1980.

[22] Marcuse D.: Gaussian approximation of the fundamental modes of graded-index fibers. J. Opt. Soc. Am. 68, 103-109, 1978.

[23] Digonnet M.J.F., Shaw H.J.: Single-mode fiber-optic wavelength multiplexer. Conf. Opt. Fiber Commun. (OFC'82), 36-37, 1982.

[24] Digonnet M.J.F., Shaw H.J.: Wavelength multiplexing in single-mode optical fiber coupler. IEEE Trans. MTT J. QE-18, 746-752, 9183.

[25] Snyder A.W., Love J.D.: Optical waveguide theory, Chapman and Hall, London, 1983, Chapter 18.

[26] Hardy A., Strafer W.: Coupled mode theory of parallel waveguides. JJ. Lightwave Tech. LT-3, 1135-1146, 1985.

[27] Bracey M.F., Cullen A.L., Gillespie E.F.F., Staniforth J.A.: Surface-wave research in Sheffield. IRE Trans. AP-7, S219-S225, 1959.

[28] Marcuse D.: The coupling of degenerate modes in two parallel dielectric waveguides. Bell Syst. Tech. J. 50, 1791-1816.

[29] Chu P.L.: Leture notes of "Optical Communication", 1989.

[30] Miller S.E.: Coupled wave theory and waveguide applications. Bell Syst. Tech. J. 33, 661-719, 1954.

---

[31] Digonnet M.J.F., Shaw H.J.: Analysis of a tunable single-mode optical fiber coupler. IEEE Trans. MTT-30, 592-600, and IEEE J. QE-18, 746-752, 1982.

[32] Snyder A.W., Ruhl F.F.: Radiation losses from couplers. IEEE J.Lightwave Tech, Vol. LT-3, No.1, 1985.

Chapter 3

Twin-core Offset Fibres

3.1 Introduction to Chapter 3

This chapter proposes a new type of fibres, the Twin-core Offset Fibres (TOF) as shown in Fig.3.1.1. The TOF is based on the idea of twin-core D fibres. However, a long of twin-core D fibre with exactly specified parameters cannot be realised using the existing fibre fabrication technology. In the preform drawing technique, the drawn fibre has a varying cross-section due to the asymmetry of the D-shape, and its D shape can not be maintained. In the fibre polishing technique, only a very short section (a few centimetres) of twin-core D fibre can be made, which can not satisfy the requirement for batch production of standard products. Comparing with the twin-core D fibre, long TOF (tens to hundred of meters) with uniform and controlled size parameters are easy to be fabricated.

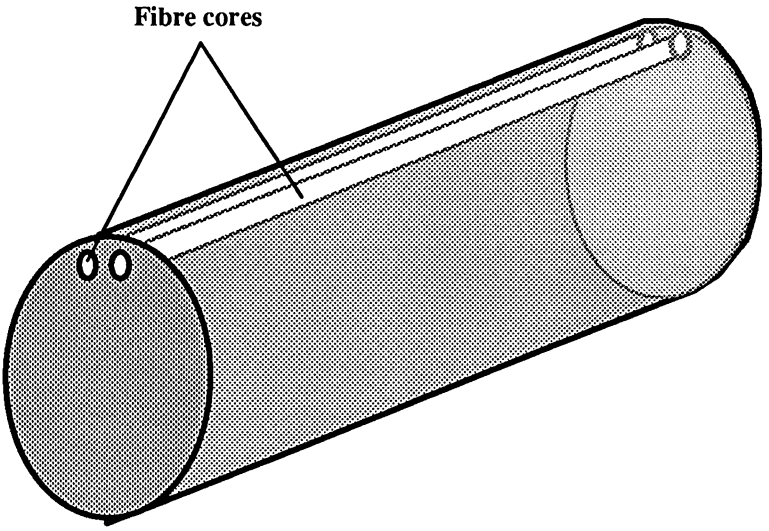

Figure 3.1.1 A section of twin-core offset fibre (TOF)

There is no ready formula for calculating the parameters and field distributions in the core or cores offset fibre, to the best of my knowledge. Although the method of working out an equivalent concentric structure using conformal transformation is thought to be feasible [1]. The assumption of infinite cladding used in the classical derivation of conventional fibre, however, is no longer valid, making the mathematics very complicated and tedious. In addition, the conformal transformation is usually not used in the time-varying situation and we are not sure if it is applicable to our case. We believe a deeper and more complete theoretical analysis of the topic exceeds the requirement of this thesis. This thesis is concerned with a qualitative rather than quantitative analysis of core offset fibres.

We first analyse the single-core offset fibres in Sec.3.2, which provides an easy path to the analysis of the twin-core offset fibres. The twin-core offset fibres are then analysed in Sec.3.3.

3.2 Analysis of Single-core Offset Fibres

3.2.1 Principles

A single-core offset fibre is shown in figure 3.2.1.1. We assume that an equivalent step-index profile exists for this fibre based on the reasons explained on Sec.2.1. The composite effective refractive index $n_{2\text{eff}}$ of the cladding near the core is a combined effect of the cladding index n_2, the refractive index of the surrounding medium (eg, air, liquid, or coating) n_3, and the nearest distance of the core to the fibre surface S. The exact calculation of $n_{2\text{eff}}$ is not known but it lies between n_2 and n_3. When the normalised core-surface distance $S_n = S/\rho$ is large enough, $n_{2\text{eff}} \approx n_2$. The smaller is S_n, the more contribution of n_3 is to the $n_{2\text{eff}}$. When the core almost touches the fibre surface, $n_{2\text{eff}}$ would have a value close to $(1-k)n_2 + kn_3$ (where k is unknown at this stage but thought to be about 0.4).

In next section, we will qualitatively discuss the parameter modifications of a conventional single-core fibre due to the core offsetting.

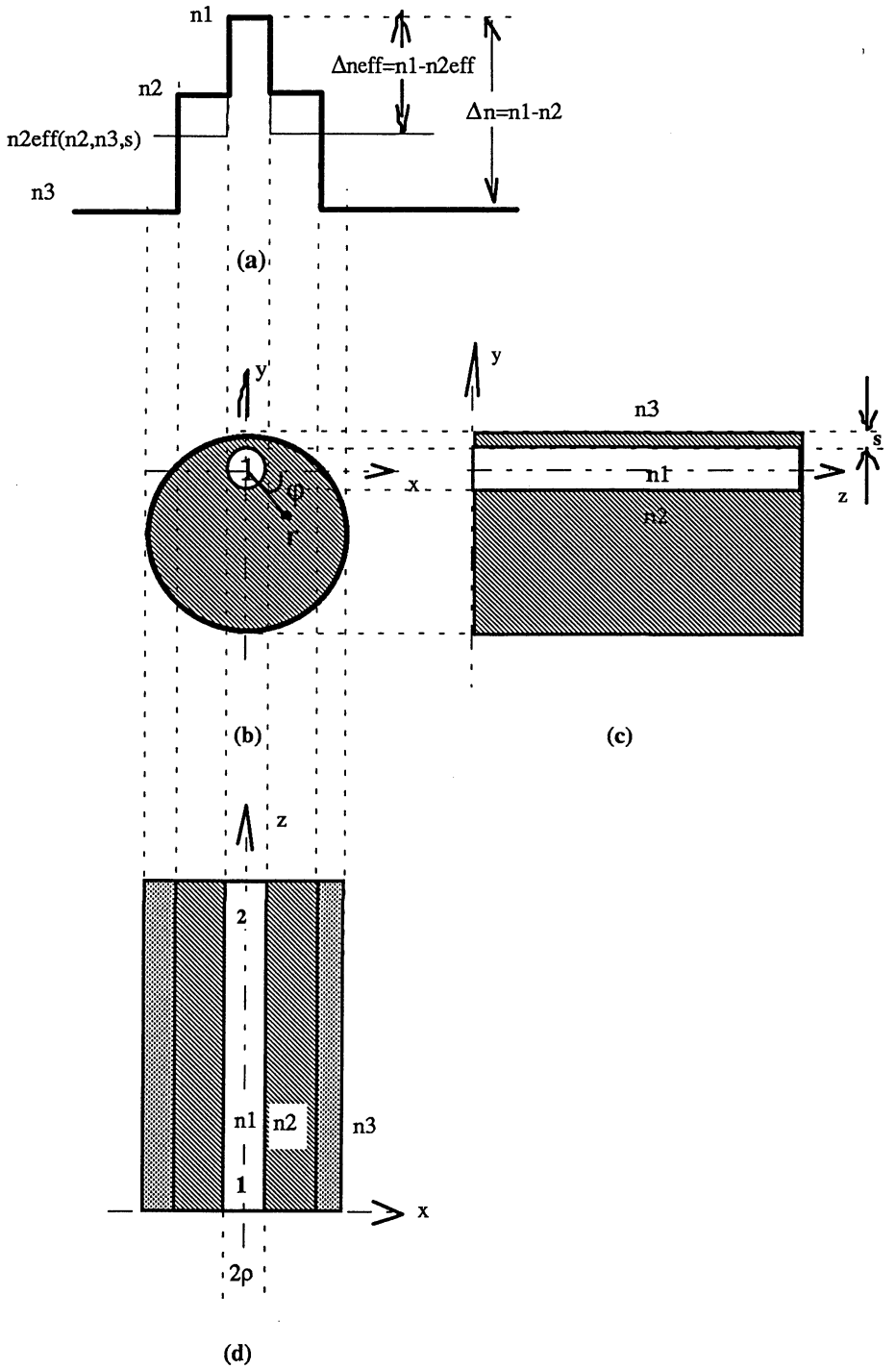

Figure 3.2.1.1 Single-core Offset fibre
(a) Refractive index profile
(b)-(d) Cross-sectional view

3.2.2 Parameters and Characteristics

Replacing n_2 by $n_{2\text{eff}}$ in some of the equations in Sec.2.2.2, we obtain the following modified parameters: the effective index difference

$$\Delta n_{eff} = n_1 - n_{2eff} \tag{3.2.2.1}$$

or effective relative index difference

$$\Delta_{eff} = \frac{n_1^2 - n_{2eff}^2}{2n_1^2}$$

$$\approx \frac{n_1 - n_{2eff}}{n_1} \tag{3.2.2.2}$$

$$(for\ weakly\ guiding, ie, \Delta n_{eff} < 0.01)$$

the normalised frequency

$$V = \frac{2\pi}{\lambda}\rho\sqrt{n_1^2 - n_{2eff}{}^2}$$

$$= \frac{2\pi}{\lambda}\rho n_1\sqrt{2\Delta_{eff}} \tag{3.2.2.3}$$

the core modal parameter

$$U = \rho\sqrt{k^2 n_1^2 - \beta^2}$$

$$\approx 2.405\frac{V}{V+1}\left[1 - \frac{2.405^2}{6(V+1)^3} - \frac{2.405^4}{20(V+1)^5}\right] \tag{3.2.2.4}$$

$$(for\ 1.5 \le V \le 2.5)$$

the cladding modal parameter (bound mode)

$$W = \rho\sqrt{\beta^2 - k^2 n_{2eff}^{\ 2}}$$

$$\approx 1.1428V - 0.996 \left(for \cdot 1.5 \le V \le 2.5\right) \qquad (3.2.2.5)$$

where propagation constant β is in the range $\kappa n_{2eff} < \beta < \kappa n_1$, the normalised spot size

$$r_0 = \frac{1}{\sqrt{2}}\left[0.65 + \frac{1.619}{V^{3/2}} + \frac{2.879}{V^6}\right] \qquad (3.2.2.6)$$

we find that the formulas for Δn, Δ, U, W, V and r_0 in Sec.2.2 are modified due to the core offsetting.

Because the value of n_{2eff} depends on n_3, it can be seen from equation (3.2.2.3) and equation (3.2.2.5) that the V and W values can be varied by varying n_3, although the exact V and W values cannot be calculated, we can at least deduce that: (1) if $n_3 \le n_2$, n_{2eff} varies between n_2 and n_3, increasing n_3 would reduce Δ_{eff} and hence V and W, and would also increase the field spreading, while reducing n_3 would strengthen the fibre's ability to confine field within the core. (2) if $n_2 < n_3 < n_1$, there will be same result as in case 1, but the power loss in this case would be greater due to the closeness of n_2/n_3 interface to the core (field loss in the interface according to the Fresnel's law); (3) If $n_3 \ge n_1$, the result should be the same as in case 1 and case 2 theoretically. However, the loss will become extremely great. In the case of the core almost touching the fibre surface ($S \approx 0$), the power is totally lost.

From Sec.2.2.2, we know that V is a measure of field confinement ability and ρ/W is a measure of field extent in the cladding. By varying n_3, the field extent in the

cladding can be controlled. Figure 3.2.2.1 shows the effects of different n_3 on field distribution.

Taking an example of a core offset fibre with core radius of 1.9μm, n_1 of 1.462, n_{2eff} varies from 1.452~1.459, in the operation wavelength of 1000nm, V value varies from 2.03 to 1.1.

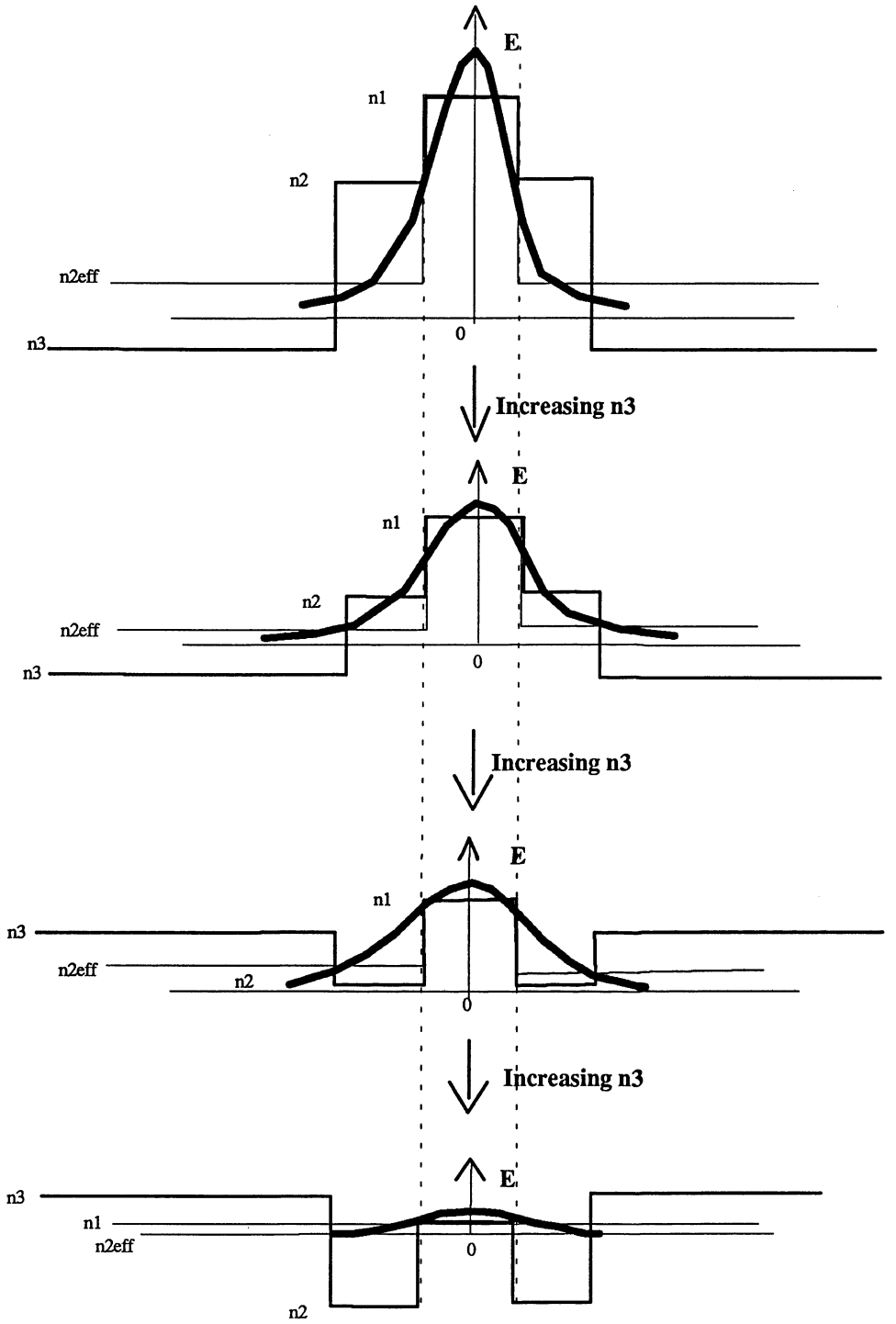

Figure 3.2.2.1 The effect of surrounding medium index n3 on the field distribution E(r)

3.3 Analysis of Twin-core Offset Fibres

3.3.1 Principles

As we mentioned in Sec.2.3, when the two cores of a single-mode fibre are parallel to one another and when the distance between the core axes is reduced until the evanescent fields of the two cores overlap, the fundamental field of one core will interact with the field from the other and power is coupled between the two. The degree of the power coupling depends on the overlap of fields from the two cores. In Sec.3.2, we indicated that by varying the index of the surrounding medium n_3, the degree of the spread of the fundamental fields from the core in a core offset fibre can be varied. For a twin-core offset fibre shown in Fig.3.3.1.1, it is apparent that by changing n_3, the degree of the fundamental field overlapping of the two cores can be changed and the power (or field) coupling is therefore changed. Figure.3.3.1.2 shows the degree of field overlap dependence on n_3.

Three cases of field distribution and coupling of different n_3 are analysed as below: (1) $n_3 \leq n_2$; In this case, n_{2eff} can be varied from a value greater than n_3 to n_2 by varying n_3, with the actual value being determined by n_2, n_3 and S. As n_3 increases, the field overlap increases and hence the power coupling increases. (2) $n_2<n_3<n_1$; In this case, n_{2eff} can be varied from n_2 to a value smaller than n_3 by varying n_3. The power coupling between the cores becomes stronger than case one; however, the loss increases due to the closeness of n_2/n_3 interface to the cores (according to Fresnel's law). (3) $n_3 \geq n_1$; In this case, S become a critical factor. If S is not very small, n_{2eff} can be varied from n_2 to a value smaller than n_1 by varying n_3, and the power in the cores are not zero and power coupling still

exists. If S is very small (cores touch the fibre surface), the power is totally lost and no power coupling can be detected.

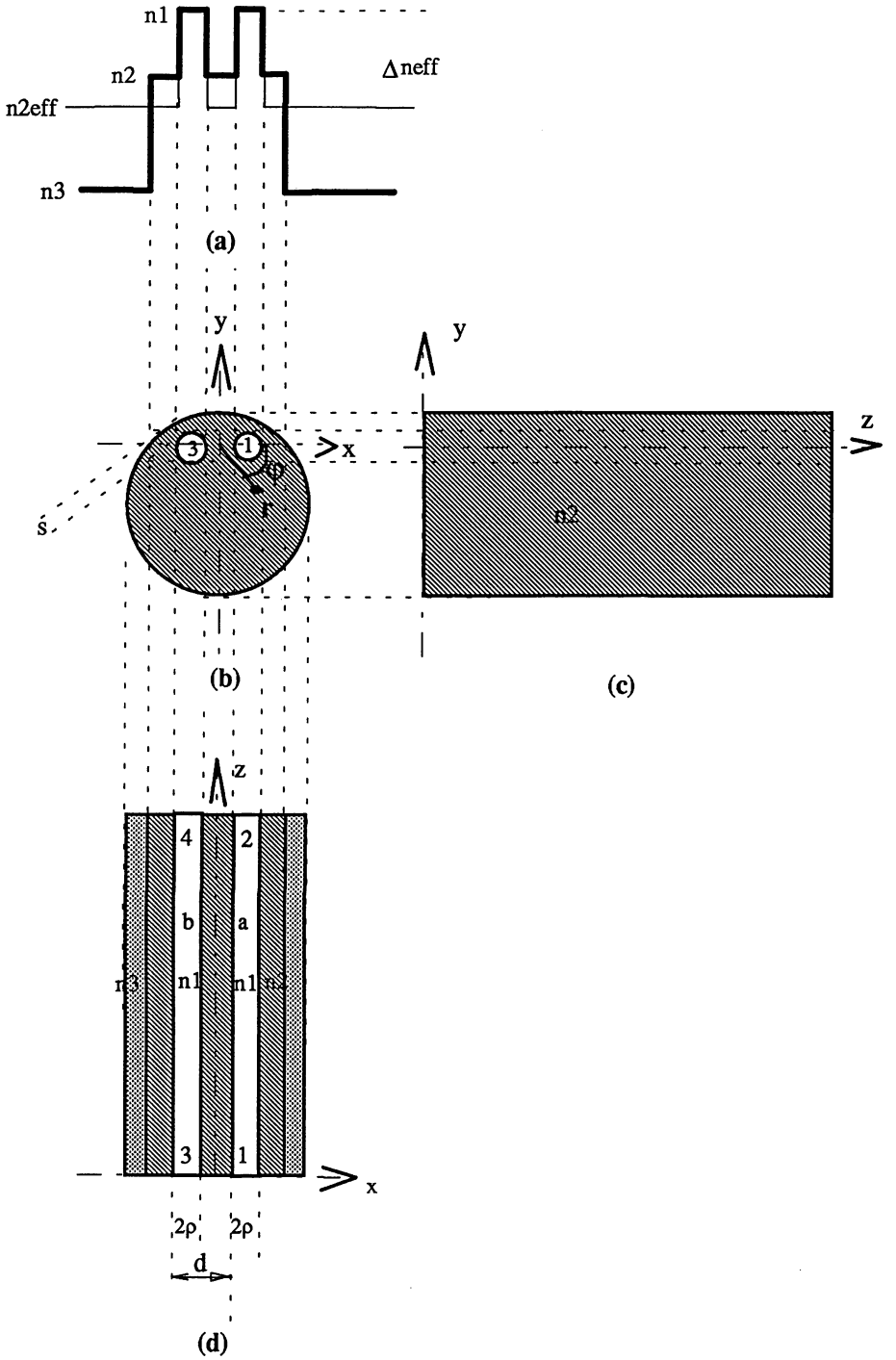

Figure 3.3.1.1 Twin-core offset fibre

(a)Refractive index profile

(b)-(d) Cross-sectional view

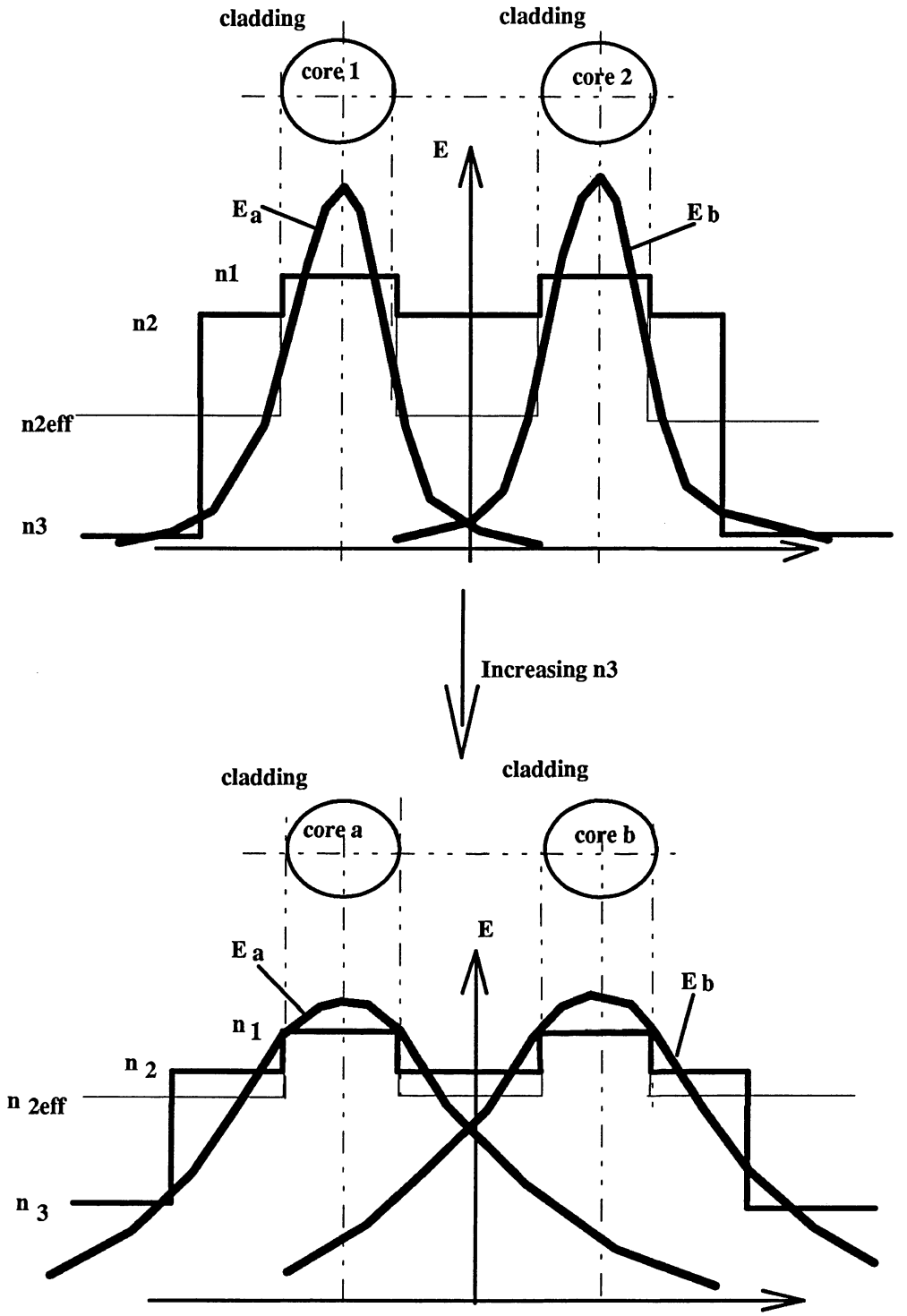

Figure 3.3.1.2 The effect of surrounding medium index n3 on the electric fields overlapping between two cores

3.3.2 Parameters and Characteristics

The dependence of the coupling strength on the refractive index of the surrounding material of a twin-core offset fibre can also be seen analytically. In Equations (3.2.2.2), (3.2.2.3) and (3.2.2.5), the values of Δ, V and W (which are the parameters of an equivalent step-index profile of a fibre of arbitrary profile) are function of n_3. Substituting these modified parameters into Eq.(2.3.2.9), we obtain a modified formula for the coupling coefficient

$$C = C_{ab} = C_{ba} \approx \left\{ \frac{\pi \cdot \Delta_{eff}}{Wd\rho} \right\}^{1/2} \frac{U^2}{V^3} \frac{\exp(-W\, d/\rho)}{K_1^2(W)} \qquad (3.3.2.1)$$

Consequently, the following parameters are also functions of n_3: The coupling length

$$L_c = \frac{\pi}{2C} \qquad (3.3.2.2)$$

and the normalised power of each core at z from the launching end

$$P_a(z) = \cos^2(C\, z) \qquad (3.3.2.3)$$

$$P_b(z) = \sin^2(C\, z) \qquad (3.3.2.4)$$

The above relations again look like those formulas used in Sec.2.3.2 for the convectional twin-core fibre except that they are determined by the effective cladding index n_{2eff}, which is a function of the cladding index n_2, the refractive index of the surrounding medium n_3, and the nearest normalised distance of the core to the fibre surface $S_n = S/\rho$, rather than just the cladding index n_2.

We should also pay attention to the modification of the V value for single-mode (fundamental modes) operation due to the cores offset. In Sec.2.3.2, we found that when $\{8/[0.967+4\ln(d/\rho)]\}^{1/2}$<V<2.405, the conventional twin-core fibre is in fundamental mode operation. In a twin-core offset fibre, the V value depends on n_3, we hence have

$$\left\{\frac{8}{0.967+4\ln(d/\rho)}\right\}^{1/2} < V = \frac{2\pi}{\lambda}\rho\sqrt{n_1^2 - n_{2eff}^{\ 2}} < 2.405 \quad (3.3.2.5)$$

Fig.3.3.2.1 shows the coupling coefficient versus wavelength for different surrounding medium with different refractive indices (the Pascal program for calculating C vs λ curves is shown in Appendix A). It indicates that C is greater for greater n_3 (when n_3<n_1). Fig.3.3.2.2 shows the normalised power in the coupled core versus the wavelength for different surrounding medium with different refractive indices at fixed propagated length z from launching end. We can see that for greater n_3 (smaller n_{2eff}) and hence greater C, the period of a power cycle become smaller. It is apparent that the phenomenon shown in Fig.3.3.2.2 represents the swapping of power in the two cores of a fixed length TOF and it becomes more frequent if n_3 is greater.

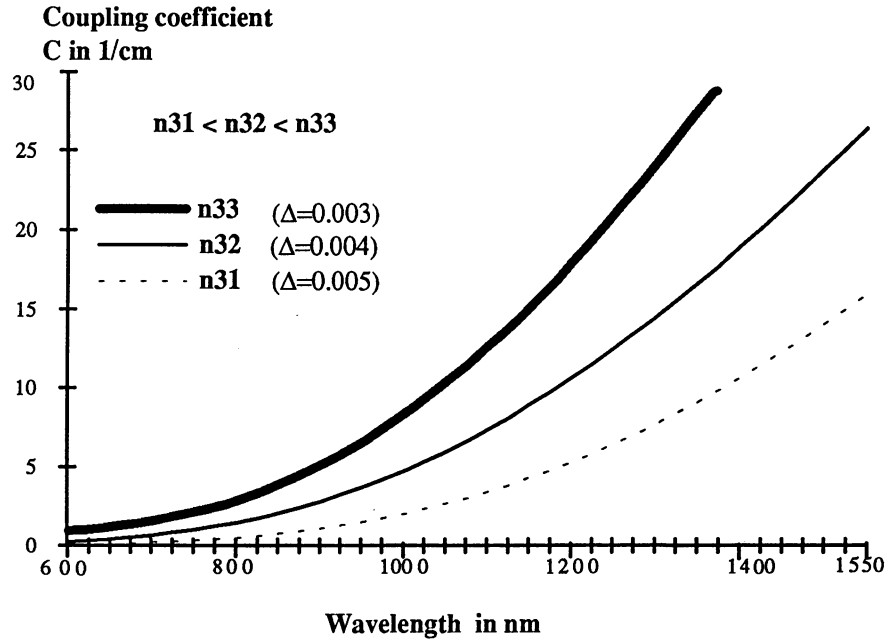

Figure 3.3.2.1 Coupling coefficient vs wavelength for different surrounging medium of different refractive index

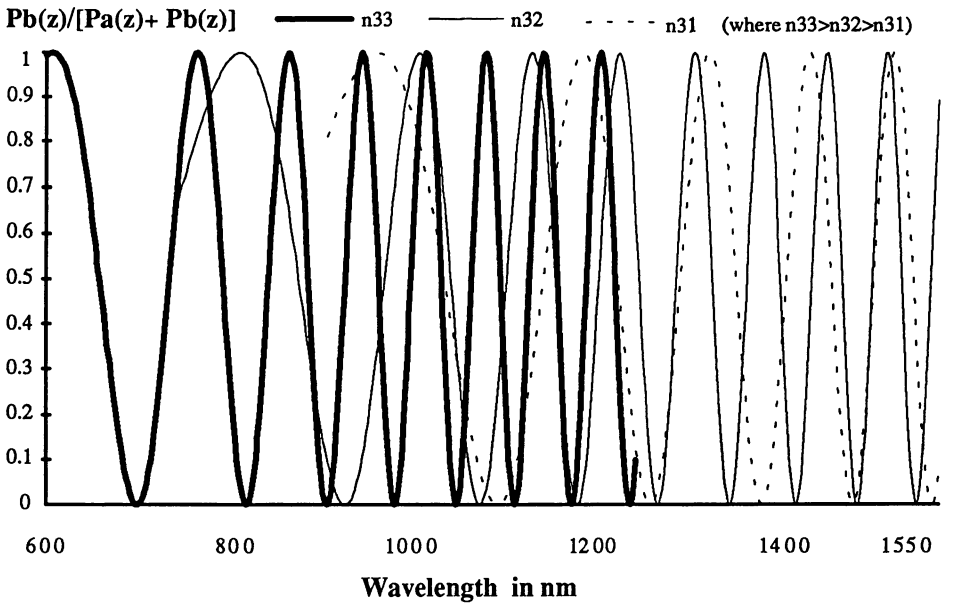

Figure 3.3.2.2 Normalized power at coupled core output vs wavelength for different surrounding medium of index n3

Reference of Chapter 3:

[1] Tsao C.Y.H., Payne D.N., Li L.: Modal propagation characteristics of radially stratified and D-shaped metallic optical fibers, Appl. Opt, Vol.28, No.3, 588--594, 1989.

Chapter 4

Process Design for Fabricating Twin-core Offset Fibres

4.1 Introduction to Chapter 4

In this chapter, we develop a systematic process of fabricating twin-core offset fibres and we call this the Step Controlled Process (SCP). The SCP process is based on the previous Cladding Removal Process (CRP) [1, 2] used for fabricating conventional twin-core fibres and twin-core D fibres. Compared with the CRP, SCP process provides an accurate and step by step controlled method of fabrication not only for twin-core offset fibres (TOF), but also for other type of twin-core fibres.

There are five steps in fabricating TOFs using SCP method. We will briefly describe the five steps in this section and details of the steps are presented in other sections of this chapter. The formulas for determining the indices and size parameters in each step are provided.

The five steps of fabricating TOFs using SCP method are (Ref to Fig.4.1.1):

Step 1: Fabricating a single-core preform. This preform **must** satisfy certain refractive index requirements as indicated in Sec.4.6. There are size requirement set out in Sec.4.6. for this step. We can choose to either modify the preform to satisfy the size requirement in this step, or to do the modification later in step 3. The size parameters of a single-core preform can be modified by stretching or sleeving it several times.

Step 2: Two pieces of equal length samples are cut from the single-core preform obtained in step 1. Equal parts of the cladding are then removed from each piece by cutting and polishing to produce two D-shaped single-core preform. The size parameters of the two D preform must satisfying the requirement shown in Sec.4.5.

Step 3: The two D-shaped single-core preform are then fused together at high temperature to form a normal twin-core preform. In this step, the size parameters must satisfy the requirement set out in Sec.4.4, otherwise, many problems will arise (eg, core twisting due to uneven stress). Stretch and sleeve method are used to modify the size parameters in this step.

Step 4: Part of the cladding are removed from the twin-core preform to form a twin-core offset preform. The size parameters must satisfy the requirement set in Sec.4.3 (If not, we can even go back to step 3 then step 4 again, although it is not desirable).

Step 5: A twin-core offset fibre is drawn from the twin-core offset preform with the indices and size parameters satisfying the requirement set out in Sec.4.2.

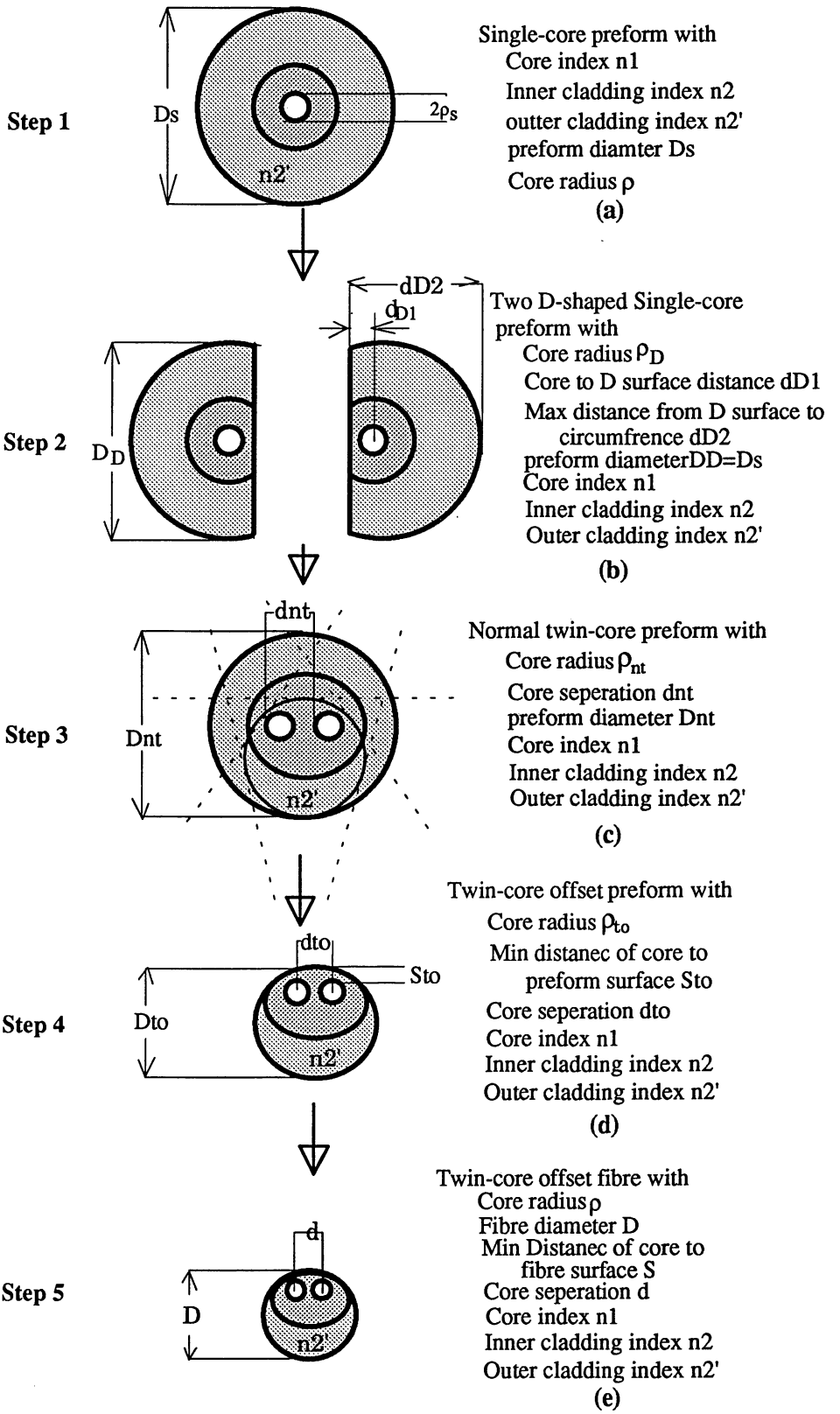

Figure 4.1.1 Twin-core offset fibre fabrication process

4.2 Design consideration of twin-core offset fibres

Before fabricating twin-core offset fibre, its parameters and variables must be determined first. These parameters include the fibre diameter D, core radius ρ, core separation d, minimum distance of core to fibre surface S, refractive index of the core n_1, refractive index of the cladding n_2, normalised frequency of each guide V, coupling coefficient C, etc. A cross-sectional view of the twin-core offset fibre is again shown in Fig.4.2.1. The refractive index of the inner cladding n_2 should be a little bit lower than the outer cladding index n_2'. This fibre structure is called the depressed cladding structure (in single-core fibre, it is called W fibre). The use of depressed cladding structure has two advantages: firstly, this structure provides a negative waveguide dispersion that cancels the positive material dispersion when operating wavelength less than 1200 nm; secondly, the outer cladding with higher refractive index can strip of most unwanted cladding modes in the inner cladding. If the thickness of the inner cladding is large enough, the effect of the outer cladding on the fibre's parameters (eg, V and Δ) can be ignored for calculation simplicity.

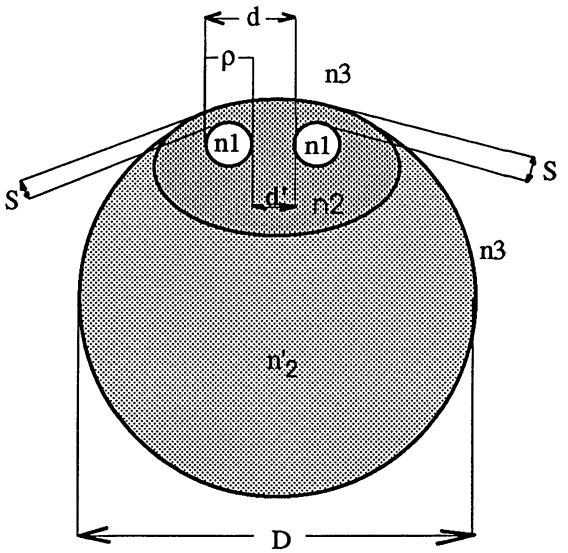

Figure 4.2.1 Cross-sectional view of twin-core offset fibre

4.2.1 Coupling coefficient, cores edge separation and relative index difference

In Sec.2.2.2, we indicated that the coupling coefficient C depends on the degree of field overlapping from two cores, and hence smaller cores edge separation d' (d'=d-2ρ) and relative index difference Δ leads to greater C.

We normally expect our twin-core fibres for making couplers or switches to have a greater coupling coefficient so that the size of the device can be smaller. However, if the coupling coefficient is too great, the splitting ratio of a coupler becomes so sensitive to the length of the fibre that it is difficult to cut to the exact required length.

Another limitation of large C is that the core separation d cannot be so small that the two cores are touching (ie, cores edge separation d'=0 or normalised core separation $d_n = d/\rho = 2$), otherwise, we can neither splice the cores of a twin-core fibre to the cores of an individual single-core fibre, nor can we launch light separately to the individual core of a twin-core fibre. A practical d' should be in the range of 3~9μm. For a fixed C value, smaller Δ needs a greater d' to compensate. We choose d'=6μm.

On the other hand, the relative index difference can be made to be very small. We prefer a smaller Δ (Δ_{eff} in core offset fibres) for two reasons. Firstly, to maintain a single-moded operation at the same wavelength range, smaller Δ_{eff} allows a greater core radius ρ, which leads to an easier splicing and connection of cores of a twin-core offset fibre to single-core fibre and reduces the losses caused by transverse misalignment. Secondly, the higher index of the core and lower index of the depressing cladding is produced by doping the glass tube with a combination of chemical materials when using the MCVD method to make preform. Since the scattering losses increase with the doping level, high doping levels should usually be avoided. Although smaller Δ_{eff} would decrease the light confinement ability and increase the bending and micro-bending losses, the twin-core offset fibre we used in making optical devices is usually relatively straight and short and hence bending and micro-bending loss is not significant. Of course, to obtain a greater varying range of coupling strength for a TOF, a greater Δ_{eff} varying range is required. However, to maintain the fibre still weakly guiding, Δ_{eff} (where $\Delta n_{eff} \cong n_1 \Delta_{eff}$) should be in the range

$$0.001 \le \Delta n_{eff} = n_1 - n_{2eff} \le 0.01 \qquad (4.2.1.1)$$

or

$$\Delta n_{effi} = n_1 - n_{2effx} = n_1 - n_2 = 0.001 \qquad (4.2.1.2.a)$$

$$\Delta n_{effx} = n_1 - n_{2effi} = 0.01 \qquad (4.2.1.2.b)$$

where n_{2effi}, n_{2effx} ($n_{2effx} = n_2$) is the minimum and maximum of n_{2eff}, Δn_{effi} and Δn_{effx} is the minimum and maximum of Δn_{eff}.

The first step of SCP process is to make a single-core preform satisfying appropriate index requirement. We employ the Modified Chemical Vapour Deposition (MCVD) method to make the single-core preform. The quartz glass tube used in MCVD (details will be described in Sec.5.2 for single-core preform fabrication) method usually have a refractive index of 1.460 (n_2'). We have to choose the core and cladding indices (n_1 and n_2) a little higher and lower respectively than the index of the glass tube. We believe that 1.4605 for n_1 and 1.4595 for n_2 would be a good choice because that would make n_{2eff} to have the greatest varying range from 1.4505 to 1.4595, according to Eq.(4.2.1.2). However, for minimum radiation loss, and for optimum visibility of power versus wavelength curve when n_3 equals n_2, which is very useful in later experimentation, we choose 1.464 for n_1 and 1.459 for n_2 to lower the C value when n_3 equals n_2. As we indicated in Sec.3.2.2 and from Eq.(4.2.1.2), we can obtain a minimum n_{2eff} as low as $n_{2effi} = n_1 - \Delta n_{effx}$=1.464-0.01=1.454 and a maximum n_{2eff} as high as $n_{2effx} = n_2 = 1.459$ by varying n_3. Thus we have the maximum and minimum relative index difference $\Delta_{effx} \cong \frac{1.464 - 1.454}{1.463}$=0.00683 and $\Delta_{effi} = \frac{n_1 - n_2}{n_1}$=0.00342.

4.2.2 Normalised frequency V

In Sec.3.2.2 of chapter 3, we indicated that for maintaining the twin-core offset fibre in fundamental mode operation, the V value should be in the range of

$$\left\{\frac{8}{0.967+4\ln(d/\rho)}\right\}^{1/2} < V = \frac{2\pi}{\lambda}\rho\sqrt{n_1^2 - n_{2eff}{}^2} < 2.405 \quad (4.2.2.1)$$

when the cores of the twin-core fibre are electromagnetically well separated. To satisfy Eq.(4.2.2.1), in reference to Sec.3.2 of chapter 3, and in the operating wavelength range $\lambda_{min} < \lambda < \lambda_{max}$, the condition below must be satisfied:

$$V_{max} = \frac{2\pi}{\lambda_{min}}\rho\sqrt{n_1^2 - n_{2effi}^2} < 2.405 \quad (4.2.2.2.a)$$

$$V_{min} = \frac{2\pi}{\lambda_{max}}\rho\sqrt{n_1^2 - n_{2effx}^2} > \left\{\frac{8}{0.967+4\ln\left[\frac{d'+2\rho}{\rho}\right]}\right\}^{1/2} \quad (4.2.2.2.b)$$

or

$$\frac{2\pi}{\lambda_{min}}\rho n_1\sqrt{2\Delta_{effx}} < 2.405 \quad (4.2.2.3.a)$$

$$\frac{2\pi}{\lambda_{max}}\rho n_1\sqrt{2\Delta_{effi}} > \left\{\frac{8}{0.967+4\ln\left[\frac{d'+2\rho}{\rho}\right]}\right\}^{1/2} \quad (4.2.2.3.b)$$

where $d'+2\rho = d$.

4.2.3 Core radius, fibre diameter and minimum distance from core to fibre surface

As indicated in Sec.3.2.2 of chapter 3, the V value in a twin-core offset fibre is $V = \frac{2\pi}{\lambda}\rho\sqrt{n_1^2 - n_{2eff}^2} = \frac{2\pi}{\lambda}\rho n_1\sqrt{2\Delta_{eff}}$. In the case where the core refractive index n_1 is fixed and the free-space wavelength λ of the launched signal is in the range $\lambda_{min} < \lambda < \lambda_{max}$, to maintain in fundamental modes operation, according to Eq.(4.2.2.2) or Eq.(4.2.2.3) set in Sec.4.2.2, the core radius ρ of the fibre must satisfy both conditions in below:

$$\rho < \frac{1.2025\lambda_{min}}{\pi\sqrt{n_1^2 - n_{2effi}^2}} = \frac{1.2025\lambda_{min}}{\pi n_1\sqrt{2\Delta_{effx}}} \qquad (4.2.3.1.a)$$

$$\frac{\pi}{\sqrt{2}\lambda_{max}}\rho\sqrt{\left(n_1^2 - n_{2effx}^2\right)\left[0.967 + 4\ln\left(2 + \frac{d'}{\rho}\right)\right]} > 1$$

or (4.2.3.1.b)

$$\frac{\pi}{\sqrt{2}\lambda_{max}}n_1\rho\sqrt{\left(2\Delta_{effi}\right)\left[0.967 + 4\ln\left(2 + \frac{d'}{\rho}\right)\right]} > 1$$

If we choose the fibre to be operated in the wavelength range 850μm~1050μm, using the parameters obtained in Sec.4.2.1, where n_1=1.464, n_{2effi}=1.454, n_{2effx}=1.459, d'=6μm, we then have ρ < 1.905μm from Eq.(4.2.3.1.a). We then set core radius to be **ρ = 1.9μm**. Substituting ρ and other known parameters into Eq.(4.2.3.1.b), we find the left hand side of Eq.(4.2.3.1.b) has the value of 1.33. Hence we know that **ρ = 1.9μm** is an appropriate value.

If we choose the fibre to operate in the wavelength range 1250~1600μm, which is the standard range for current communication channel, we can obtain ρ = 2.8μm in the same manner.

The fibre diameter should be in the range of 70~130μm, but it is more desirable to have a larger fibre for making optical devices. The fibre will be fragile and difficult to handle if it is too thin.

A very small core to fibre surface distance S is preferred to maximise the effect of the surrounding medium n_3. We set S≈1μm.

4.2.4 Summary of designed fibre parameters

In the 850~1050μm wavelength operation range, the designed parameters for the twin-core offset fibre are shown in table 4.2.4.1 below.

n_1	n_2	n_3	ρ	d	s	D
1.464	1.459	1.454~1.459	1.9um	9.8um	1um	70~130um

Table 4.2.4.1 Designed parameters of our twin-core offset fibre

4.3 Design Consideration of the Twin-core Offset Preform

In the step 4 to step 5 of twin-core fibre fabrication process mentioned in Sec.4.1 (ie, the twin-core preform to twin-core fibre drawing process in Fig.4.1.1.d to Fig.4.1.1.e), the total glass volume of the fibre does not changed when compare with the preform so that if the fibre length is L and the twin-core preform length is L_t, we have

$$\pi(D/2)^2 L = \pi(D_{to}/2)^2 L_{to}$$

and

$$\pi\rho^2 L = \pi\rho_{to}^2 L_{to}$$

and hence

$$\frac{\pi\rho^2 L}{\pi(D/2)^2 L} = \frac{\pi\rho_{to}^2 L_{to}}{\pi(D_{to}/2)^2 L_{to}}$$

thus we have:

$$\rho_{to} = \rho\frac{D_{to}}{D} \qquad (4.3.1)$$

Assume d, S and d_{to}, S_{to} are the diameters of cylinders in fibre and preform respectively, we can derive, as we did above, that:

$$d_{to} = d\frac{D_{to}}{D} \qquad (4.3.2)$$

$$S_{to} = S\frac{D_{to}}{D} \qquad (4.3.3)$$

where d, D, ρ, S have be set in Sec.4.2.3 and Sec.4.2.4. As it is best to have a preform diameter of about 9mm when drawing preform to fibre, we take the D_{to} to be 7~10mm. d_{to}, S_{to}, ρ_{to} are the corresponding parameters in twin-core offset preform shown in Fig.4.1.1.(d).

Summarise Eq.(4.3.1)~(4.3.3), the size parameters of a twin-core offset fibre are related to the size parameters of the fibre as

$$\frac{\rho_{to}}{\rho} = \frac{d_{to}}{d} = \frac{S_{to}}{S} = \frac{D_{to}}{D} \qquad (4.3.4)$$

The refractive indices in each part of the fibre remain unchanged as in the twin-core offset preform (ie, index parameters unchanged).

substituting the ρ, d, S, D, n_1, n_2 values from Table.4.2.4.1, we can obtain the required size parameters of the twin-core offset preform as shown in Table 4.3.1 below.

d_{to}/ρ_{to}	D_{to}/ρ_{to}	D_{to}/d_{to}	d_{to}/ρ_{to}
5.158	36.842~68.421	7.143~13.265	70~130

Table 4.3.1 Designed size parameters for twin-core offset preform

If we set the fibre diameter to be 110μm and preform diameter to be D_{to} =9mm, then we have ρ_{to} =0.1555; core separation d_{to} =0.8018mm; minimum distance from core to preform surface S_{to} ≈0.0818mm

4.4 Design Consideration of the Normal Twin-core Preform

In the step 3 to step 4 of the twin-core offset fibre fabrication process (from normal twin-core preform to twin-core offset preform shown in Fig.4.1.1.c to Fig.4.1.1.d), part of the cladding are removed by cutting (along dotted line in Fig.4.1.1.c) and polishing (sharp angles). In this process, core radius ρ_{nt} and core separation d_{nt} are not changed, they are:

$$\rho_{nt} = \rho_{to} = \rho \frac{D_{to}}{D} \tag{4.4.1}$$

and

$$d_{nt} = d_{to} = d \frac{D_{to}}{D} \tag{4.4.2}$$

and hence

$$\frac{\rho_{nt}}{d_{nt}} = \frac{\rho_{to}}{d_{to}} = \frac{\rho}{d} \tag{4.4.3}$$

However, the preform diameter is changed due to the cutting and polishing. The diameter of the normal twin-core preform is approximately equal to

$$\begin{aligned} D_{nt} &\cong 2(D_{to} - S_{to} - \rho_{to}) \\ &\cong 2D_{to}\left(1 - \frac{S}{D} - \frac{\rho}{D}\right) \\ &\approx 2D_{to} \quad \left(if\ \frac{S}{D}, \frac{\rho}{D}\ very\ small\right) \end{aligned} \tag{4.4.3}$$

A relation between the size parameters of a normal twin-core preform and twin-core offset fibre is

$$\frac{\rho_{nt}}{\rho} = \frac{d_{nt}}{d} \cong \frac{D_{nt}}{2D} \qquad (4.4.4)$$

The index parameters would not change in this step of process.

By substituting the known parameters from Sec.4.2 and Sec.4.3, we can obtain the size parameters of the normal twin-core preform as in Table 4.4.1 below:

d_{nt}/ρ_{nt}	D_{nt}/ρ_{nt}	D_{nt}/ρ_{nt}
5.158	73.68~136.8	14.286~26.53

Table 4.4.1 Designed size parameters of normal twin-core preform

If $\frac{D_{nt}}{\rho_{nt}}$ or $\frac{D_{nt}}{d_{nt}}$ is not within the required range, the normal twin-core preform must be stretched and sleeved to satisfy the requirement at this step. When setting the fibre diameter to 110μm and the twin-core preform diameter D_{to} to 9mm, we have core radius remains ρ_{nt} =0.155mm; core separation d_{nt} =0.8018mm, preform diameter D_{nt}≈18mm.

4.5. Design Consideration of the D-shaped Single-core Preform

From step 2 to step 3 of the process described in Sec3.1, two D-shaped single-core preform are joined by their D surface and fused together. Due to the extremely high temperature in fusion, part of the exposed surface are vaporised. After fusion, the diameter of a preform is reduced 10% by observation. However, the core and the D surface are not exposed to the air and hence are not suffered from vaporisation. The most important size parameter to be decided in this step is the minimum distance form core centre to D surface d_{D1}, it must satisfy that

$$\frac{d_{D1}}{\rho_D} = \frac{d}{2\rho} \tag{4.5.1}$$

where ρ_D is core radius of the D-shaped preform. The distance from D surface to the far end of the preform circumference (must be very accurate) is

$$d_{D2} \cong \frac{D_D}{2} + d_{s1} \tag{4.5.2}$$

core radius unchanged

$$\rho_D = \rho_{nt} = \rho_{to} = \rho\frac{D_{to}}{D} \tag{4.5.3}$$

The diameter of a D-shaped single-core preform should be greater than the diameter of a normal twin-core preform due to fusion loss

$$D_D = 1.1D_{nt} \tag{4.5.4}$$

In the high temperature fusion process, the refractive indices of the preform would suffer a small amount of changes. However, this change is not significant and is normally neglected.

The parameters of the D preform are calculated to be those shown in Table 4.5.1.

n_1	n_2	d_{D1}/ρ_D
1.464	1.459	2.579

Table 4.5.1 Design parameters of the single-core D preform

If the fibre diameter must be 110um and the preform before fibre drawing must be 9mm, the D-shaped preform diameter D_D must be 20mm unless further stretch and sleeve will be done on step 3.

4.6 Design Consideration of the Single-core Preform

Single-core preform making is the first stage in twin-core offset fibre fabrication process From the discussion in the previous sections, we can easily obtain a set of parameters characterising the single-core preform which can finally be used to draw the desired twin-core offset fibre. This preform should have the same refractive indices as the desired fibre as indicated in Sec.4.2. If we are not going to stretch and sleeve the preform in step 3, this single-core preform must satisfies (or stretch and sleeve it so that it satisfies)

$$\frac{D_s}{\rho_s} = 2.2\frac{D}{\rho} \qquad (4.6.1)$$

If a single-core preform does not satisfy Eq.(4.6.1) and we are not going to modify it in this step, we can leave it to step 3. The thickness of the inner cladding n_2 is not critical and we prefer it to be as thick as possible, but that is not possible because it is limited by many factors, for example, in deposition of the inner cladding by MCVD method, too many layers of disposition would block the tube.

The parameters of the preform are calculated and shown in Table 4.6.1.

n_1	n_2	n_2'	D_{s1}/ρ_s
1.464	1.459	1.460	81.05~150.5

Table 4.6.1 Designed parameters of single-core preform

If the D_{s1}/ρ_s is not in the designed range, we can modify it either in this step or in step 3. When the fibre diameter must be 110μm and the twin-core offset preform before fibre drawing (twin-core offset preform) must be 9mm, and we do not need further stretching and sleeving before fibre drawing, this single-core preform must be has diameter of 20mm and core radius of 0.156mm.

Reference of Chapter 4:

[1] Wong K.K.: Comparisons of different non linear directional fibre coupler, M.Eng.Sc. Thesis, The University of New South Wales, 1992.

[2] Tjugiarto T.: Multi-core optical fibre and its applications in the presence of acousto-optics interactions, M.Eng.Sc. Thesis, The University of New South Wales, 1988.

Chapter 5

Fabrication of Twin-core offset fibres

5.1 Introduction to Chapter 5

This chapter reports the detailed fabrication process of a twin-core offset fibre using the Step Controlled Process described in chapter 4, which starts from the fabrication of a primary single-core preform, and then a twin-core preform, and the modification of a twin-core preform to a twin-core offset preform, and finally the drawing and measurements of the twin-core offset fibre.

5.2 Fabrication of A Single-core Preform

5.2.1 Method description

In our laboratory, the Modified Chemical Vapour Deposition (MCVD) method is used to fabricate primary single-core preforms. The MCVD method is based on the activated homogeneous oxidation of reagents in high temperature inside a

rotating quartz glass tube [1]. Chemical substances are first entrained in a gas stream into the quartz tube in controlled amounts by passing carrier O_2 gas through the liquid dopant sources. The quartz tube has a refractive index value of 1.460 which latter become the outer cladding n_2' of the preform. The quartz tube used in the process is not only a substrate for the chemical vapour deposition but also a support to ensure the tubular flow of gases. The chemical gas mixture flowing inside the tube are thermally triggered by the torch to start vapour oxidisation and to form glass soot . As the hot soot flows downstream, it is attracted by the cold walls of the tube (not yet heated by the torch) and is deposited onto the inner surface of the tube as a thin layer. When the torch passes over the deposited soot, it will consolidate and become a transparent glass film. Using different combination of chemical gas mixture, the glass film can have different refractive indices. By repeatedly traversing the torch, more layers of glass film can be built up and hence increase the total thickness of the glass film. Finally, the quartz tube with glass films of different refractive indices in the inner wall can be collapsed to a solid glass rod by traversing the torch at higher temperature, a preform with any required indices in the centre part is ready for further processing [2, 3]. Fig.5.2.1 is a schematic diagram showing the MCVD apparatus and process.

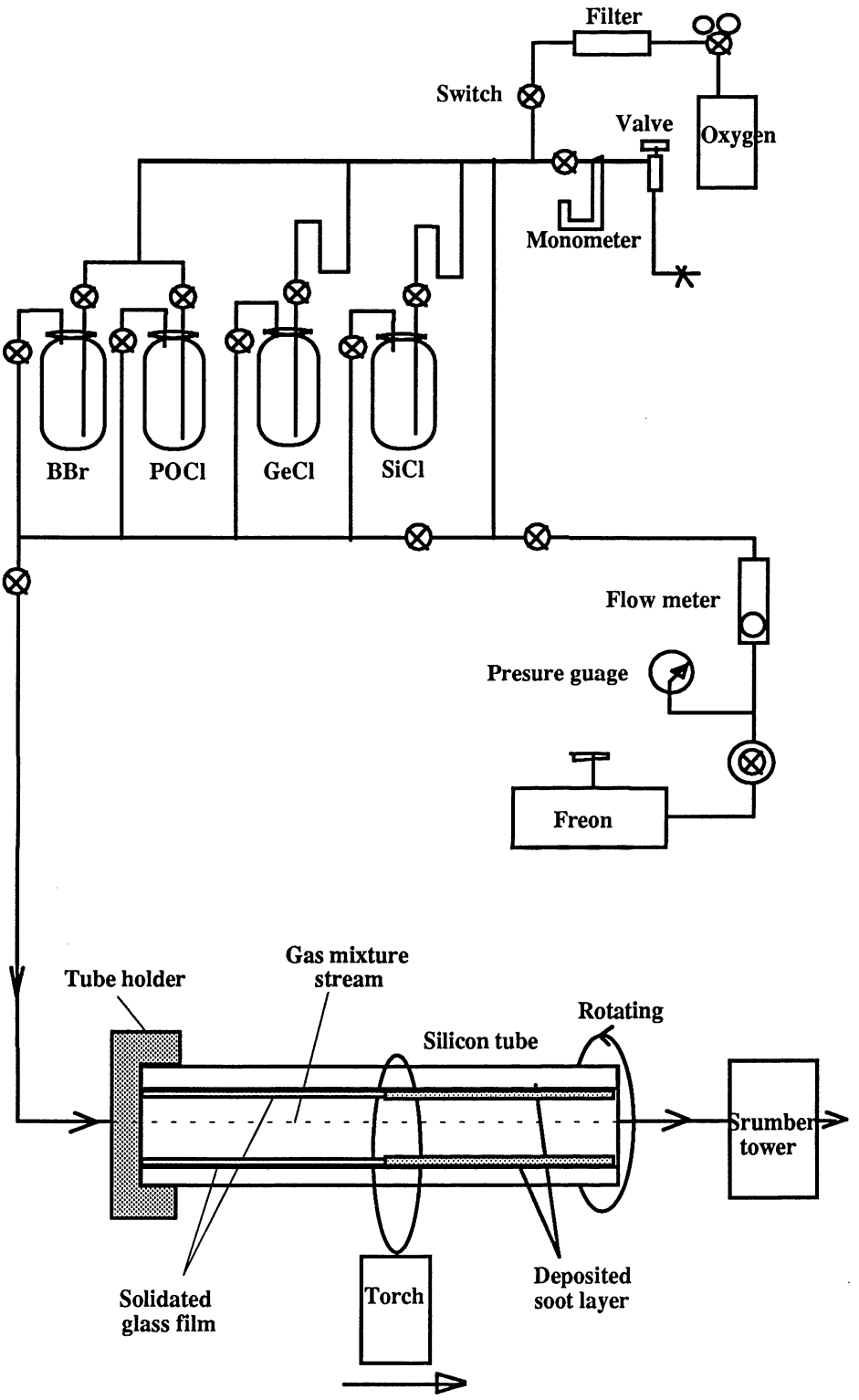

Figure 5.2.1.1 Schematic diagram of MCVD apparatus for making primary preform

5.2.2 Fabrication procedure

As indicated in the process design of the twin-core offset fibre fabrication in chapter 4, the first step in the SCP process is to make a single-core preform with the required indices and geometric specification. From Sec.4.6 of chapter 4, we know that a single-core preform with core index 1.464, inner cladding index 1.459, outer cladding index 1.460 is required. If we are going to make a single-core preform which can be modified by cuting and fusion only to form a twin-core offset preform with 9mm diameter and final drawn fibre with 110mm diameter, the single-core preform should have core radius of 0.156mm (for 850~1050nm wavelength operation range), preform diameter ($\mathbf{D_s}$) of approximatly 20mm, and a thicker but not exact defined inner cladding is required.

We should select a quartz tube of end face ring area (between inner and outer surface) satisfying $\mathbf{A_t = A_s - A_f}$, where $\mathbf{A_t}$ is the tube end face ring area, $\mathbf{A_f}$ is the deposited film ring area of the tube or inner cladding area of the preform end-face, $\mathbf{A_s}$is the preform end-face area, because generally $\mathbf{A_f << 0.1A_t}$, we can have a safety value of $\mathbf{D_o^2 - D_i^2 = 0.9D_s^2}$, where $\mathbf{D_o}$, $\mathbf{D_i}$.and $\mathbf{D_s}$ are outer, inner tube and preform diameters. The selection of the inner diameter of the tube is very critical and several factors have to be considered. Smaller inner diameter can reduce the outer diameter and also leads to easy tube collapsing, but small inner diameter would induce gas flow blockage and hence less layers of glass film can be formed on the inside wall of the tube. Smaller inner diameter also make the thickness of the tube wall too great. This causes difficulty for the heat to reach the inside wall of the tube in glass forming process. For the case where $\mathbf{D_s}$ is 20mm, if we choose a tube of 15/24 ($\mathbf{D_i}$=15mm, $\mathbf{D_o}$=24mm) with glass index 1.460, the tube wall may be too thick (9mm) for heat reach the inside wall. If we use a tube with wall thickness of 5mm, its diameters will be 33.5/38.5 which probably too big that

reduces the air mixture usage rate. It is also hard to obtain a torch flame which is strong or wide enough for the above two cases.

In addition, only 16mm tube holder (shown in Fig.5.2.1.1) is available, which can hold a tube of 16mm outer diameter and pass the gas mixture through the tube, and the only tube having 16mm outer diameter is 13/16 quartz tube. It seems that we have no option but making a single-core preform from 13/16 tube then modify it to the required size by stretching and sleeving.

After choosing a quartz tube, we come to the cladding deposition process. A glass film of index lower than 1.460 (which is the index of the quartz tube) can be obtained by passing gas mixture of $SiCl_4$, O_2, BBr_3 and $GeCl_4$ in to the tube as shown in Fig.5.2.2.1, where $SiCl_4$ is the main substances to form glass. O_2 is the carrier for the other chemical substances and helps for chemical reaction. BBr_3 is used to reduce the refractive index and $GeCl_4$ to increase the index. The ratio of BBr_3 or $GeCl_4$ to the total amount of gas mixture determines the index value of the deposited glass, while this ratio can be controled by the delivery flow rate of the individual chemical substance. For obtaining a glass film of index 1.459, the delivery flow rate of each chemical substance is shown in Table.5.2.2.1. We deposited as much as 20 layers of glass films for the cladding.

We then deposited glass films of higher refractive index as core. We used the gas mixture with the same composition of chemical substances as in making the cladding, but the amount (or ratio) of different substances was changed. Tabel 5.2.2.1 also shows the delivery flow rate of different chemical substances in core glass film deposition. Only one layer of glass film has be deposited on the tube inner wall as core glass because large diameter thin film will become glass rod with relativly large radius when it is collapsed.

When finishing the cladding and core glass film diposition, we collapsed the quartz tube to a solid glass rod by traversing the torch with higher temperature (~2100° C). During the collapsing process, all chemical flows are stopped except for the oxygen gas. The torch has to traverse a couple of times until the tube is completely collapsed. The oxygen gas is gradually reduced to zero. We then obtained a primary single-core preform with diameter D_s' of 9.4mm.

Chemical Substance	Delivery flow rate in ml/min (Cladding)	Delivery Flow Rate in ml/min (Core)
$SiCl_4$	100	100
O_2	300	300
BBr_3	80	50
$GeCl_4$	35	50

Tabel 5.2.2.1 Delivery flow rate of different chemical substances in primary preform fabrication using MCVD method

5.2.3 Measurements and estimations of the fabricated single-core preform

By using a method of direct display of the preform deflection function [4], we obtained the index profile of the above preform as shown in Fig.5.2.3.1.

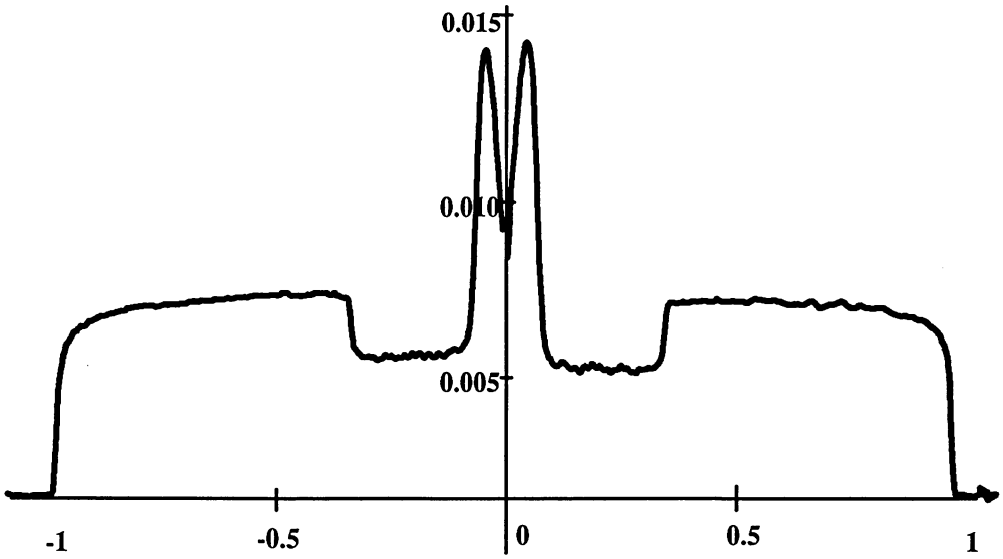

Figure 5.2.3.1 Refractive index profile of our primary single-core preform

From Fig.5.2.3.1, using the ESI (Equivalent Step Index) approximation, we know that the preform has core index n_1 ≈1.464, inner cladding index n_2 ≈1.459, outer cladding index n_2'=1.460, core radius ρ_s' =0.325mm, D_s'=9.4mm.

We found that this preform has indices in core and cladding roughly matched to the design. However, the out diameter to core radius ratio of this preform of 28.9 is much too low than the required range of 81.05~150.5 as indicated in Sce.4.6. If we use this preform to make fibre directly, withn a core radius at ρ = 1.9μm, according to Eq.(4.6.1), the fibre diameter will be 25mm (much too thin, not in the range of 70~130mm). The twin-core offset preform for fibre drawing will have diameter 4.3mm (what required is about 9mm).

To increase the fibre diameter while maintaining its core as thin as required (ie, to increase the outer diameter to core radius ratio of the twin-core offset fibre), we have to either modify (by stretch and sleeve) the primary single-core preform to the designed diameter to core radius ratio range of 81.05~150.5 as shown in

Sec.4.6, or modify (tretch and sleeve) the normal twin-core preform to the designed diameter to core radius ratio range of 73.68~136.8 (or preform diameter to core seperation ratio $\frac{D_{nt}}{d_{nt}}$ of 14.286~26.53) as shown in Sec.4.4. We took the second choice in our TOF fabrication precess.

5.3 Fabrication of Normal Twin-core Preform

We cut two 4cm length sections from the single-core preform obtained in Sec.5.2 (the longer the pieces, the easier to maintain the two cores parallel to each other). These two pieces of preform are then glued to a supporting iron block by wax, the block then mounted to a high precision cutting machine with diamond blade and lubricant oil. A part of the cladding with D-shaped cross-section is then removed (reference to Sec.4.5) [5, 6, 7]. The depth of the remaining part of the D-shaped preform d_{D2} should be just larger than 5.538mm ((9.4/2)+0.325*2.579, Eq.4.5.1 and Eq.4.5.2), the flat D surface are then polished using the polishing machine and 20μm, 12μm and 5μm diamond paste to exactly 5.538mm thick from flat D surface to far end of the round circumference. The flat D surface obtained this way would be flat, clean and smooth enough for later two D preform fusion. The two D preform then immersed in alcohol and placed in ultrasonic wave oven for one hour to remove the wax and dirt before fusion.

The two D-shaped single core preform are then fused together to form a twin-core normal preform as shown in Fig.4.1.1.b ~ 4.1.1.c. This twin-core preform was measured to have a diameter of 9.5mm, its cores radius was unchanged (0.325mm). Core to core separation was 1.676mm. Its preform diameter to core

separation ratio was calculated to be 5.667, much smaller than the allowed range of **14.286~26.53** indicated in Table 4.4.1 (preform diameter to core radius ratio was 29.23, not in the range of **73.68~136.8**). To increase the above ratio, we firstly stretched the preform to have 5mm diameter. After stretching, the core to core separation is calculated to be 0.882mm, and core radius was calculated to be 0.171mm. Then we use a 8/11 quartz glass tube to sleeve the 5mm preform and obtained a new preform of diameter 8.9mm. We again used a 9/11 glass tube to sleeve the 8.9mm preform and then a 13/16 glass tube to sleeve the previously obtained preform. Finally, we got a normal twin-core preform of diameter 14.1mm, core separation of 0.882mm and core radius of 0.171mm. The new preform diameter to core separation ratio is about 16 and is in the allowed range (same as preform diameter to core radius ratio because cores separation to core radius ratio is constant).

5.4 Fabrication of Twin-core Offset Preform

Taking the preform obtained from Sec.5.3, we cut it using the diamond saw on a cutting machine and polish it using 20μm diamond paste on a polishing machine to a cylindrical preform with cores close to the preform out surface. The cutting and polishing procedure has been mentioned in chapter 4 and shown in Fig.4.1.1.c ~ 4.1.1.d. We tried to polish one side of the cores as close to the preform surface as possible while not hurting the cores themself by firstly using 20μm diamond paste, then 12μm and 5μm diamond paste. After cutting and polishing, the twin-core offset preform has a diameter of 7.27mm, unchanged core to core seperation (0.882mm) and core radius(0.171mm). The minimum distance from cores to preform surface is very small. The preform diameter to cores separation and to

core radius ratio is 8.295 and 42.69 respectively, satisfying the requirement indicated in Sec.4.3.

5.5 Twin-core Offset Fibre Drawing and Measurement

In twin-core offset preform to twin-core offset fibre drawing process, the core radius and core to core separation are the most concerned parameters. However, the ratio between the core to core separatin and the core radius is constant during the drawing process. We can pay attention to either one of these two paramers only. To obtain a single-mode twin-core offset fibre designed in Sec.4.2, from the preform obtained in Sec.5.4, using Eq.(4.3.4), we decided we should draw a fibre of out diameter 80.7μm (7.27*1.9/0.171). The fibre diameter can be easily controlled by the fibre drawing machine in our laboratory. Finally, a twin-core offset fibre was fabricated and ready for later measurement and experimentation. The fibre's near field end face can be seen using a special microscope with light launched from one end and objectives and inspector on the other end. A photograph of this near field end face is shown in Fig.5.5.1. We can measure the size parameters of this fibre from its near field image. The measured results are: core separation 9.8μm, fibre diameter 79μm, core radius approxmatly 2.6μm, minimum distance of core to fibre surface approximatly 6μm. The actual core radius may be much smaller than the measured result because the strong light intensity output from the core makes the near field image of the core appear to be bigger than its real size.

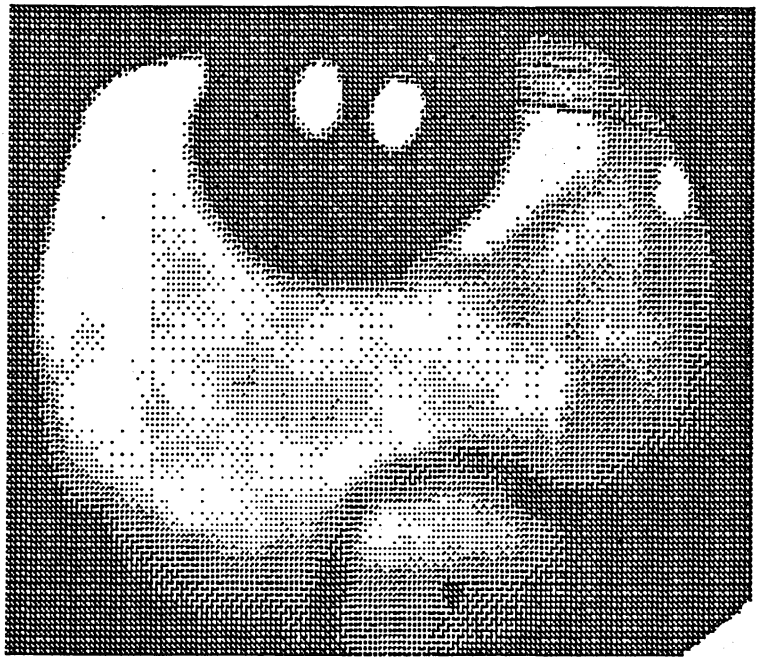

Figure 5.5.1 Near field end face image of twin-core off-set fibre

Reference of Chapter 5:

[1] Chu P.L.: Lecture notes of "Theory of optical fibres and optical signal processing", 1989.

[2] Fan K.: Private Commuincation.

[3] Whitbread T.W.: Private communication

[4] Peri D., Chu P.l., Whitbread T.: Direc display of the deflection function of optical fibre preforms, Appl.Opt., Vol.21., No.5, 809-814, 1982.

[5] Tjugiarto T.: "Multicore optical fibre and its application in the presence of acousto-optics interactions", M.Eng.Sc. Thesis, University of New South Wales, 1988.

[6] Tjugiarto T.: Private communication.

[7] Peng G.D.: Private communication

Chapter 6

Twin-core Offset Fibre Directional Couplers

6.1 Introduction to Chapter 6

This chapter introduced a new idea of making tunable directional couplers, based on twin-core offset fibres. We call this type of directional couplers the Twin-core Offset Fibre Directional Couplers (TOFDC). We first review the basic concept of the directional couplers, followed by a discussion of existing directional couplers, then we describe the TOFDCs, as well as their principles and the formulas characterising them. We then propose some applications of the TOFDCs. The fabrication of a TOFDC were not carried out in this project due to three reasons. Firstly, in the experiments done in our laboratory, the light signal input to a TOFDC is directly from a free space beam source such as laser and LED. We can launch this light into a core of the twin-core offset fibre and immerse the fibre in liquids of different refractive indices to obtain the same results as done on a real TOFDC. This greatly simplifies and speeds up our experiments. Secondly, the reported excess insertion loss induced in the joint of a twin-core fibre to a single-core fibre using the GRIN Rod Len Method [1] is large, but there is no other better method available. Finally, the limitation of time in the submission of the thesis

makes it impossible to spend more time on the experiment and on improvement of the jointing technique.

6.2 Basic Concepts of Directional Couplers

An optical directional coupler is a four-port device that accepts optical signals into one or two of the input ports and produces a signal on the output ports subjected to certain selective criteria of the device. Fig.6.2.1 shows a generalised directional (four-port) coupler. The main parameters that characterise a four-port directional coupler are: the splitting ratio

$$R_S = \frac{P_4}{P_2 + P_4} \tag{6.2.1}$$

which is often expressed in decibels as

$$A_S = 10 \cdot \log\left[\frac{P_2 + P_4}{P_4}\right] \tag{6.2.2}$$

the directivity in decibels

$$A_d = 10 \cdot \log\left(\frac{P_1}{P_3}\right) \tag{6.2.3}$$

the insertion loss (or excess loss) in decibels

$$A_i = 10 \cdot \log\left[\frac{P_1}{P_2 + P_4}\right] \tag{6.2.4}$$

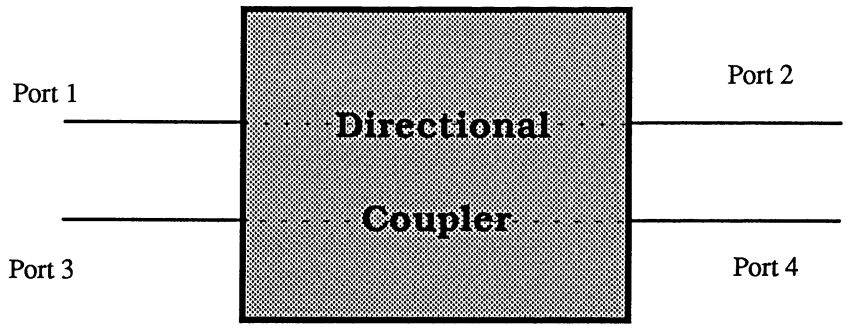

Fig 6.2.1 Directional Coupler

Optical directional couplers are required for power splitting and combining. Directional couplers are mainly employed in optical communication system for duplexing the signal and the local oscillator wave for coherent detection, for wavelength multiplexing/demultiplexing, for laser redundancy, for monitoring backscatter, and as a power tap.

6.3 Brief Revision of the Existing Types of Fibre Directional couplers

Many types of single-mode directional couplers using different fabrication methods have been developed and analysed during the last two decades. Among these are: (1) Fibre-Etched Directional Couplers[2] [3] [4], (2) Fibre-Polished Directional Couplers [5] [6] [7] [8] [9] [10] [11] [12] [13] [14], (4) Preform-Polished (or Twin-Core Fibre) Directional Couplers [15] [16] [17] [18] [19] [20] [21] [22] [23], (4) Fusion-Taped fibre Directional Couplers [24] [25] [26] [27] [28] [29], and (5) Fusion-Taped Twin-Core Fibre Directional Couplers [30] [31] [32] [33]. The fabrication processes and main characteristics of these types of directional couplers will be briefly described below.

A fibre-etched directional coupler is made by first stripping the coating from two single core fibres, the claddings of the fibres are then etched in a bottle filled with a solution of hydrofluoric acid to a diameter close to that of the core. Finally the two etched fibres are twisted together, giving an overlap of the evanescent field in the cladding of one fibre which is sufficient for power coupling to the other fibre. The coupling efficiency of this type of couplers can be adjusted by turning a threaded cap to control the number of twists between the two etched fibers as well as their separation. This type of couplers seems to suffer from the problems of aging and are delicate, non-rugged. They are only suitable for use under laboratory conditions. The insertion loss of this type of couplers is of the order of 1 dB.

Fibre-polished directional couplers are obtained by first cementing two single-core fibres in separate fused silica block with a curved groove cut in it. Parts of the claddings are then removed by grinding, polishing, and lapping both blocks, and finally placing one block on top of the other with a thin film of index-matching

liquid between the two blocks. The coupling can be varied by sliding one block laterally relative to the other. A simplified picture of the fibre-polished directional coupler is shown in fig.6.3.1. This type of directional couplers exhibits low loss, high directivity, and can be tuned to any required coupling ratio. However, elaborate fixturing is required to maintain a stable coupling ratio (the stability of the coupler would still be affected by the temperature dependence of the index-matching liquid between the blocks) and hence a convenient, smooth coupling ratio changing after fixturing is impossible.

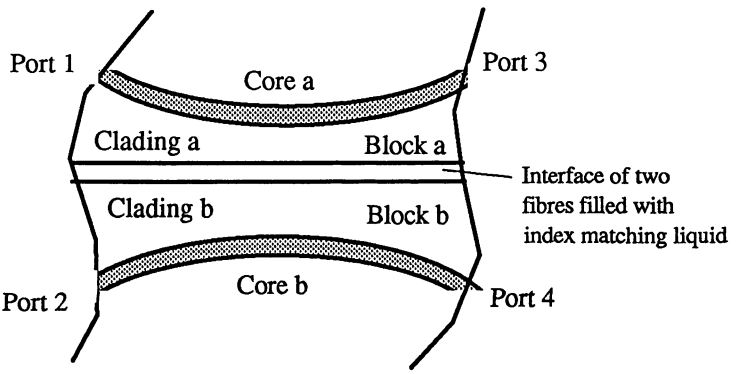

Figure 6.3.1 Fibre-polished directional coupler

Preform-polished (Twin-core Fibre) Directional Couplers are produced by first cutting part of two single-core preforms with cut surfaces parallel to the fibre axises. The surfaces are then polished until they are close to the cores of the individual fibres. The two D-shaped single-core preforms are then fused together to form a twin-core preform from which a twin-core fibre can be drawn. A directional coupler can be realised from this fibre with coupling ratio depending on the normalised separation of the cores, the length of the twin-core fibre used, and the index differences between the core and cladding (The exact required coupling coefficiency of a twin-core fibre made from this method is not easy to be obtained

and hence we have to select different fibre length to achieve required power splitting ratio). The stability of this type of couplers is excellent, but their coupling ratio cannot be changed easily.

Fusion-tapered fibre Directional couplers are made by twisting two single-core fibre around each other and flame-heated and fused while the two stages of the fusion station are moved apart to form biconical tapers in the fused regions of the two fibres. The basic phenomenon which permits coupling in this process is that the biconical taper brings the two fiber cores close to each other, but simultaneously decreases the core diameters (which increases the mode spot size), both of which contribute to strong coupling through the evanescent tails of the guided modes. The coupling ratio can be roughly tuned by monitoring the power output value from the output port during the fusion-taping process and finely tuned by controlling the bending of the tapered region. Fig.6.3.2 shows a Twin-fibre fusion-taped directional coupler and its fabrication process. This type of couplers has low insertion loss, good thermal and mechanical stability, but they are difficult to be fabricated from depressed cladding fibres, which are often needed to provide negative waveguide dispersion to cancel the positive material dispersion in the wavelength range of the contemporary practical semiconductor laser (800-1100 nm).

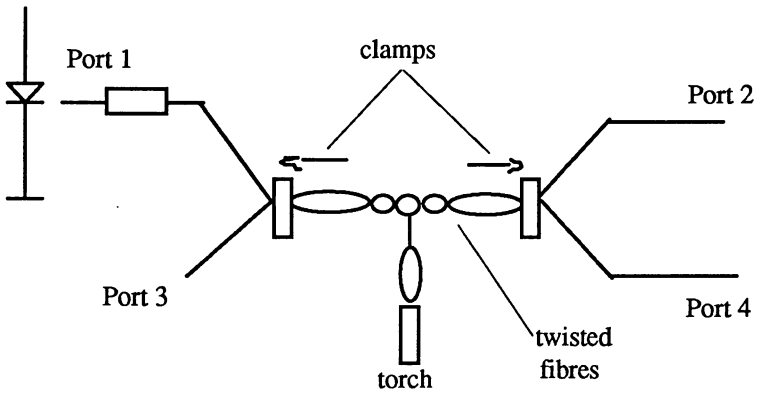

Figure 6.3.2 Fusion-taped Fibre Directional Coupler

A Fusion-taped Twin-core Fibre Directional Coupler is very similar to the Fusion-taped fibre Directional Coupler in its fabrication process except that it is made from one twin-core fibre and hence there is no need to twisting fibres, and it also eliminates the difficulties of being fabricated from depressed cladding fibres (twin-core) and hence is suitable for operating in the systems where dispersion cancellation in the wavelength range less than 1200 nm are required.

6.4 Principles of Twin-core Offset Fibre Directional Couplers

This type of directional couplers are actually a twin-core offset fibre (shown in Fig.3.3.1) inserted in a small tube with both tube ends sealed by soft corks. The two fibre ends are led out from the corks and the core ends of the fibre are joined with four single-core fibres using the method described by Lui and Chu [34]. The tube is filled with liquid with certain refractive index according to the required power splitting ratio. The index of the liquid in the tube can be smoothly varied by extracting and injecting liquid with different refractive index of different amount through the corks from and to the tube using injection needle. Fig.6.4.1

shows a directional coupler of this type. The power coupling of this coupler is based on the fundamental field of one core interacting with the fundamental field in other core just as those five types of couplers previously described does. The reason of the variable power splitting ratio lies on the fact that the two cores of the modified twin-core fibre are so close to the out surface and hence the index change of the liquid in the tube would greatly affects the composite (effective) refractive index value of the cladding, which produces a change in the normalised frequency of the fibre and hence the coupling strength between the two cores. More detailed explanations of the effects of surrounding liquid on coupling strength between two cores of a TOF are given in chapter 3. The main advantage of this type of couplers is that they can provide more convenient and smooth variation on the power splitting ratio and less disturbance to the coupler and coupler/fibre connection.

The parameters characterising a directional coupler mentioned in Sce.6.2 can be applied to a TOFDC. In the ideal case, ie, when the two cores are exactly identical, its splitting ratio is

$$R_S = \frac{P_4}{P_2 + P_4} \approx \sin^2(C \cdot L) \tag{6.4.1}$$

or in decibel

$$A_S = 10 \cdot \log\left(\frac{P_2 + P_4}{P_4}\right) = 10 \cdot \log\left[\frac{1}{\sin^2(C \cdot L)}\right] \tag{6.4.2}$$

the directivity in decibel

$$A_d = 10 \cdot \log\left(\frac{P_1}{P_3}\right) = \infty \tag{6.4.3}$$

the insertion loss in decibels

$$A_i = 10 \cdot \log\left[\frac{P_1}{P_2 + P_4}\right] = 0 \qquad (6.4.4)$$

The splitting ratio versus wavelength for different surround liquid of different refractive index n_3 is shown in Fig. 6.4.2. Fig.6.4.3 shows the splitting ratio versus the index value n_3 of surrounding medium for fixed operation wavelength (the program used for the calculation of the curve is shown in Appendix B), while Fig.6.4.4 shows the splitting ratio versus the relative index difference Δ for fixed operation wavelength λ.

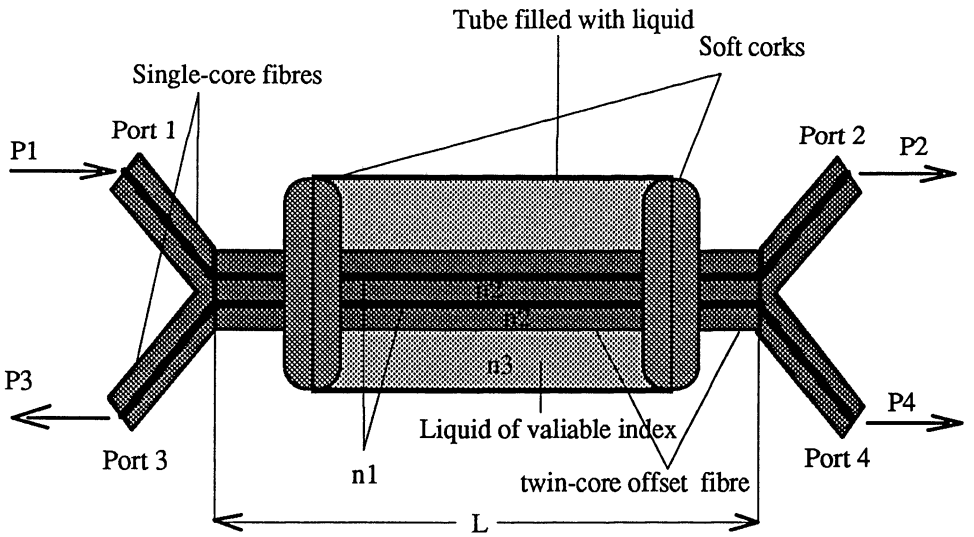

Figure 6.4.1 Twin-core Offset Fibre Directional Coupler (TOFDC)

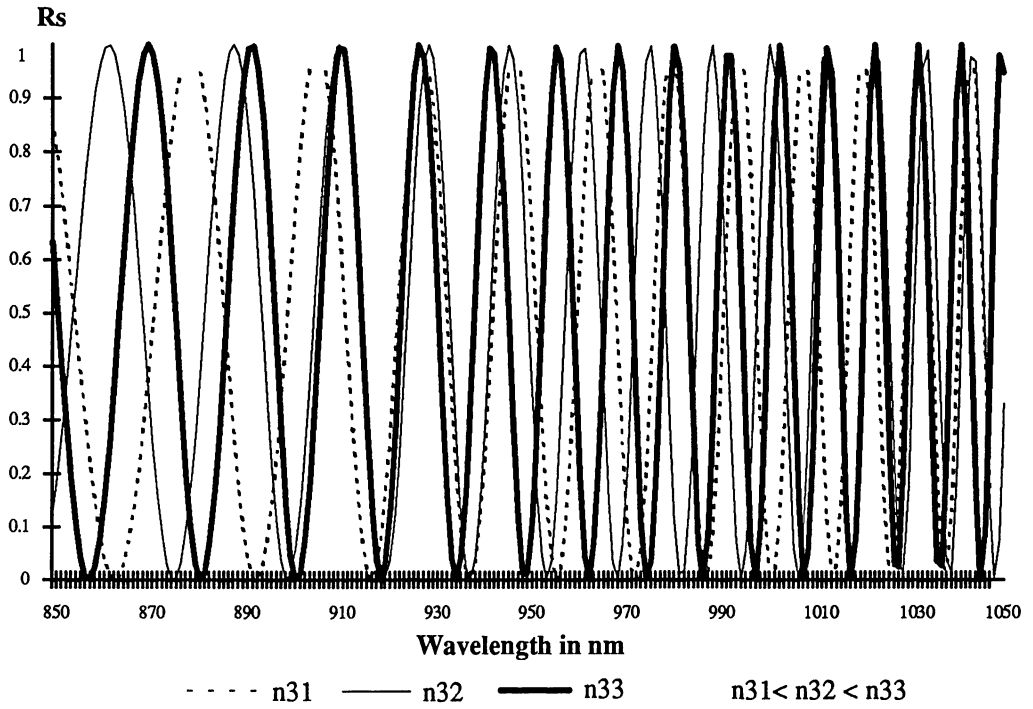

Figure 6.4.2 Power splitting ratio of a TOFDC vs wavelength for different surrounding medium of index n31,..,n33

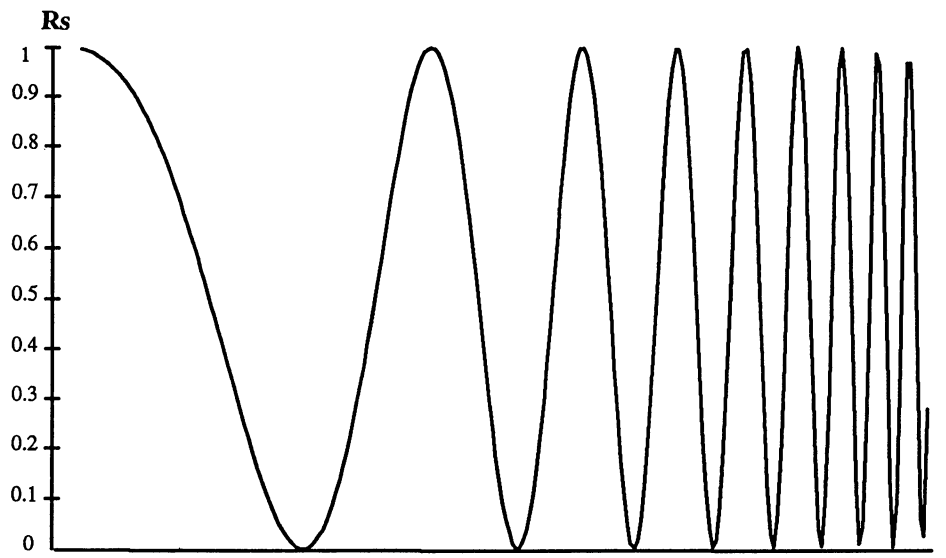

Figure 6.4.3 Power splitting ratio vs index value of the surrouning medium

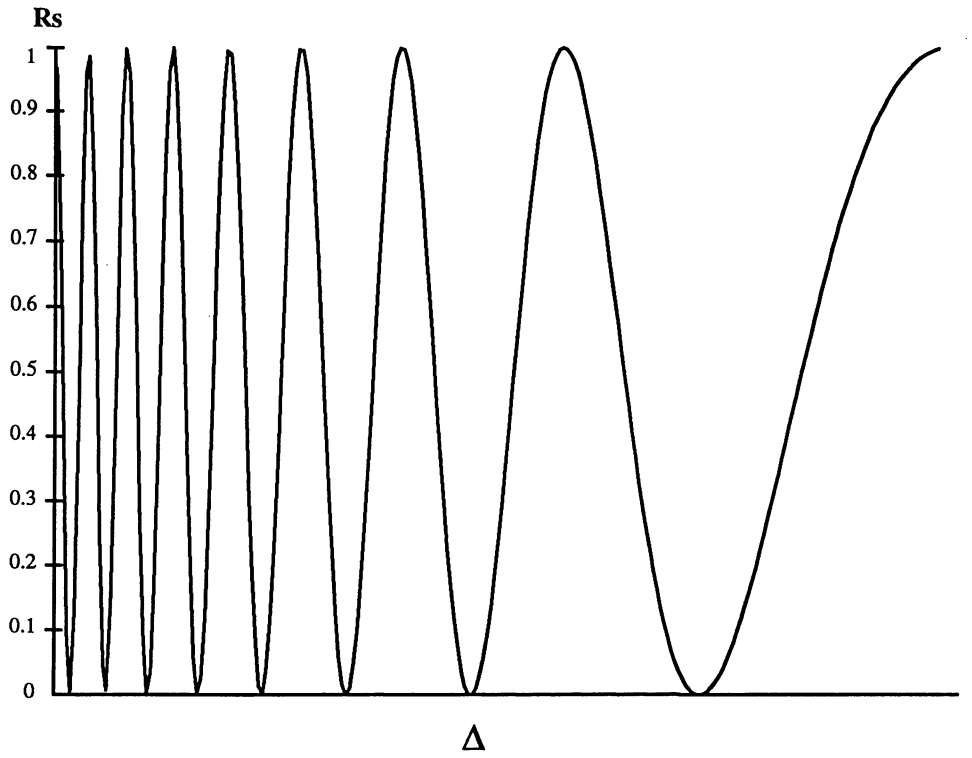

Figure 6.4.4 Power splitting ratio vs relative index difference

6.5 Applications of the Twin-core Offset Fibre Directional Couplers

Many applications can be found for a TOFDC (Twin-core Offset Fibre Directional Coupler). We will briefly describe some of these applications in the following of the section. These applications include: (1) TOFDC as a variable attenuator; (2) TOFDC as a tunable power splitter or combiner; (3) TOFDC as a fibre tap; (4) TOFDC as a tunable signal intensity switch; (5) TOFDC as a temperature sensor; (6) TDFDC as a tunable bandpass filter.

6.5.1 TOFDC as a variable attenuator

Fig.6.5.1.1 shows the throughput and coupled output power of an ideal TOFDC (no insertion loss, reference to Sec.6.4 and Fig.6.4.1) as a function of surrounding medium index.. From the figure, it is apparent that by choosing n_3 to be n_{31}, the throughput power of the TOFDC will be attenuated to 20 percent of its input. By choosing n_3 to be n_{32}, the throughput power will be attenuated to zero. When n_3 equal to n_{33} or n_{34}, the throughput power will be 50 percent attenuated or no attenuation to the input power. Variable attenuators are used, eg, for measuring the bit error rate as a function of the received optical power.

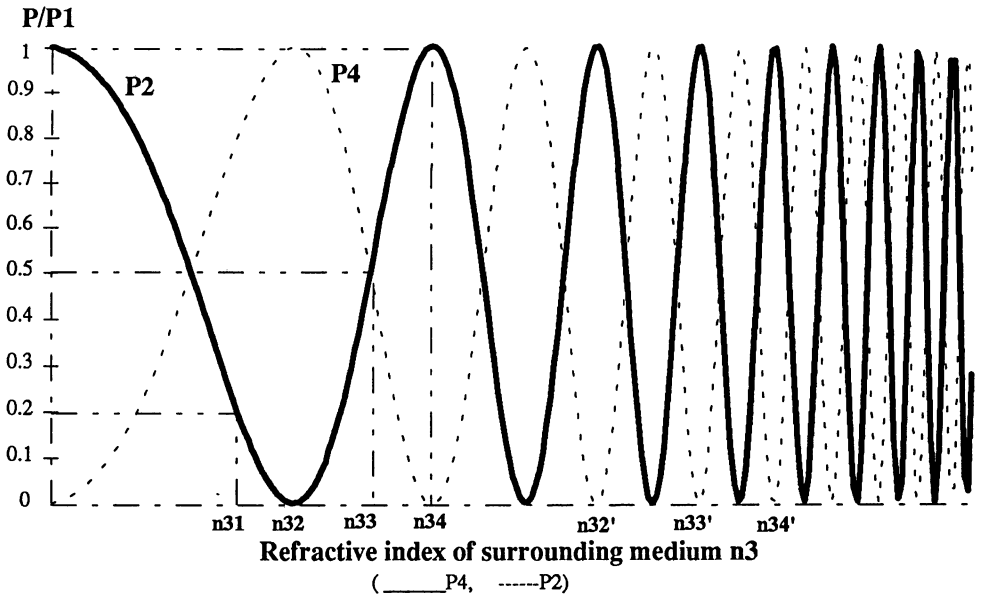

Figure 6.5.1.1 Throughput and coupled normalised power of a TOFDC vs index of the surrounding medium

6.5.2 TOFDC as a tunable power splitter

The principle of the TOFDC tunable power splitter is similar to the TOFDC variable attenuator indicated in Sec.6.5.1 except that three ports of a TOFDC are used, where port 1 is the input port, port 2 and port 4 are the output ports. By varying n_3, the ratio of power from two output ports P_2 and P_4 can be varied from 0:1,.., 0.5:0.5,.., 1:0, etc, and hence one single transmitted signal can be sent to two receivers in different signal intensity.

6.5.3 TOFDC as a fibre tap

When signal goes into a TOFDC, a very small part (variable) of the signal power is extracted from one of the output port without having to disturb the transmitted signal which goes to a fibre channel via the other output port. A TOFDC for the above usage can be regarded as a tap. Taps can be used for identifying fibers carrying traffic, for providing a feedback signal for controlling the launched light power, and also for eavesdropping [35]. If we select port 4 in Fig.6.4.1 as the taping port, a tapping efficiency can be defined by

$$\eta = P_4/(P_1 - P_2) \qquad (6.5.3.1)$$

6.5.4 TOFDC as a signal intensity switch with tunable switching power

By carefully adjusting the refractive index of the surrounding liquid of a TOFDC to some finite values (eg, n_{34}, n_{32}', n_{33}' or n_{34}', etc, in Fig.6.5.1.1, we can make the coupled output power to be equal to the input power (assuming no insertion loss) and no output power at the throughput port at all. When the signal intensity in the cores of the twin-core offset fibre within a TOFDC reaches certain value, the refractive index of cores will increase rapidly due to the nonlinearity of the core material. The index difference of the cores and the composite (effective) cladding then become so large that no power coupling can occur between the two cores, and the input signal remains in the launched core and only the throughput port has the signal. This is called intensity switching. By selecting different n_3 value (must be one of the n_{34}, n_{32}', $.n_{33}'$, n_{34}'), the signal intensity and hence the signal power which causes the switching (we call this power as critical power P_c) can be varied. A signal intensity switch with tunable critical power thus obtained. We can find that the greater the n_3 (ie, the small the $\Delta n=n_1-n_{2eff}$), the smaller the switching power P_c. Fig.6.5.4.1 shows the power switching curve of a TOFDC intensity switch.

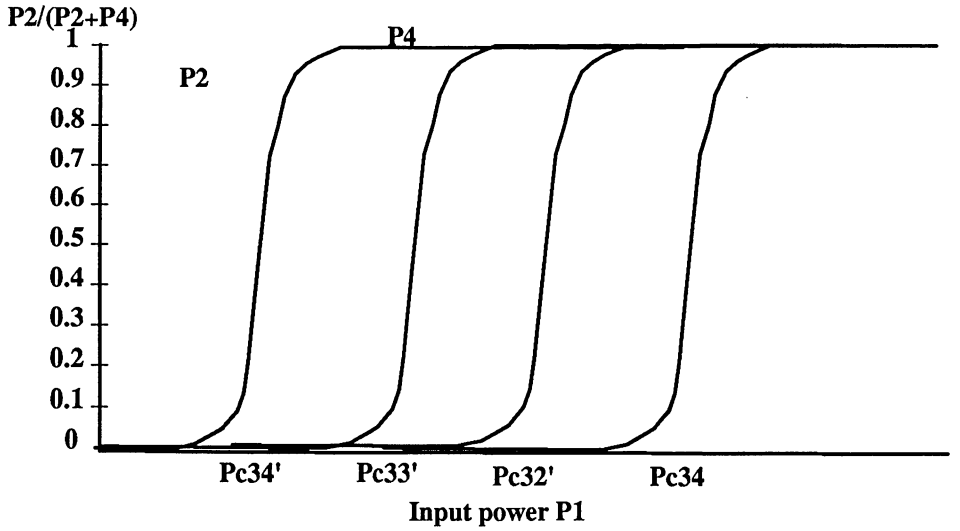

Figure 6.5.4.1 Switching curve of a TOFDC intensity switch

6.5.5 TOFDC as a temperature sensor

By filling the tube with liquid whose refractive index is sensitive to temperature, the reading of output power can represent the temperature scale if the input power is fixed. In this use of TOFDC, the index varying range of the liquid has to be controlled in a small range.

6.5.6 TOFDC as a tunable band-pass filter

As indicated in [36], two or more concatenated fibre couplers can work as a band-pass filter. If we can change the liquid index in the TOFDCs simultaneously, concatenated TOFDCs can form a tunable bandpass filter, where the selected signal passing wavelength range can be varied by varying n_3 in TOFDC shown in Fig.6.2.1.

References of Chapter 6:

1 Lui F., Chu P.L.: A twin-core fibre to twin fibre connector, 12th Australian conference on Optical fibre Technology, pp. 185-188, 1987.

2 Sheem S.K., Giallorenzi T.G.:Single-mode fiber-optical power divider: encapsulated etching technique. Opt. Lett. 4, 29-31, 1979.

3 Sheem S.K., Cole J.H.: Acoustic Sensitivity of single-mode optical power dividers. Opt. Lett. 4, 322-324, 1979.

4 Liao F.J., Boyd J.T.: Single-mode fiber coupler. Appl. Opt. 20, 2731-2734, 1981.

5 Bergh R.A., Kotler G., Shaw H.J.: Single-mode fiber optic directional coupler. Electron. Lett. 16, 260-161, 1980.

6 Parriaux O., Gidon S., Kuznetsov A.A.: Distributed coupling on polished single-mode optical fibers. Appl. Opt. 20, 2420-2423, 1981.

7 Bergh R.A., Digonnet M.J.F., Lefevre H.C., Newton S.A., Shaw H.J.: "Single-mode fiber optic components" in Fiber-Optic Rotation Sensors, ed. by S. Ezekiel and H.J.Arditty, (Springer, Berlin, Heidelberg, New York), pp. 136-143, 1982.

8 Digonnet M.J.F., Shaw H.J.: Analysis of a tunable single-mode optical fiber coupler. IEEE Trans. MTT-30, 592-600, and IEEE J. QE-18, 746-752, 1982.

9 Nayar B.K., Smith D.R.: Monomode-polarization-maintaining fiber directional couplers. Opt. Lett. 8, 543-545, 1983.

10 Pleibel W., Stolen R.H., Rashleigh S.C.: Polarization-preserving coupler with self aligning birefringent fibers. Electron. Lett. 19, 825-826, 1983.

11 Jaccard P., Scheja B., Berthou H., Parriaux O.: A batch fabrication technique for single-mode fiber couplers. 9th Europ. Conf. Opt. Commun. 1983, 409-412, 1983.

12 Jaccard P., Scheja B., Berthou H., Cochet F., Parriaux O., Brugger A.: A new technique for low-cost all-fiber device fabrication. Proc. Spie 479, 16-19, 1984.

13 Georgiou G., Boucouvalas A.C.: Low-loss single-mode optical couplers. Proc. Inst. Electr. Eng. 132, P2. J, 297-302, 1985.

14 Mao Z., Fang X., Li B.: Mode excitation theory and experiment of single-mode fiber directional coupler with strong coupling. J. Lightwave Tech. LT-4. 466-472, 1986.

15 Wong D, Darbowiak A.E., Chu P.L.: A twincore variable optical coupler/switch for local area network, 12th Australian Conference on Optical fibre Technology, pp. 29-32, 1987.

16 Schiffner G., Schneider M., Schoner G.: Double-core single-mode optical fiber as directional coupler, Appl. Phys., vol. 23, pp 41-45, 1980.

17 Kitayama K., Shibata N., Ohashi M.: two-core optical fibers: Experiment, J. Opt. Soc. Am. A, vol. 2, no. 1, pp 84-89, 1985.

18 Kitayama k., Ishida Y.: "Wavelength-selective coupling of two-core optical fiber: Application and design", J. Opt. Soc. Am. A, vol. 2, no. 1, pp90-94, 1985.

19 Taylor H.F.: Frequency-selective coupling in parallel dielectric waveguides, Optics Communications, vol. 8, no. 4, pp 421-425, 1973.

20 Taylor H.F.: Frequency-selective coupling in parallel dielectric waveguides, Optics Communications, vol. 8, no. 4, pp 421-425, 1973.

21 Schoner G., Schiffner G.: Coupling properties of a double-core single-mode optical fiber, Siemens Forsch-u. Entwickl-Ber. Bd. 10, No. 3, 1981.

22 Barr s.: Optical fibre Directional Coupler, B.E thesis, UNSW, 1985.

23 Tjugiarto T.: Multi-core optical fibre and its applications in the presence of acousto-optics interactions, M.E.Sc thesis, UNSW, 1988.

24 Villarruel C.A., Moeller R.P.: Fused single-mode fiber access couplers. Electron. Lett. 17, 243-244, 1981.

25 Kawasaki B.S., Hill K.O., Johnson D.C.: Biconical-taper single-mode fiber coupler. Opt. lett. 6, 327-328, 1981.

26 Slonecker M.H.: Single-mode fused biconical taper coupler. conf. Opt. Fiber Commun. (OFC'82), 336-37, 1982.

27 Villarruel C.A., Abebe M., Burns W.K.: Polarisation preserving single-mode-fiber coupler. Electron. Lett. 19, 17-18, 1983.

28 Kawasaki B.S., Johnson D.C., Hill K.O.: Configurations, performance, and applications of biconical taper optical fiber coupling structures. Canadian J. Phys. 61, 352-360, 1983.

29 Ragdale C.M., Slonecker M.H., Williams J.C.: Review of fused single-mode coupler technology. Proc. sPIE 479, 2-8, 1984.

30 Schiffner G., Schneider H., Schoner G.: Double-core single-mode optical fiber as directional coupler. Appl. Phys. 23, 41-45, 1980.

31 Schoner G., Schiffner G.: Coupling properties of a double-core single-mode optical fiber. Siemens Forsch.-u. Entwickl.-Ber. 10, 172-178, 1981.

32 Truesdale C.M., Nolan D.A., Keck D.B., Berkey G.E.: Multiple-index waveguide coupler. Conf. Opt. Fiber commun. (OFC'86), 60-61, 1986.

33 Truesdale C.M., Nolan D.A..: Core/clad mode coupling in a new multiple-index waveguide structure. 12th Europ.Conf. Opt. commun. 1986, 181-184, 1986.

34 Lui F., Chu P.L.: A twin-core fibre to twin fibre connector, 12th Australian conference on Optical fibre Technology, pp. 185-188, 1987.

35 Neumann E. -G.: Single-mode fibers Fundamentals, Springer-Verlag, Berlin, 1988, Chapter 12

36 Yataki M.S., Payne D.N., Varnham M.P.: All-fiber wavelength filters using concatenated fused-taper couplers. Electron.Lett. 248-249, 1985.

Chapter 7

Experiments

7.1 Introduction to Chapter 7

The purpose of this chapter is to prove our predictions in chapter 3 and chapter 6, where we indicated that by varying the refractive index n_3 of the surrounding medium of the TOF (twin-core offset fibre) or filled liquid of a TOFDC (Twin-core Offset Fibre Directional Coupler), the coupling coefficient of the TOF and the splitting ratio of the TOFDC will vary. From the experiments below, we can also obtain a quantitative view of the effect of n_3 on TOF and TOFDC.

As explained in Sec.6.1, a short section of twin-core offset fibre (TOF) immersed in liquid of certain refractive index with light launched into one of the cores can be regarded as a TOFDC (Twin-core Offset Fibre Directional Coupler), the experiment on TOF and TOFDC thus become the same. In other words, experiment on either TOF or TOFDC gets results of both.

The TOF used in the experiment is the one described in chapter 5 (Sec.5.5). The fibre core radius may be larger than the designed value in chapter 4. Larger core

radius could introduce higher order modes if the operation wavelength remains in 850~1050μm. The fibre also has a minimum distance from core to fibre surface which is greater than the designed fibre. This may result in the performance of the TOF and TOFDC less dependent on the surrounding liquid. Nothing we can do to change the core radius except restarting the whole TOF fabrication process. However, the minimum distance from core to fibre surface can be minimised by polishing the TOF. We start our experiments directly on the unmodified fibre obtained in our fabrication (chapter 5). The polishing to minimise core to surface distance will be done if necessary.

This chapter describes the theoretical basis of the experiment, the experimental setup, the experimental procedure, the experimental data obtained, the data processing to get the coupling coefficient of a TOF, and a discussion of the experiment results.

7.2 The Theoretical Basis of the Experiment

As we have indicated in chapter 3 and chapter 6, when equal amplitude optical signals with consecutive wavelength launched in one core of a fixed length TOF (or one port of a TOFDC), the output power (both throughput and cross-coupled) will vary sinusoidally with the wavelength, but the period of the sinusoidal variation will get smaller as the wavelength increases. This is because that increasing wavelength can increases the coupling coefficient and hence increases the number of the signal power swap between the two cores of the TOF (ie, reduces the coupling length). By increasing the index n_3 of the surrounding medium of a TOF (or liquid in the tube of a TOFDC) towards cladding index n_2,

we can reduce the effective relative index difference Δ_{eff} and hence obtain the same result as increasing the input signal wavelength. If we first launch equal intensity power with consecutive wavelength into one core of the TOF input end and measure the power at any one core of the output end to obtain a power versus wavelength curve, then increase the n_3 and repeat the above procedure to obtain another power versus wavelength curve, we would find more cycles in the same wavelength interval in the second curve than in the first one. Fig.7.2.1 shows the above theoretical prediction.

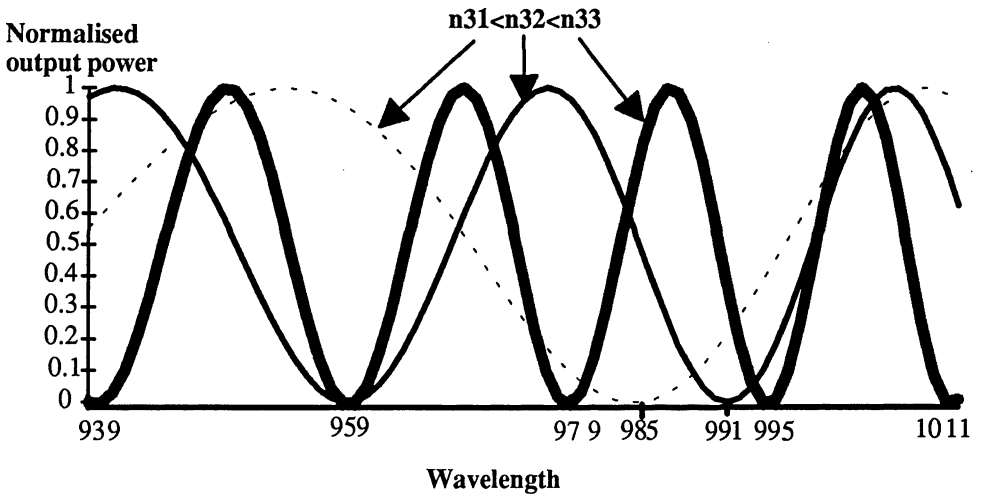

Figure 7.2.1 Normalised output power (one port) Vs wavelength for different surrounding medium

Instead of launching signal of consecutive wavelength, we can launch white light, which contain all wavelength components, into a core of a TOF at one end (or one input port of a TOFDC), then consecutively select different wavelength components at any one core of the output end and measure their amplitudes. The

result should be exactly the same as launching signal of consecutive wavelength. This is what we are going to do in our experiment.

There are two methods that utilise the power versus wavelength curve described above to obtain coupling coefficient of a twin-core fibre.

The first method is based on a modified formula of Eq.(3.3.2.3) or Eq.(3.3.2.4), which is

$$P_a(\lambda) = \cos^2[C(\lambda) \cdot z] \tag{7.2.1}$$

We take a piece of twin-core fibre (can be TOF, of course) and measure its power versus wavelength curve, then remove a very short section of the fibre and repeat the measurement again. At a certain wavelength, the output powers between these two measurement will have changed. The fibre can further be cut and measurement repeated until the power measured reaches its starting value. The total cut fibre length is twice the coupling length $2L_c$. Using Eq.(3.3.2.2), we can have coupling coefficient at the selected wavelength

$$C = \frac{\pi}{2L_c} \tag{7.2.2}$$

Using this method, coupling coefficient C at only the pre-selected wavelength is measured. To know C at other wavelength, it is necessary to repeat the above procedure. This method cannot be used when the coupling coefficient is large because the coupling length is then too short to be cut. Generally, it is necessary to have a prior knowledge of the approximate coupling length before this method is used.

The second method uses the relation of wavelengths at maximum and minimum power in the coupling spectrum [1]:

$$z \cdot C(\lambda_n) = m\pi + n\pi + \frac{\pi}{2} \quad (at\ \min ima) \tag{7.2.3.a}$$

$$z \cdot C(\lambda_n) = m\pi + n\pi + \pi \quad (at\ \max ima) \tag{7.2.3.b}$$

where z is the fibre length, $C(\lambda_n)$ is the coupling coefficient in wavelength λ_n, m is one of the integer in 0~M which makes Eq.(7.2.3) to be a true coupling coefficient versus wavelength (C vs λ) curve (M represents how many possible C vs λ curves will be taken for determination) and n=0,1,2,....,N is the count of the minimum (or maximum) power wavelength (where N is the number of minimum or maximum power wavelength to be taken in calculation). $C(\lambda_n)$ can be modelled as a polynomial

$$C(\lambda_n) = c_0 + c_1\lambda_n + c_2\lambda_n^2 + c_3\lambda_n^3 + ... + c_N\lambda_n^N \tag{7.2.4}$$

with c_n the expansion coefficient of the n^{th} order. By launching white light to one core of a twin-core fibre of length z_1 at its input end, and measuring the power versus wavelength spectrum (by consecutively select different wavelength components) at any one core of the output end, taking N+1 values of the minimum power wavelength $\lambda_0..\lambda_N$, we obtained equations

$$\begin{cases} c_0 + c_1\lambda_0 + c_2\lambda_0^2 + ... + c_N\lambda_0^N = \left(m + \frac{1}{2}\right)\frac{\pi}{z_1} \\ c_0 + c_1\lambda_1 + c_2\lambda_1^2 + ... + c_N\lambda_1^N = \left(m + \frac{3}{2}\right)\frac{\pi}{z_1} \\ \quad ..... \\ c_0 + c_1\lambda_N + c_2\lambda_N^2 + ... + c_N\lambda_N^N = \left(m + \frac{2N-1}{2}\right)\frac{\pi}{z_1} \end{cases} \tag{7.2.5}$$

Solving the above equations, we obtain a group of M C vs λ curves. To determine which one of the M curves is the true C vs λ curve, we cut the fiber to length z_2 and then repeat the measurement and calculation as for fibre z_1 to obtain another group of M C vs λ curves. We would find at least one curve at one group coincide with a curve of the other group. If more than one curves at one group coincide with the curves of the other group, we can take more cuts on the fibre then repeat what we did on z_1 and z_2 until each group has one curve coincide with one curve of each other group. The curve thus obtained is the real C Vs λ curve. An automated Pascal program that accepts measured minimum power wavelength and automatically plot the C Vs λ curve is written in Appendix D.

7.3 Experiment Setup

The experiment setup is shown in Fig.7.3.1. The white light source is a lamp emitting light of all wavelength components. The pin-hole is used for making the white light become a point source. The left Lens is used for focusing the light in one core only and the right Lens is used for separating light from the two cores at the fibre output. We use the 60x lens in our experiment. The three micro-positioner are used for minor position adjustment. The fibre holder is a steel block with a groove at the centre of the top surface, which is used to hold the fibre and the testing material (as surrounding medium of the twin-core offset fibre). All the above apparatus are mounted on a rail for easy alignment. The chopper is used for improving the signal to noise ratio. We set its rotating speed to approximately 333rpm. The pin-hole at the right is used to block all light except those from the core to be detected. The monochromator automatically scans to select the signal

of different wavelengths consecutively (passing only one wavelength component and block the others). The detector can be silicon or germanium detector, depending on the wavelength of the detected signal (Si for under 1100nm and Ge for over 1100nm. We use Si detector in our experiment). The lock-in amplifier amplifies and measures the detected signal and its amplification (or attenuation) can be adjusted according to the amplitude of the input signal. The computer controls the scanning (stepping) of the monochromator, samples the signal power from the amplifier and stores the sampled power value and the wavelength. Note that the pin-hole, the centre of the lens, the centre groove of the fibre holder, the centre of the inlet and outlet of the monochromator, and the detector must be in a straight line.

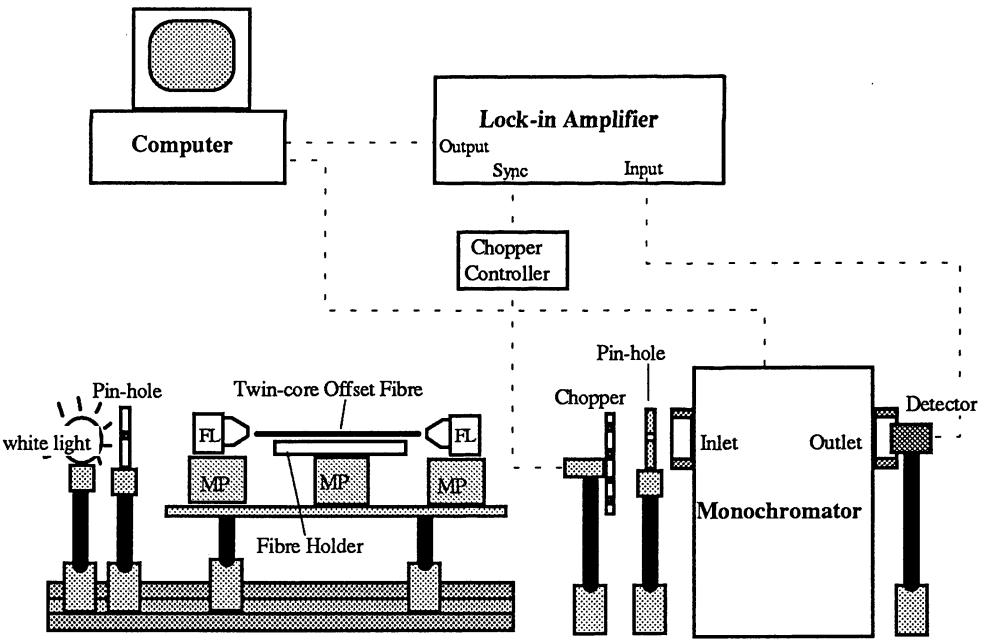

(FL: Focusing Len; MP: Micro-Positioner)

Figure 7.3.1 Diagram for experiment setup

7.4 Experiment Procedure and the Data Obtained

We first cut a section of twin-core offset fibre of 7.9cm in length (the end face must be cut to perpendicular to the fibre axis), and place it in the groove of the fibre holder and fix it using two small drop of fixing glue at each end of the groove (we use the mixture of silicon resin and silicon hardener because of its low refractive index). The fibre holder is then heated so that the fixing glue is set. We then place the fibre holder back to the micro-positioner and make final adjustment to the experiment setup. We launch the point white light through the pin-hole and lens to only one core of the twin-core offset fibre. Due to the coupling mechanism of the twin-core offset fibre, two bright spots can be observed at the output of the fibre (the straight through and the coupled outputs). After chopping the light, we allow only one bright spot at a time pass through the pin-hole to the inlet of the monochromator. We place a small drop of index matching liquid of liquid of value 1.333 to the fibre surface. We then cover the fibre with some cotton to keep the liquid in place. Based on our analysis on Sec.3.2, we should have used liquid of index 1.446 so that the effective cladding index n_{2eff} has a value of approximately 1.455 if the core is very close to the fibre surface. Unfortunately, the minimum distance from core to fibre surface of our fabricated TOF is rather large. We therefore use a liquid of lowest obtainable index to compensate for the closeness of the core to the surface. We then adjust the micro-positioner so that the bright spot from the straight through core goes into the monochromator and scan the output spectrum from the monochromator by means of a computer program (called pro47.exe). A straight through output power versus wavelength (P_2 vs λ) curve is thus obtained and stored in the computer. We again adjust the right hand side micro-positioner in Fig.7.3.1 so that another bright spot come from the coupled core goes into the monochromator and repeat the scanning and a coupled

power versus wavelength (P_4 vs λ) curve is obtained and stored. The stored P_2 vs λ and P_4 vs λ curves is reproduced in Fig.7.4.1. After some processing of the P_2 vs λ and P_4 vs λ curves, a normalised straight through and coupled power spectrum for surrounding liquid of index 1.333 (fibre length 7.9cm) is shown in fig.7.4.2.

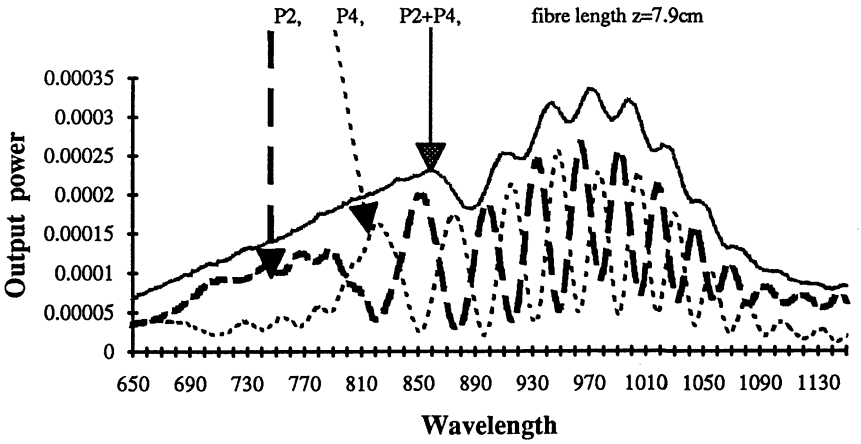

Figure 7.4.1 Experimentally measured power vs wavelength for our fabricated TOF with n3=1.333

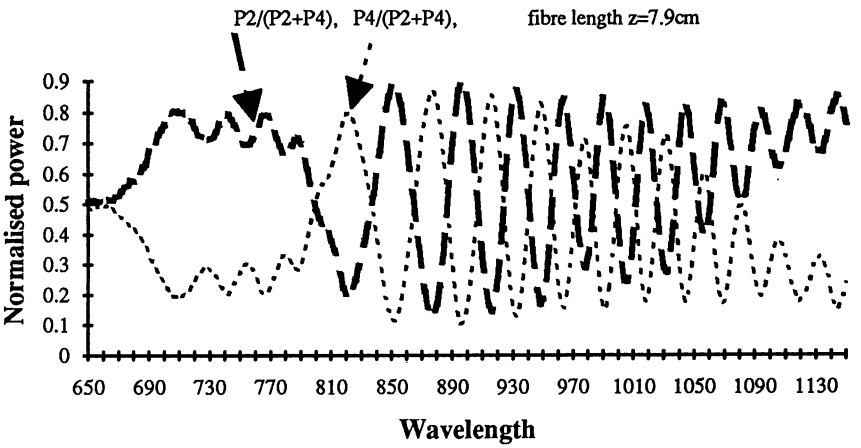

Figure 7.4.2 Experimentally measured normalised power vs wavelength for our fabricated TOF with n3=1.333

We repeat the above experiment by replacing the liquid of index 1.333 with the liquid of index 1.440 (wish to obtain an effective cladding index n_{2eff} of 1.457), while not moving any of the setup (can be realised by removing the cotton with 1.333 index liquid, washing the fibre with alcohol carefully, and drop some liquid of index 1.440 on the fibre and cover it with cotton). After finishing the same steps as we did in using 1.333 index liquid, we obtained another normalised power spectrum shown in Fig.7.4.3.

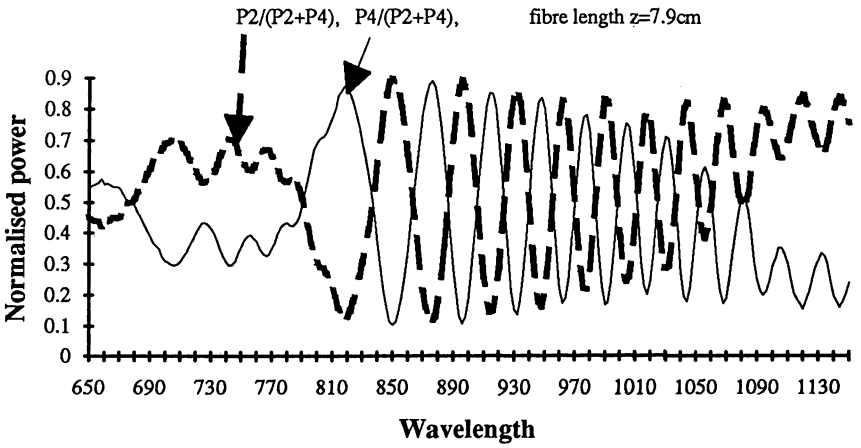

Figure 7.4.3 Experimentally measured normalised power vs

Again, we replace the 1.448 index liquid with 1.459 index liquid, which matches the cladding index value to make a 1.459 effective cladding index. Then we repeat the steps and another normalised power spectrum for n_3=1.459 is obtained and shown in Fig.7.4.4.

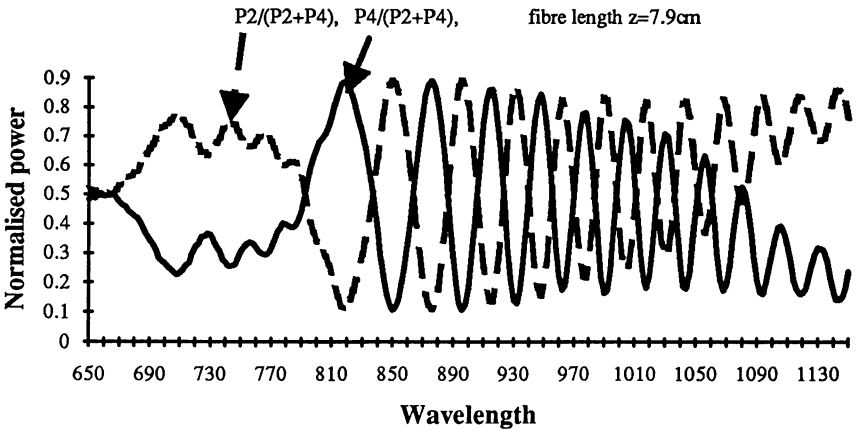

Figure 7.4.4 Experimentally measured normalised power vs wavelength curve for our fabricated TOF with n3=1.459

We again replace the 1.459 index liquid with 1.460 index liquid, which has higher index value than the inner cladding, then repeat the steps as we did before. Another power spectrum for n_3=1.460 is shown in Fig.7.4.5.

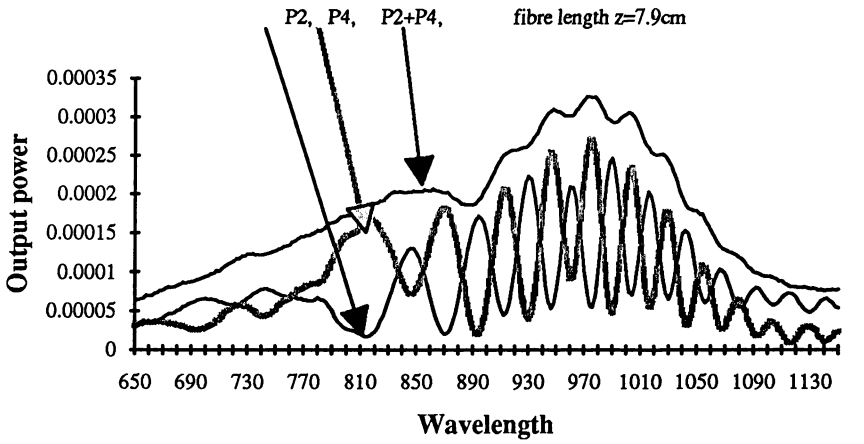

Figure 7.4.5 Experimentally measured output power vs wavelength curve for our fabricated TOF with n3=1.460

We extract only the coupled normalised power spectrum in the 850~1050 wavelength range from Fig.7.4.2~Fig.7.4.4 and combine them in Fig.7.4.6 for later reference.

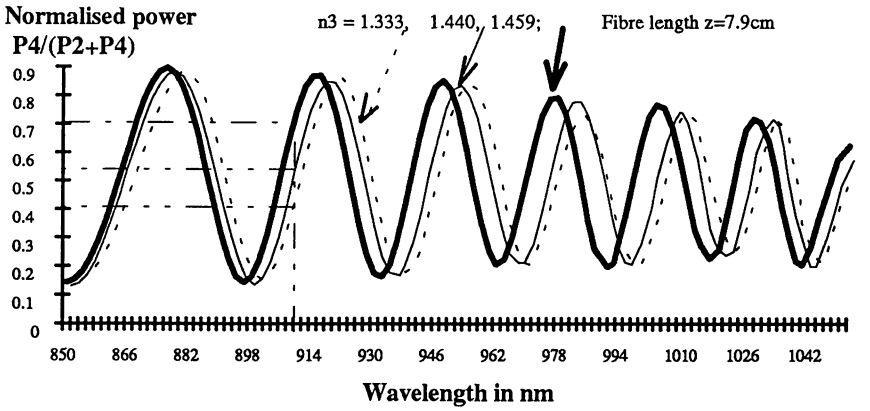

Figure 7.4.6 Measured normalised coupled power spectrum of our TOF (extracted figure, fibre length z=7.9cm)

We can find the wavelengths where the normalised coupled output power have the minimum value from Fig.7.4.6. These wavelength points are useful in the later coupling coefficient calculation, we list them in Table.7.4.1.

Refractive Index n_3 (surrounding liquid)	1.333	1.440	1.459
Wavelength #1	900nm	898nm	896nm
Wavelength #2	938nm	936nm	934nm
Wavelength #3	970nm	968nm	966nm
Wavelength #4	997nm	995nm	992nm
Wavelength #5	1021nm	1020nm	1017nm
Wavelength #6	1043nm	1042nm	1039nm

Table.7.4.1 The wavelength where detected coupled power reaches minimum for different n_3 when fibre length is 7.9cm

We then cut one end of the twin-core offset fibre (not remove it from the setup) so that its length become 7.7cm, and repeat the same experiment procedures as we did on 7.9cm length twin-core offset fibre. The normalised coupled power output

spectrum for using 1.333, 1.440, 1.459 are shown in Fig.7.4.7. The wavelengths for the detected minimum power also listed in Table.7.4.2.

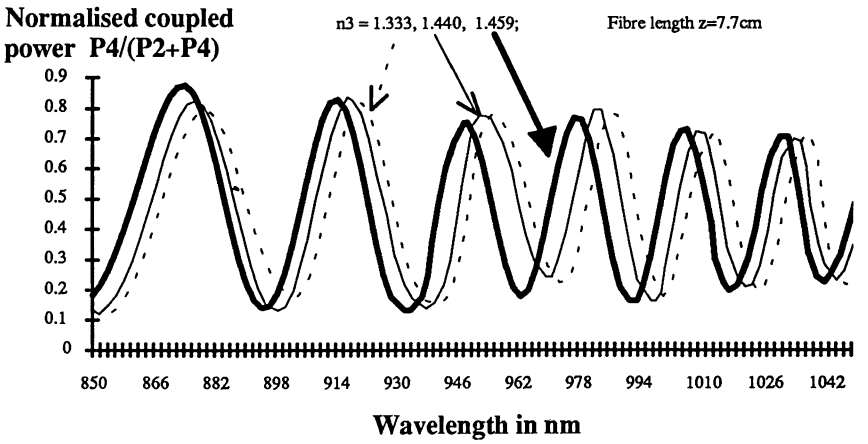

Figure 7.4.7 Measured normalised coupled power spectrum of our TOF (extracted figure, fibre length z=7.7cm)

Refractive index n_3 (surrounding liquid)	1.333	1.440	1.459
Wavelength #1	853nm	852nm	850nm
Wavelength #2	903nm	901nm	899nm
Wavelength #3	941nm	940nm	937nm
Wavelength #4	973nm	972nm	969nm
Wavelength #5	1001nm	999nm	996nm
Wavelength #6	1026nm	1024nm	1021nm
Wavelength #7	1048nm	1046nm	1043nm

Table.7.4.2 The wavelengthsa where detected coupled power reaches minimum for different n_3 when fibre length is 7.7cm

We again cut another end of the twin-core offset fibre so that the fibre length become 7.5cm and repeat the experiment exactly the same as for 7.7cm length fibre. The obtained normalised coupled output power versus wavelength is shown in Fig.7.4.8. The minimum power wavelengths listed in Table.7.4.3.

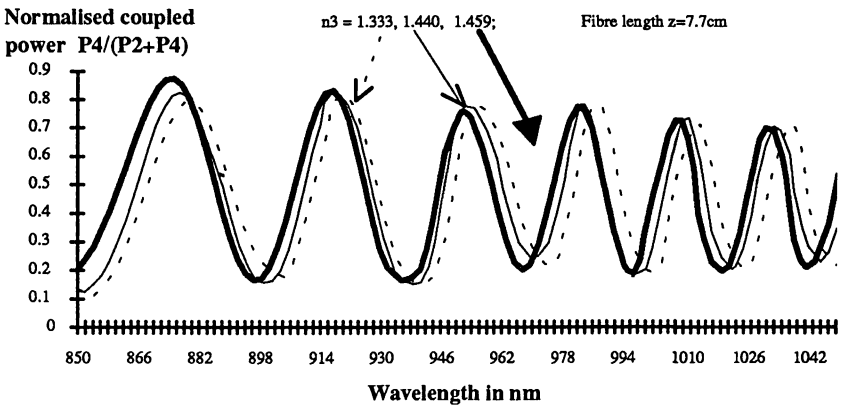

Figure 7.4.8 Measured normalised coupled power spectrum of our TOF (extracted figure, fibre length z=7.5cm)

Refractive index n_3 (surrounding liquid)	1.333	1.440	1.459
Wavelength #1	856	855	853
Wavelength #2	960	905	902
Wavelength #3	945	943	941
Wavelength #4	977	975	973
Wavelength #5	1005	1003	1001
Wavelength #6	1030	1028	1025
Wavelength #7	1052	1050	1048

Table.7.4.3 The wavelength where detected coupled power reaches minimum for different n_3 when fibre length is 7.5cm

7.5 Getting Coupling Coefficient From the Experiment Data

From the information shown in Table.7.4.1, Table.7.4.2 and Table.7.4.3, using the computer program in Appendix D, the coupling coefficient versus wavelength curves of our twin-core offset fibre with surrounding medium index of 1.333, 1.440 and 1.459 can be plotted directly in separate paper sheets. We can just run the program in Appendix D and follow the instruction to complete the calculation. After some processing, the three curves are combined in Fig.7.5.1 for comparison.

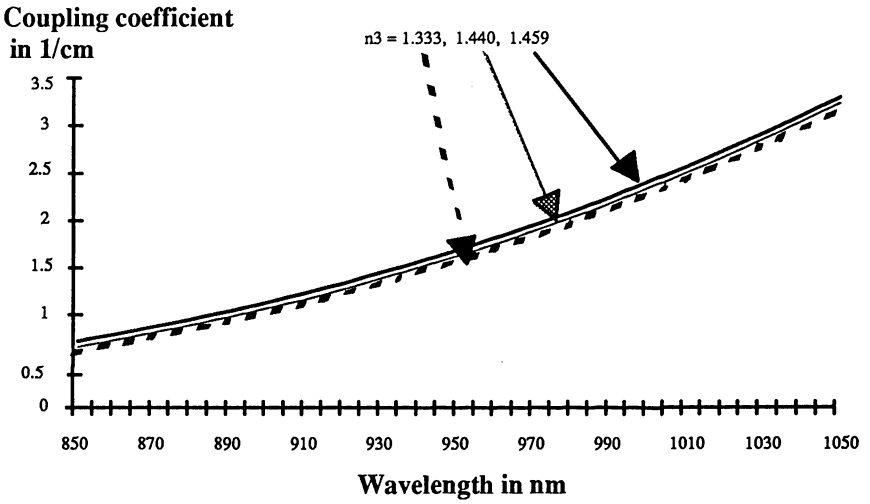

Figure 7.5.1 Coupling coefficient calculated from the experimental data

7.6 Discussion of the Experiment Results

For our designed twin-core offset fibre described in chapter 4, its theoretical normalised coupled power versus wavelength ($P_4/(P_2+P_4)$ Vs λ) curves (7.9cm in length) and coupling coefficient versus wavelength (C Vs λ) curves for effective cladding index of 1.455, 1.457, 1.459 are shown in Fig.7.6.1 and Fig.7.6.2.

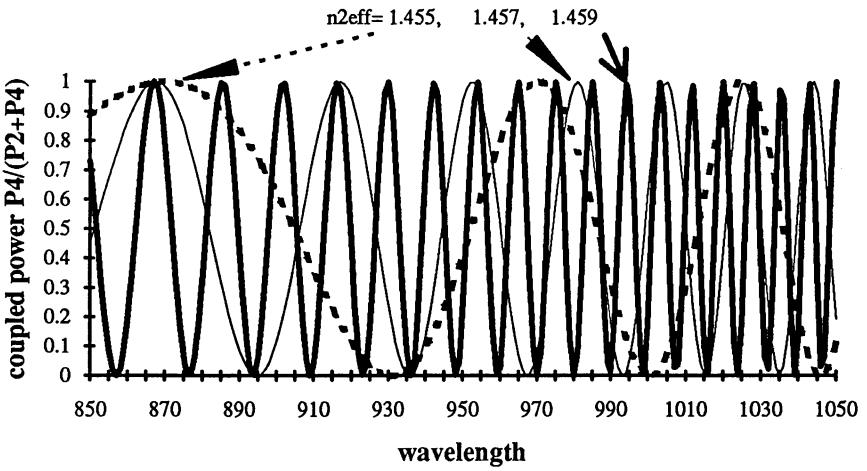

Figure 7.6.1 Theoretical calculated normalised coupled power vs wavelength curve of our designed TOF with

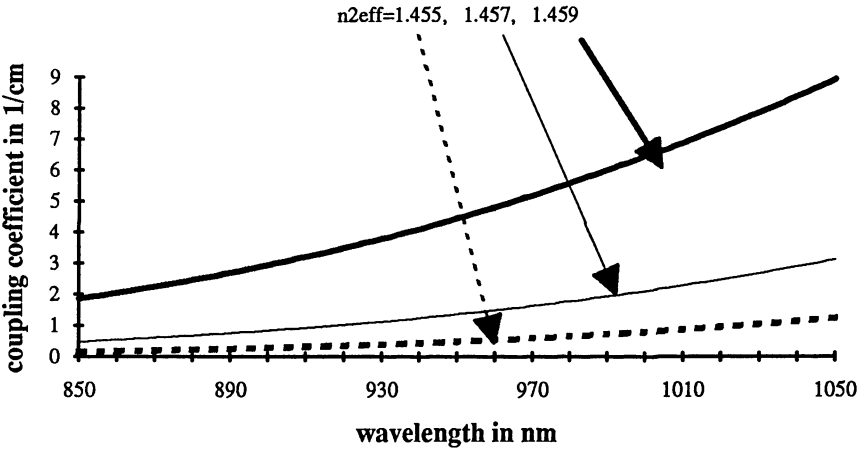

Figure.7.6.2 Theoretical calculated Coupling coefficient vs wavelength of our designed TOF with different n2eff

We again plot the theoretical normalised coupled power $P_4/(P_2+P_4)$ versus wavelength λ (7.9cm in length) and coupling coefficient C versus wavelength λ curve of our fabricated fibre described in chapter 5 in Fig.7.6.3 and Fig.7.6.4.

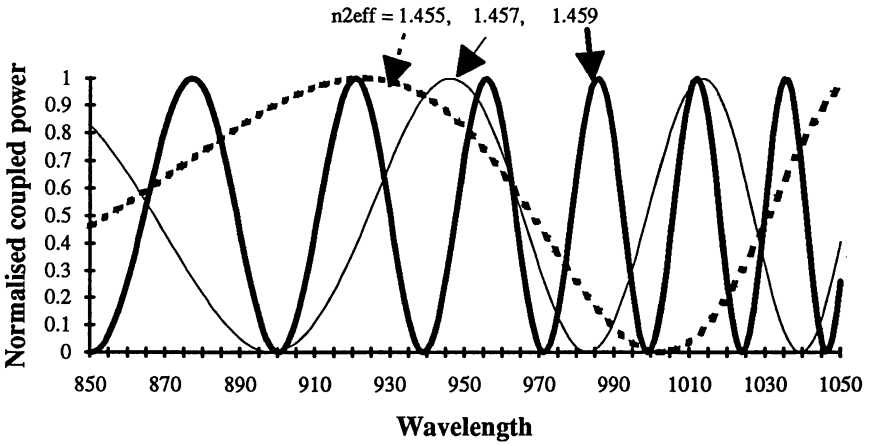

Figure 7.6.3 Theoretically calculated normalised coupled power vs wavelength for our fabricated TOF with different

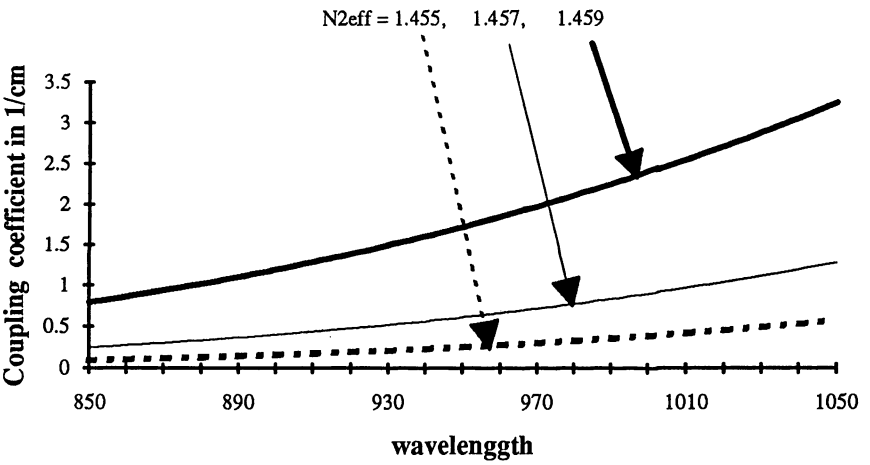

Figure 7.6.4 Theoretical calculated coupling coefficient vs wavelength of our fabricated TOF with different n2eff

From Fig.7.4.5~7.4.7 and Fig.7.5.1, we find small changes due to the index change of surrounding liquid, although the change is not as large as our expected one shown in Fig.7.6.1~7.6.4. We believe the insignificant change of coupling power with the index of surrounding liquid is due to the cores being too far from the fibre surface. However, for a twin-core offset fibre directional coupler (TOFDC), low index sensitivity is an advantage in many case, because the index of

most liquids are temperature sensitive, a low index sensitivity TOFDC can avoid the influence of temperature fluctuation, making it easy to control the splitting ratio and to increase the stability of the TOFDC. For example, a TOFDC made from our twin-core offset fibre is 7.9cm long. If the operation wavelength is 900nm, then from Fig.7.4.5, we can find that by varying the index of the surrounding liquid from 1.333, 1.440 to 1.459, the coupled output power can be varied from 40, 55 to 70 percent of the total output power, ie, the splitting ratio of the TOFDC can be varied from approximately 4, 2.6, to 1.55 decibels (ref Eq.6.2.1 and Eq.6.2.2). The best situation should have certain minimum core to fibre surface distance so that by varying the index of the surrounding liquid from 1.333 to 1.459, the splitting ratio of the TOFDC varies from 0 to 100 percent (or 0 to ∞ in decibel).

Again, we compare the 1.459 curves in Fig.7.5.1 and Fig.7.6.4, and find them quite similar. This proves that our measurement described in chapter 5 on the TOF's parameters is generally correct.

We expect that some higher order modes exist in short wavelength range less than 850nm because the core of our fabricated fibre is larger than our designed fibre. We cannot find this however in Fig.7.4.1 because the effective cladding index cannot be reduced to the designed value of 1.454. Actually, using the liquid of the lowest index we can get, the TOF remains in single moded more or less than 820nm wavelength with a thicker core.

Incomplete coupling is found in the experiment and is, we believe, due to the fact that the cores are not identical.

Only minor output power drop can be be seen when comparing Fig.7.4.1 and Fig.7.4.5, which indicated a very small amount of power lose in the n_2/n_3 interface. Because of the large distance of the interface to the core and the value of $|n_2 - n_3|$ is small (although negative), there is no wonder why we have this result.

References of chapter 7:

[1] Peng G.D., Tjugiarto T., Chu P.L.: Twin-core Optical Fibre With Large Core Ellipicity, Appl. Opt., Vol.30, No.6, 632-634, 1991.

Chapter 8

Summary

We proposed a new type of fibres, the twin-core offset fibres (TOF). The TOF is based on the idea of Twin-core D fibre. However, it is difficult to obtain a twin-core D fibre with the required parameters using the preform drawing method because its cross-sectional shape, thickness and hence core radius, core separation, etc, vary in the fibre drawing process due to the asymmetry of the preform. On the other hand, the length of a twin-core D fibre fabricated by fibre polishing method is very limited. A long TOF with uniform and controlled parameters is easy to obtain, in contrast. In addition, little analysis has been done on twin-core D fibre previously. We performed the analytical work on TOF both theoretically and experimentally, which can be applied to twin-core D fibres. Although our analytical work on TOF is not comprehensive, we believe it is a worthy start.

We then developed a systematic method of designing and fabricating TOFs based on the previous twin-core fibre fabrication method. Comparing with the previous method, the new method provides a step by step control of not only the TOF

fabrication process, but also the general twin-core fibres. A TOF has been fabricated using the newly developed method in our laboratory. However, we find the core radius and the minimum distance from core to fibre surface of the TOF are larger than our designed values. We believe some mistakes have been made during the fabrication process. Fortunately, we find later that larger minimum distance from core to fibre surface can improve the stability of a twin-core offset fibre directional coupler (TOFDC) and reduce the influence of temperature fluctuation. A compromise should be made between too close and too far a distance from core to fibre surface.

We then propose a new type of tunable directional couplers, the twin-core offset fibre directional couplers (TOFDC). This type of couplers is not actually been fabricated due to the reason explained in Sec.6.1 of chapter 6. We believe the advantage of TOFDCs is that they can provide more convenient and smooth tunning of the power splitting ratio than the previous tunable directional couplers. Some application of the TOFDCs are also discussed.

We finally conducted experiments on the TOF. The results of the experiments shows the effect we expected, although not exactly in agreement. We believe that further reducing the minimum distance from core to fibre surface, the effect would be much more dominant.

By further understanding the characteristics of the TOFs and TOFDCs, and improving the accuracy in the fabrication process, we believe that they can eventually be applied to practical uses.

Appendix A

Pascal program for calculating the electric field distribution in a conventional single-core fibre

---

```
program EvsR_exact;
uses crt, specfunc;
var
  i,x,y, errflag:integer;
  E1, E2: array [-40..40] of real;
  K, Wg, V, U, W, r: real;
  outfile: text;
  filename: string[20];
begin
  write('enter V value: ');
  readln(V);
  Wg:=0.65+(1.619/(sqrt(v*v*v)))+(2.879/(v*v*v*v*v*v));
  W:=1.1428*V - 0.996;
  U:=sqrt((V*V)-(W*W));
  write('enter filename to store E-r_ext result: ');
  readln(filename);
  assign(outfile,filename);
  rewrite(outfile);
  r:=0.2;
  x:=1;
  y:=-1;
  K:=Bessel(0,U,errflag)/ModbesselK(0,W);
  while r<=3 do
  begin
    if r<=1 then
      E1[x]:=bessel(0,U*r,errflag)
    else
      E1[x]:=K*ModBesselK(0,W*r);
    E2[x]:=exp(-sqr(r/Wg));
    E1[y]:=E1[x];
    E2[y]:=E2[x];
    x:=x+1;
```

```
    y:=y-1;
    r:=r+0.2;
  end;
  for I:=(y+1) to (x-1) do
  begin
    writeln(i,',',E1[i],',',E2[i]);
    writeln(outfile,i,',',E1[i],',',E2[i]);
  end;
  close(outfile);
end.
```

Appendix B

Pascal Program for Calculating Output Spectrum of A Twin-core Fibre

---

```
program FibreValueCalcu;
uses
   crt,printer,specfunc;
const
   order=1;
   Z=6{cm};
var
   wl,wlx,wli:integer;
   P,wlr,wlxr,wlir,N1,N2eff,d,r,
   Dalta,U,V,W,C,K1:real;
   Errflag:integer;
   outfile:text;
   filename:string[20];

Begin
   clrscr;
 {  write('Enter N1: ');
   readln(N1);          }
   Nco:=1.464;
   write('Enter N2eff: ');
   readln(N2eff);
 {  write('Enter Distance between cores in um: ');
   readln(d);    }
   d:=9.8;
   d:=d*1e-4;
{   write('Enter Diameter of the core in um: ');
   readln(d);}
```

```
    r:=1.9;
    r:=r*1e-4;
{     write('Enter Minumn Wavelength in nm: ');
    readln(wli);
    write('Enter Maximun Wavelength in nm: ');
    readln(wlx);}
    wli:=850;
    wlx:=1050;
    Dalta:=(n1-n2eff)/n1;
    write('Enter file name for store WL and p: ');
    readln(filename);
    assign(outfile,filename);
    rewrite(outfile);
    wl:=wli;
    while wl<=wlx do
    begin
     wlr:=wl*1e-7;
     V:=2*Pi*r*sqrt((N1*N1)-(N2eff*N2eff))/Wlr;
     if ((v<1.4)  or (V>2.5)) then
      writeln('V out of range, V=',v);
     W:=(1.1428*V)-0.996;
     U:=sqrt((V*V)-(W*W));
     K1:=ModBesselK(1,W);
     C:=sqrt((Pi*Dalta)/(W*d*r))*(U*U)/(V*V*V*(exp(W*d/r))*K1*k1*w);
     P:=sin(C*Z)*sin(C*Z);
     writeln(outfile,wl,',',P);
     writeln(wl,',',P);
     wl:=wl+1;
    end;
    close(outfile);
end.
```

Appendix C

Pascal program for plotting coupling coefficient versus relative refractive index difference curve

---

```
program FibreValueCalcu;
uses
   crt,printer,specfunc;
const
   order=1;
   z=5;
var
   wl,N1,N2eff,N2effi,N2effx,d,r,
   p,Dalta,U,V,W,C,K1,x,y:real;
   Errflag:integer;
   outfile:text;
   filename:string[20];

Begin
   clrscr;
 {  write('Enter N1: ');
   readln(Nco);          }
   N1:=1.464;
   write('Enter wavelength: ');
   readln(wl);
 {  write('Enter Distance between cores in um: ');
   readln(d);    }
   d:=12;
   d:=d*1e-4;
{   write('Enter Diameter of the core in um: ');
   readln(d);}
   r:=3;
   r:=r*1e-4;
{    write('Enter Minumn Wavelength in nm: ');
   readln(wli);
```

```
    write('Enter Maximun Wavelength in nm: ');
    readln(wlx);}
    N2effi:=1.450;
    N2effx:=1.463;
    wl:=wl*1e-7;
    write('Enter file name for store Dalta and p: ');
    readln(filename);
    assign(outfile,filename);
    rewrite(outfile);
    N2eff:=N2effx;
    dalta:=0.00007;
    while dalta<=0.009 do
    begin
     Dalta:=(N1-N2eff)/N1;
     V:=2*Pi*r*sqrt((N1*N1)-(N2eff*N2eff))/Wl;
     if ((v>2.5) or (v<1.5)) then
      writeln('v out of range ');
{    W:=(1.1428*V)-0.996;
     U:=sqrt((V*V)-(W*W));}
     x:=(v+1)*(v+1)*(v+1);
     y:=x*(v+1)*(v+1);
     U:=2.405*V*(1-(0.964004/x)-(1.67274726/y))/(v+1);
     w:=sqrt((v*v)-(u*u));
     K1:=ModBesselK(1,W);
     C:=sqrt((Pi*Dalta)/(W*d*r))*(U*U)/(V*V*V*(exp(W*d/r))*K1*k1*w);
{     P:=sqr(cos(C*z));}
     writeln(outfile,dalta,',',c);
     writeln(dalta,',',c);
     N2eff:=N2eff-0.0002;
    end;
    close(outfile);
    {writeln('Nco=',Nco:6:4,'Delta=',Dalta,'WL=',WL,'s/r=',Ds/R,'z=',z);}
end.
```

Appendix D

Pascal Program for Deriving Coupling Coefficient C and Plot a C Versus Wavelength Curve of a Twin-core Fibre According to the Experimental Data

(Just run the program and follow the instruction)

```
program FindOutCCoef(input, output, infile, outfile);
uses  crt, stdhdr, gj, mulreg, segraph, worlddr, curvefit, dos, plotunit;
const
  NoOfCutPpt='How many cuts on fibre? Enter a number:  ';
  NoMinCut=2;      NoMaxCut=6;
  NoOfCurvPpt='How many curves take for each cut, Enter a number:  ';
  NoMinCurv=2;      NoMaxCurv=40;
  NoOfMinPonPpt='Enter Number of min  power wavelength taken in P Vs wavelength curve:';
  MinNoMinPon=2;     MaxNoMinPon=12;
  StartWalenPpt='Enter starting wavelength of your calculation: ';
  MinStartWalen=500; MaxStartWalen=1000;
  EndWalenPpt='Enter ending wavelength of your calculation: ';
  MinEndWalen=700;   MaxEndWalen=1600;
  WalenStepPpt='Enter wavelength step of your calculation: ';
  MinWalenStep=1;    MaxWalenStep=100;
  MinWalen=500;      MaxWalen=1600;
  FitOrderPpt='Enter fitting order: ';
  minfitorder=3;     maxfitorder=8;
Type
  FibreLenNoRange=0..NoMaxCut;
  MinPonNoRange=0..MaxNoMinPon;
  CurvNoRange=0..NoMaxCurv;
  FLType=Array [FibreLenNoRange] of real;
  MPWType=Array [FibreLenNoRange,MinPonNoRange] of integer;
  MPWRtype=array [fibrelenNoRange,MinPonNoRange] of real;
```

```
  FilenameType=string[20];
  UnitType=string[2];
  ArrayFileNameType=Array [0..NoMaxCut] of FilenameType;
Var
  CurvNo, Walen, MinPonNo, GroupNo, NoOfCut, NoOfCurv,NoOfMinPon,
  StartWalen, EndWalen, WalenStep, fitorder, OutPutUnit: integer;
  FibreLen,fibrelenr: FLType;
  MinPonWalen: MPWType;
  MinPonWalenr:MPWrtype;
  infile,outfile, outfile1, outfile2: text;
  filename, filename1, filsname2: Filenametype;
  startwalenr,endwalenr,walenstepr:real;
  units:UnitType;
  tem: ArrayFilenameType;
  Elem_Switched:boolean;

procedure pause;
begin
  writeln('Press Enter to continue....');
  readln;
end;

procedure refresh;
var     i:integer;
begin
   clrscr;
   for i:=0 to 8 do
      writeln;
end;

procedure Instruction;
begin
  clrscr;
  write('  This is the program for calculating the coupling ');
  write('coefficient of a twin-core fibre, the following ');
  writeln('steps should be done before using this program:');
  writeln;
  write('A. Cut a piece of twin-core fibre, note down its length,');
  write(' then measure its output power vs wavelength curve using');
```

```
  write(' monochrometer, from this curve, find as many minmun ');
  write('power points as possible, note down the wavelengths of ');
  writeln('these points. ');
  writeln;
  write('B. Cut the same fibre again, repeat the work in A, it ');
  writeln('require 3 or more cuts for a accurate calculation. ');
  writeln;
  write('C. From the noted down record obtained above, select ');
  write('a set of same number consecutive minmun power point ');
  write('wavelengths in each cut, they are required when performing');
  writeln(' the calculation. ');
  writeln;
  write('D. Performing the calculation follow the instruction, you');
  write(' will get data files for each fibre cut, the first column');
  write(' of these data file are wavelenths, the other columns are');
  write(' coupling coefficiences of different n (from 0 to Number ');
  write('of curves you indicated minus 1), we draw them as a ');
  write('series of Coupling coefficients vs wavelength curve, we');
  write(' can find one curve in each group of curves of the same ');
  write('cut would be almost the same, this curve is the coupling ');
  writeln('coefficient vs wavelength curve we want.');
  writeln;
  write('After you sure what to do and get the measured data ready, ');
  pause;
  writeln;
end;

Function Get_Require(prompt: string; Min, Max: integer): integer;
Var     Require: integer;
Begin
    write(prompt);
    readln(require);
    while (require<min) or (require>max) do
    begin
        writeln(prompt);
        readln(require)
    end;
    Get_Require:=require
end;
```

```
procedure read_data_from_file(var infile4:text; filename4:filenametype;
          var noc4,nomp4:integer; var fl4:fltype; var mpw4:mpwtype);
var       count1,count2:integer;
begin
  refresh;
  write('Enter filename from which to obtain data: ');
  readln(filename4);
  assign(infile4,filename4);
  reset(infile4);
  readln(infile4,noc4);
  readln(infile4);
  readln(infile4,nomp4);
  readln(infile4);
  for count1:=0 to (noc4-1) do
  begin
   readln(infile4,fl4[count1]);
   for count2:=0 to (nomp4-1) do
    read(infile4,mpw4[count1,count2]);
   readln(infile4);
  end;
 close(infile4)
end;

procedure Create_A_Data_File(Var Outfilec:text; Filenamec
        :FilenameType; var nocc,nompc:integer; var flc:fltype; var
        mpwc:mpwtype);
Var       count1,count2:integer;
begin
   refresh;
   write('Enter filename for saving data: ');
   readln(filenamec);
   writeln;
   assign(outfilec,filenamec);
   rewrite(outfilec);
   refresh;
   nocc:=get_require(NoOfCutPpt,NoMinCut,NoMaxCut);
   writeln;
   writeln(outfilec,nocc);
```

```
    writeln(outfilec);
    refresh;
    nompc:=get_require(NoOfMinPonPpt,MinNoMinPon,MaxNoMinPon);
    writeln;
    writeln(outfilec,nompc);
    writeln(outfilec);
    for count1:=0 to (nocc-1) do
     begin
      write('Enter length(mm) of the No',count1+1,' fibre cut of total ',nocc,': ');
      readln(flc[count1]);
      writeln;
      writeln(outfilec,flc[count1]);
      for count2:=0 to (nompc-1) do
       begin
        write('Enter the No',count2+1,' minumun power point wavelength');
        write('(nm) of total ',nompc,': ');
        readln(mpwc[count1,count2]);
        writeln;
        write(outfilec,mpwc[count1,count2],' ');
       end;
      writeln(outfilec);
     end;
   close(outfilec);
end;

procedure Get_Experiment_Info(var infiles,outfiles:text; var filenames:
          filenametype; var nocs,nomps:integer; var fls:fltype;
          var mpws:mpwtype);
var       choice:integer;
begin
 refresh;
 write('Press 1 to use existing data file or 2 to create a new one: ');
 readln(choice);
 writeln;
 while ((choice <> 1) and (choice <> 2)) do
   begin
    write('Press 1 to use existing data file or 2 to create a new one: ');
    readln(choice);
    writeln;
```

```
    end;
  if choice=1 then
     read_data_from_file(infiles,filenames,nocs,nomps,fls,mpws)
  else
     create_a_data_file(outfiles,filenames,nocs,nomps,fls,mpws);
end;

procedure check_input_info(NoOfCut1:integer;fibrelen1:fltype;NoOfMinPon1:
          Integer;MinPonWalen1:MPWtype);
var       GroupNo1,MinPonNo1:integer;
begin
   clrscr;
   writeln;
   writeln;
   Writeln('Please Check whether the entered information match the measured ones!');
   writeln;
   writeln;
   for GroupNo1:=0 to (NoOfCut1-1) do
   begin
     writeln('The entered Fibre Length of the No',GroupNo1+1,' Cut is ',
                FibreLen1[GroupNo1]);
     writeln('The entered ',NoOfMinPon1,' Minmum Point Wavelength are shown below: ');
     for MinPonNo1:=0 to (NoOfMinPon1-1) do
        write(MinPonWalen1[GroupNo1, MinPonNo1],' ');
     writeln;
     writeln;
   end;
   pause;
end;

procedure Calculation_requirement(Var NoOfCurva,StartWalena,Endwalena,
          WalenStepa,fitordera,OutPutUnita:integer);
  var     option:integer;
  begin
    refresh;
    write('If you want to use the preseted Calculation requirement (NOCU25 ');
    writeln('SW600 EW1200 ');
    writeln('WS20 FO3 OPUcm), press 1 then enter');
    writeln;
```

```
  writeln('If you want to specify your own, press 2 then enter. ');
  writeln('Suggest specify your own requirements!');
  write('Number of cuts prefer 3 or more, number of minimum power savelengths ');
  write('depends on the wavelength range of C you want, number of curves recommdnds 8');
  writeln;
  write('Enter your option: ');
  readln(option);
  while (option<>1) and (option<>2) do
      readln(option);
  If option=1 then
   begin
      NoOfCurva:=25;
      StartWalena:=600;
      EndWalena:=1200;
      WalenStepa:=20;
      FitOrdera:=3;
      OutPutUnita:=2;
   end
   else
    begin
     refresh;
     NoOfCurva:=Get_require(NoOfCurvPpt,NoMinCurv,NoMaxCurv);
     writeln;
     StartWalena:=Get_require(StartWalenPpt,MinStartWalen,MaxStartWalen);
     writeln;
     EndWalena:=Get_Require(EndWalenPpt,MinEndWalen,MaxEndWalen);
     writeln;
     WalenStepa:=Get_Require(WalenStepPpt,MinWalenStep,MaxWalenStep);
     writeln;
     writeln('recommeded fitting order: 3');
     fitordera:=get_require(fitorderPpt,minfitorder,Maxfitorder);
     writeln;
     write('Choose output unit (1-m,2-cm,3-mm,4-um,5-nm), recommends 2: ');
     readln(OutPutUnita);
     writeln;
    end;
 end;

procedure Unit_Conversion(mpw2:mpwtype; sw2,ew2,ws2,noc2,nomp2,OutPutUnit2:
```

```
        integer;fl2:fltype; var mpw2r:mpwrtype; var sw2r,ew2r,ws2r:real;
        var fl2r:fltype; var units2:UnitType);
var      gn2,mpn2:integer;
begin
   case OutPutUnit2 of
     1:
     begin
      for gn2:=0 to (noc2-1) do
      begin
       fl2r[gn2]:=fl2[gn2]*1e-3;
       for mpn2:=0 to (nomp2-1) do
         mpw2r[gn2,mpn2]:=mpw2[gn2,mpn2]*1e-9;
      end;
      sw2r:=sw2*1e-9;
      ew2r:=ew2*1e-9;
      ws2r:=ws2*1e-9;
      units2:='m';
     end;
     2:
     begin
      for gn2:=0 to (noc2-1) do
      begin
       fl2r[gn2]:=fl2[gn2]*1e-1;
       for mpn2:=0 to (nomp2-1) do
         mpw2r[gn2,mpn2]:=mpw2[gn2,mpn2]*1e-7;
      end;
      sw2r:=sw2*1e-7;
      ew2r:=ew2*1e-7;
      ws2r:=ws2*1e-7;
      units2:='cm';
     end;
     3:
     begin
      for gn2:=0 to (noc2-1) do
      begin
       fl2r[gn2]:=fl2[gn2];
       for mpn2:=0 to (nomp2-1) do
         mpw2r[gn2,mpn2]:=mpw2[gn2,mpn2]*1e-6;
      end;
```

```
        sw2r:=sw2*1e-6;
        ew2r:=ew2*1e-6;
        ws2r:=ws2*1e-6;
        units2:='mm';
      end;
      4:
      begin
        for gn2:=0 to (noc2-1) do
        begin
          fl2r[gn2]:=fl2[gn2]*1e3;
          for mpn2:=0 to (nomp2-1) do
            mpw2r[gn2,mpn2]:=mpw2[gn2,mpn2]*1e-3;
        end;
        sw2r:=sw2*1e-3;
        ew2r:=ew2*1e-3;
        ws2r:=ws2*1e-3;
        units2:='um';
      end;
      5:
      begin
        for gn2:=0 to (noc2-1) do
        begin
          fl2r[gn2]:=fl2[gn2]*1e6;
          for mpn2:=0 to (nomp2-1) do
            mpw2r[gn2,mpn2]:=mpw2[gn2,mpn2];
        end;
        sw2r:=sw2;
        ew2r:=ew2;
        ws2r:=ws2;
        units2:='nm';
      end;
    end{case};
    refresh;
    writeln('Unint conversion completed.');
    pause;
end{unit_conversion};

Procedure Calcu_Cs_and_Output(Var Outfile3, outfile2:text; Filename3, filename2:
      FilenameType; mpw3r:mpwrtype;NOMP3,NOC3,NOCU3,SW3,EW3,
```

```
        WS3,fitorder3:integer; sw3r,ws3r:real; fl3,fl3r:FLType;
        units3:UnitType; var tem3: ArrayFilenameType);
Var     GN3,CN3,wl3,order:integer;
        WL3r,cc3:real;
        directry,LenSymbal:string;
  Function C_Calcu(GN1, CN1, NOMP1, fitorder1:integer; WLr1:real; MPWr1:MPWrType;
          FLr1:FLType): real;
  Var     x, y, yest, resid: longvector;
          coefsig, solution: shortvector;
          wlx, count1: integer;
          wlxr, c, see, det, rval: real;
          cferror: boolean;
  Begin
    for count1:=0 to (nomp1-1) do
       x[count1]:=mpwr1[gn1,count1];
    for count1:=0 to (nomp1-1) do
       y[count1]:=(cn1+count1+0.5)*Pi/flr1[gn1];
    PolyCurveFit(x,y,nomp1,fitorder1,solution,yest,resid,see,coefsig,det,rval,cferror);
    c:=0;
    wlxr:=wlr1;
    for count1:=0 to fitorder1 do
    begin
      c:=c+solution[count1]*wlxr/wlr1;
      wlxr:=wlxr*wlr1;
    end;
    c_calcu:=c;
  End;
Begin
    refresh;
    write('Indicate the drive & directry where you want to save C files to, ');
    writeln('or non ');
    writeln;
    write('for current directry, the files will be named automatically ');
    writeln('according to their ');
    writeln;
    write('output unit & fibre lengths: ');
    readln(directry);
    writeln;
    for GN3:=0 to (NOC3-1) do
```

```
    begin
      str(round(fl3[gn3]),LenSymbal);
      filename3:=concat(directry,'C_',units3,LenSymbal);
      filename2:=concat(filename3,'.csv');
      tem3[GN3]:=filename3;
      assign(outfile3,filename3);
      assign(outfile2,filename2);
      rewrite(outfile3);
      rewrite(outfile2);
      refresh;
      writeln('Now write to ',filename3);
      wl3:=sw3;
      wl3r:=sw3r;
      repeat
        write(wl3,' ');
        write(outfile3,wl3,' ');
        write(outfile2,wl3,',');
        for cn3:=0 to (nocu3-1) do
        begin
          cc3:=c_calcu(gn3,cn3,nomp3,fitorder3,wl3r,mpw3r,fl3r);
          write(cc3,' ');
          write(outfile3,cc3,' ');
          write(outfile2.cc3,',');
        end;
        writeln;
        writeln(outfile3);
        writeln(outfile2);
        wl3:=wl3+ws3;
        wl3r:=wl3r+ws3r;
      until wl3>ew3;
      close(outfile3);
      close(outfile2);
    end;
end;

Procedure FindOutRealC(Var infile,outfile,outfile1:text; var filename,filename1:filenametype;
        tem:ArrayFilenameType;NoOfCut,NoOfCurv,startWalen,WalenStep:integer);
label
    DropCurenCurv;
```

```
var
   FirstC, SecondC: Array [0..(MaxWalen-MinWalen)] of real;
   GN,CurvPairNo,CN1,StepNo,count,CN2,tempCurvNo0yxy_0,tempCurvNo0yxy_x,
   TotalMatch,G0G1CN_0,G0GxCN_0:integer;
   Accumulator,tempC,realC,wl:real;
   CDiff0yxy:array [0..((NoMaxCurv*NoMaxCurv)-1)] of real;
   CurvNo0yxy_0,CurvNo0yxy_x:array [0..((NoMaxCurv*NoMaxCurv)-1)] of integer;
   CDiff:array [0..(NoMaxCut-1),0..2] of real;
   GNCN0yxyMin_0,GNCN0yxyMin_x:array [0..(NoMaxCut-1),0..2] of integer;
   G0GxCN_x:Array [1..(NoMaxCut-1)] of integer;
   elem_switched:boolean;
Begin{findoutc}
 clrscr;
 writeln('Wait while the data being processed...');
 {The whole process below are: choose first curve from file0, then find the
 difference between this curve and all the curves in file1, save their
 difference and curve No in both file; choose second curve from file0,
 repeat the above process, until all curves in file0 processed. Note that
 there is only one array sequence in file0 and any other file pair. After
 obtained the differences, bubble sort to find the smallest three C curve
 difference pairs, save their curve No in individual file}
 for GN:=1 to (NoOfCut-1) do
 begin
  Writeln('Now looking for common C curves of file No0 and No',GN);
  CurvPairNo:=0;
  for CN1:=0 to (NoOfCurv-1) do
  begin
   writeln('Choose Curve No',CN1,' of file No0..');
   Assign(infile,tem[0]);
   reset(infile);
   StepNo:=0;
   while not EOF(infile) do
   begin
    read(infile,wl);
    for count:=0 to CN1 do
     read(infile,FirstC[StepNo]);
    readln(infile);
    StepNo:=StepNo+1;
   end;
```

```
  close(infile);
  For CN2:=0 to (NoOfCurv-1) do
  begin
   writeln('Choose Curve No',CN2,' of file No',GN,'...');
   Assign(infile,Tem[GN]);
   reset(infile);
   StepNo:=0;
   while not EOF(infile) do
   begin
    read(infile,wl);
    for count:=0 to CN2 do
     read(infile,SecondC[StepNo]);
    readln(infile);
    StepNo:=StepNo+1;
   end;
   close(infile);
   write('Compare C difference between Curve No',CN1);
   writeln(' File0 and Curve No',CN2,' File',GN);
   accumulator:=0;
   for count:=0 to (StepNo-1) do
    Accumulator:=Accumulator+abs(FirstC[count]-SecondC[count]);
    {Find difference of 2 C curves in different files}
   CDiff0yxy[CurvPairNo]:=Accumulator/StepNo;
   {Save C difference of curtain curve in 0 file and a curve in other file}
   CurvNo0yxy_0[CurvPairNo]:=CN1;
   {Save Curve No in 0 file}
   CurvNo0yxy_x[CurvPairNo]:=CN2;
   {Save Curve No in another file}
   CurvPairNo:=CurvPairNo+1;
  end;
end;
{Bubble sort the first 3 smallest C difference between a curve in file0
 and a curve in another file, save both the curve No in file0 and fileK}
write('Now looking for first 3 smallest C difference curve pair of ');
writeln('file0 and file',GN);
Count:=0;
Elem_Switched:=true;
while ((count<=2) and (elem_switched=true))  do
begin
```

```
    CurvPairNo:=Sqr(NoOfCurv)-1;
    elem_switched:=false;
    while (CurvPairNo>=count+1) do
    begin
     if CDiff0yxy[CurvPairNo-1]>CDiff0yxy[CurvPairNo] then
     begin
      tempC:=CDiff0yxy[CurvPairNo-1];
      tempCurvNo0yxy_0:=CurvNo0yxy_0[CurvPairNo-1];
      tempCurvNo0yxy_x:=CurvNo0yxy_x[CurvPairNo-1];
      CDiff0yxy[CurvPairNo-1]:=CDiff0yxy[CurvPairNo];
      CurvNo0yxy_0[CurvPairNo-1]:=CurvNo0yxy_0[CurvPairNo];
      CurvNo0yxy_x[CurvPairNo-1]:=CurvNo0yxy_x[CurvPairNo];
      CDiff0yxy[CurvPairNo]:=tempC;
      CurvNo0yxy_0[CurvPairNo]:=tempCurvNo0yxy_0;
      CurvNo0yxy_x[CurvPairNo]:=tempCurvNo0yxy_x;
      elem_switched:=true;
     end;
     CurvPairNo:=CurvPairNo-1;
    end;
    Count:=Count+1;
  end;
  For CurvPairNo:=0 to 2 do
  begin
   CDiff[GN,CurvPairNo]:=CDiff0yxy[CurvPairNo];
   GNCN0yxyMin_0[GN,CurvPairNo]:=CurvNo0yxy_0[CurvPairNo];
   {Save the curve No in file0 of the 3 smallest difference C curve of
   file0 and fileK}
   write('The curve No in file0 of the No',curvpairNo,' smallest ');
   writeln('difference C curve pair is ',GNCN0yxyMin_0[GN,CurvPairNo]);
   GNCN0yxyMin_x[GN,CurvPairNO]:=CurvNo0yxy_x[CurvPairNo];
   {Save the curve No in fileK of the 3 smallest difference C curve of
   file0 and fileK}
   write('The curve No in file',GN,' of the No',curvpairNo,' smallest ');
   writeln('difference C curve pair is ',GNCN0yxyMin_x[GN,CurvPairNo]);
  end;
end;
{The following statement looks for the common C curve in file0 which has
 smallest C difference with a curve in different fileX}
count:=0;
```

```
repeat
  TotalMatch:=0;
  G0G1CN_0:=GNCN0yxyMin_0[1,count];
  {The Curve No in the file0 of file0, file1 pair}
  G0GxCN_x[1]:=GNCN0yxyMin_x[1,count];
  {The Curve No in file1 of file0, file1 pair}
  GN:=2;
  repeat
   CurvPairNo:=0;
   repeat
    G0GxCN_0:=GNCN0yxyMin_0[GN,CurvPairNo];
    {The Curve No in the file0 of file0,fileX pair}
    CurvPairNo:=CurvPairNo+1;
   until ((G0GxCN_0=G0G1CN_0) or (CurvPairNo=3));
   if (G0GxCN_0<>G0G1CN_0) then
    goto DropCurenCurv
   else
   begin
    totalmatch:=totalmatch+1;
    G0GxCN_x[GN]:=GNCN0yxyMin_x[GN,CurvPairNo-1];
    {Curve No in filex in file0,fileX pair}
   end;
   GN:=GN+1;
  until (GN=NoOfCut);
DropCurenCurv:
  count:=count+1;
 until ((TotalMatch=NoOfCut-2) or (count=3));
 If (Totalmatch<>NoOfCut-2) then
 begin
  refresh;
  writeln('Error in Data input!');
  pause;
 end
 else
 begin
  assign(infile,Tem[0]);
  reset(infile);
  stepNo:=0;
  while not EOF(infile) do
```

```
begin
  read(infile,wl);
  for count:=0 to G0G1CN_0 do
    read(infile,FirstC[StepNo]);
  readln(infile);
  StepNo:=StepNo+1;
end;
close(infile);
for Gn:=1 to (NoOfCut-1) do
begin
  Assign(Infile,tem[GN]);
  reset(infile);
  StepNo:=0;
  While not EOF(infile) do
  begin
    read(infile,wl);
    for count:=0 to G0GxCN_x[GN] do
      read(infile,secondC[StepNo]);
    readln(infile);
    StepNo:=StepNo+1;
  end;
  close(infile);
  for count:=0 to (stepNo-1) do
    firstC[count]:=firstC[count]+secondC[count];
end;
refresh;
write('Enter file name for C vs Wavelength (without extension name): ');
readln(filename);
filename1:=concat(filename,'.csv');
writeln;
assign(outfile,filename);
assign(outfile1,filename1);
rewrite(outfile);
rewrite(outfile1);
clrscr;
wl:=StartWalen;
for count:=0 to (StepNo-1) do
begin
  realC:=firstC[count]/NoOfCut;
```

```
      writeln(Wl:4:0,' ',RealC);
      writeln(outfile,wl,' ',realC);
      writeln(outfile1,wl,',',realc);
      wl:=wl+WalenStep;
    end;
    close(outfile);
    close(outfils1);
  end;
end;

procedure PlotCvsWL(var infile:text; filename:filenametype; Units:unittype);
const
    TitlePart='C Vs Wavelength for ';
    X_Label='Wavelength in nm';
    Y_LabelPart='Coupling Coefficient in 1/';
Var
    Title,Y_Label:string[30];
    X,Y:array [0..(MaxWalen-MinWalen)] of real;
    Count,FileLength:integer;
    Xmin,Ymin,Xmax,Ymax:real;
Begin
    assign(infile,filename);
    reset(infile);
    FileLength:=0;
    while not EOF(infile) do
    begin
      readln(infile,X[FileLength],Y[FileLength]);
      FileLength:=FileLength+1;
    end;
    Xmin:=X[0];
    Ymin:=Y[0];
    Xmax:=X[0];
    Ymax:=Y[0];
    for Count:=1 to (FileLength-1) do
    begin
      if X[count]>Xmax then Xmax:=X[count];
      if X[count]<Xmin then Xmin:=X[count];
      if Y[count]>Ymax then Ymax:=Y[count];
      if Y[count]<Ymin then Ymin:=Y[count];
```

```
    end;
    SetPlotter(' ');
    expect(Xmin,Xmax,Ymin,Ymax);
    border;
    Xaxis(Ymin,Xmin,Xmax,(Xmax-Xmin)/20);
    Xlabel(Ymin,Xmin,Xmax,(Xmax-Xmin)/20,0);
    Yaxis(Xmin,Ymin,Ymax,(Ymax-Ymin)/20);
    Ylabel(Xmin,Ymin,Ymax,(Ymax-Ymin)/20,4);
    Xtitle(X_Label);
    Y_Label:=ConCat(Y_LabelPart,Units);
    Ytitle(Y_Label);
    Title:=concat(TitlePart,Filename);
    Lettersize(1.5,1.5);
    Figure_Title(Title);
    penup;
    for count:=0 to (FileLength-1) do
     Plot(X[count],Y[count]);
    plotend(0);
end;

BEGIN{main}
  Instruction;
  Get_experiment_Info(infile,outfile,filename,NoOfCut,NoOfMinPon,FibreLen,
    MinPonWalen);
  Check_Input_Info(NoOfCut,FibreLen,NoOfMinPon,MinPonWalen);
  Calculation_requirement(NoOfCurv,StartWalen,EndWalen,WalenStep,Fitorder,
    OutPutUnit);
  Unit_Conversion(MinPonWalen,StartWalen,EndWalen,WalenStep,NoOfCut,
    NoOfMinPon,OutPutUnit,FibreLen,MinPonWalenr,StartWalenr,EndWalenr,
    WalenStepr,FibreLenr,units);
  Calcu_Cs_and_output(outfile,filename,MinPonWalenr,NoOfMinPon,NoOfCut,
    NoOfCurv,StartWalen, EndWalen,WalenStep,fitorder,startwalenr,
    walenstepr,fibrelen,FibreLenr,units,tem);
  FindOutRealC(infile,outfile,filename,tem,NoOfCut,NoOfCurv,startWalen,WalenStep);
  PlotCvsWL(infile,filename,Units);
end.
```